Effects of transgenic overexpression of polysialyltransferase (PST) on myelination and impacts of increased sulfatide accumulation in arylsulfatase A deficient mice and its relevance to human metachromatic leukodystrophy

Dissertation

zur

Erlangung des Doktorgrades (Dr. rer. nat.)

der

Mathematisch-Naturwissenschaftlichen Fakultät

der

Rheinischen-Friedrich-Wilhelms-Universität Bonn

vorgelegt von

Hariharasubramanian Ramakrishnan

aus

Chennai, India

Bonn 2007

Angefertigt mit Genehmigung der Mathematisch-Naturwissenschaftlichen
Fakultät der Rheinischen-Friedrich-Wilhelms-Universität Bonn

1. Referent: Prof. Dr. Volkmar Gieselmann
2. Referent: Prof. Dr. Klaus Willecke

Tag der Promotion: 18.10.07

Diese Dissertation ist auf dem Hochschulschrifterserver der ULB Bonn
http://hss.ulb.uni-bonn.de/diss_online elektronisch publiziert

Thesis supervisors:
Prof. Dr. Volkmar Gieselmann
PD. Dr. Matthias Eckhardt

Defence Committee:
Prof. Dr. Volkmar Gieselmann
Prof. Dr. Klaus Willecke
Prof. Dr. Albert Haas
Prof. Dr. Klaus Mohr

Erklärung:

Hiermit versichere ich, Hariharasubramanian Ramakrishnan, dass ich die vorliegende Arbeit selbstständig angefertigt und keine anderen als die angegebenen Hilfsmittel und Quellen benutzt habe. Ferner erkläre ich, die vorliegende Arbeit an keiner anderen Hochschule als Dissertation eingereicht zu haben.

Bonn, June 2007

Hariharasubramanian Ramakrishnan

In advance publication of the dissertation

Parts of the results of this study have been published in advance by permission of the Mathematisch-Naturwissenschaftlichen Fakultät, presented by supervisor of this study.

Publications

Fewou S.N.*, Ramakrishnan H.*, Bussow H., Gieselmann V., Eckhardt M. (2007) Downregulation of polysialic acid is required for efficient myelin formation. J. Biol. Chem. 282(22):16700-11.
* Equal contribution.

Ramakrishnan H., Hedayati K.K., Lullmann-Rauch R., Wessig C., Fewou S.N., Gieselmann V., Eckhardt M. (2007) Increasing sulfatide synthesis in arylsulfatase A deficient mice causes demyelination and neurological symptoms related to metachromatic leukodystrophy. (Manuscript in preparation)

Acknowledgements

I would like to thank and express my sincere gratitude to Prof. Dr. Volkmar Gieselmann for providing me an opportunity to work on this interesting topic and also for his constant support and supervision throughout my doctoral thesis.

I wish to express my heartfelt thanks to PD. Dr. Matthias Eckhardt who was my mentor and thesis supervisor, for his supervision, support, patience and great co-operation whenever needed. His scientific advice and the discussions I had with him aroused my scientific curiosity to a great extent. I thank him for teaching me the various laboratory techniques including the art of slogging.

I would like to thank my co-supervisor Prof. Dr. Klaus Willecke for his interest in my work and for his time and willingness to be my referee. I would like to thank Prof. Dr.Albert Hass and Prof. Dr. Klaus Mohr for their time and for accepting to be part of my defence committee.

I would like to thank, Dr. Franken, PD. Dr. Kappler, Dr. Matzner and Dr. Yaghootfam, for their assistance and inputs as and when I needed them.

I take this opportunity to thank my fellow colleagues Inge, Rebekka, Marion, Abbas, Mandy, Ivonne, Stefan, Frank, Rainer, Heidi, Angela, Simon, Annette, Ayse, Heba, Peter, Mekky, Norbert, Saravanan, Preethi, Ula, Ali, Nevzat, Ms. Reninger, Ms. Ragut, Ms. Blanke and Mr. Pflüger for their support, co-operation and assistance.

I would like to thank all the co-authors, Prof. Heinrich Bussow, Prof. Renate Lüllmann-Rauch, Ms. Kerstin Khalaj Hedayati and Dr. Carsten Wessig, for their valuable contributions to this work and for the publications.

Finally, this thesis would not have been possible without the moral support, understanding and encouragement of my family and all my friends.

I. Table of contents

II. Abbreviations

µCi	Microcurie
µg	Microgram
µl	Microliter
AIDA	Advanced image data analyzer
APS	Ammonium persulfate
ASA	Arylsulfatase A (EC-3.1.6.8)
ATP	Adenosine triphosphate
BrdU	Bromodeoxyuridine
BSA	Bovine serum albumin
bp	Base pair
CAII	Carbonic anhydrase II
CGT	UDP-galactose: Ceramide galactosyl transferase (EC-2.4.1.45)
CMAP	Compound muscle action potential
CNPase	2', 3-cyclic nucleotide 3-phosphodiesterase
CNS	Central nervous system
CO_2	Carbon dioxide
cpm	Counts per minute
CST	Galactosylceramide sulfotransferase (EC-2.8.2.11)
Da	Dalton
DAB	Diamino benzidine hydrochloride
DAPI	4,6-Diamidino 2-phenylindole
dCTP	Deoxycytidine 5-phosphate
ddH_2O	Double distilled water
DEPC	Diethyl pyrocarbonate
DMEM	Dulbecco´s Modified Eagle's Medium
DNA	Deoxyribonucleic acid
dNTP	Deoxyribonucleotide triphosphate
DTT	Dithiothreitol
dUTP	Deoxyuridine triphosphate

E-cup	Eppendorf cup
EDTA	Ethylenediamine tetraacetic acid
eEF1A	Eukaryotic elongation factor 1A
eEF2	Eukaryotic elongation factor 2
EGTA	Ethylene glycol bis (2-aminoethyl ether)-N, N, N', N'-tetraacetic acid
eIF1A	Eukaryotic initiation factor 1A
eIF4A2	Eukaryotic initiation factor 4A2
eIF4b	Eukaryotic initiation factor 4b
eIF2 γ	Eukaryotic initiation factor 2 γ subunit
EMG	Electromyography
ENCAM	Embryonic neural cell adhesion molecule
EndoN	Endoneuraminidase
ERT	Enzyme replacement therapy
FCS	Fetal calf serum
FGF	Fibroblast growth factor
GalC	Galactosylceramide
GFAP	Glial fibrillary acidic protein
GPI	Glycosylphosphatidylinositol
HBSS	Hank's balanced salt solution
HCl	Hydrochloric acid
HEPES	4-(2-hydroxyethyl)-1-piperazineethanesulfonic acid
hnRNA	Heterogeneous nuclear RNA
HPTLC	High performance thin layer chromatography
HRP	Horseradish peroxidase
Ig	Immunoglobulin
IPTG	Isopropyl-β-D-thiogalactopyranoside
K^+	Potassium ion
Kb	Kilobase
kDa	Kilodalton
ko	Knock-out
LiCl	Lithium chloride

LV	Lateral ventricle
MAG	Myelin associated glycoprotein
MBP	Myelin basic protein
MBq	Megabecquerel
$MgCl_2$	Magnesium chloride
min	Minutes
MLD	Metachromatic leukodystrophy
mm^2	Square millimeter
MOPS	3-(N-Morpholino) propanesulfonic acid
mRNA	Messenger ribonucleic acid
ms	Milliseconds
MuLV	Murine leukaemia virus
mV	Millivolts
MW	Molecular weight
Na_2SO_4	Sodium sulphate
Na^+	Sodium ion
NaCl	Sodium chloride
NaOH	Sodium hydroxide
NCAM	Neural cell adhesion molecule
ng	Nanogram
NCV	Nerve conduction velocity
OD	Optical density
o/n	Overnight
OPCs	Oligodendrocyte precursor cells
PAPS	3'-phosphoadenosine-5'-phosphosulfate
PBS	Phosphate buffered saline
PCR	Polymerase chain reaction
PEI	Polyethyleneimine
PFA	Paraformaldehyde
PLP	Proteolipid protein
PMSF	Phenylmethylsulfonylfluoride
PNS	Peripheral nervous system
POD	Peroxidase

PSA	Polysialic acid
PST	α2, 8-polysialyltransferase IV
RNA	Ribonucleic acid
RT	Room temperature
SD	Standard deviation
SDS	Sodium dodecyl sulfate
SDS-PAGE	SDS-polyacrylamide gel electrophoresis
sec	Seconds
SSC	Sodium citrate
ssDNA	Salmon sperm DNA
STX	α2, 8-polysialyltransferase II
SVZ	Subventricular zone
TAE	Tris-acetic acid EDTA
TBS	Tris buffered saline
tg	Transgenic
TLC	Thin layer chromatography
TGF-β	Transforming growth factor-beta
TUNEL	Terminal deoxynucleotidyl transferase-mediated dUTP nick end labelling
VZ	Ventricular zone
wt	Wild-type
X-Gal	5-bromo-4-chloro-3-indolyl-β-D-galactopyranoside

III. Tables

IV. Figures

1. Abstract

The process of oligodendrocyte differentiation and myelination involves biosynthesis and degradation of various lipids, proteins and carbohydrates. Alterations in these metabolic pathways can lead to neuropathological symptoms and demyelinating diseases like Metachromatic leukodystrophy (MLD). This study aims at addressing the roles of two molecules namely (a) polysialic acid (PSA), an oligosaccharide and (b) sulfatide, a glycosphingolipid, in the process of oligodendrocyte differentiation, myelination and in demyelinating disorder, MLD.

Oligodendrocyte precursor cells express neural cell adhesion molecule (NCAM) which is post-translationally modified by addition of polysialic acid (PSA). As these cells undergo differentiation, they downregulate the synthesis of PSA. To understand whether downregulation of PSA is a prerequisite for oligodendrocyte differentiation and myelination, transgenic mice overexpressing polysialyltransferase, PST, under the control of proteolipid protein (PLP) promoter were generated, so that these mice do not downregulate polysialylation and show an increased level of PSA on NCAM-120 in mature oligodendrocytes. The transgenic mice sustained PSA modification of NCAM-120 in all developmental stages. These mice displayed partial co-localization of PSA and myelin basic protein (MBP) with localization of PSA-NCAM in myelin. Sustained PSA expression resulted in a decrease in myelin content and MBP protein. Structural analysis of these mice showed normal myelination in the central nervous system (CNS) and peripheral nervous system (PNS), but adult mice displayed structural abnormalities like axonal degeneration and redundant myelin. *In situ* hybridization indicated a reduction in the number of differentiated oligodendrocytes in the forebrain with no reduction in the number of oligodendrocyte precursor cells. Analysis of primary oligodendrocyte cultures displayed a less differentiated morphology with fewer processes and membranous extensions without any changes in the localization of NCAM and myelin associated glycoprotein (MAG) and with no significant difference in the percentage of MBP positive cells. Altogether these observations indicate that downregulation of PSA is essential for myelination but is not the only prerequisite for efficient myelin formation and that PSA is also involved in myelin maintenance and stability.

Lipids play an important role in maintaining membrane stoichiometry as well as in the process of myelination. De-regulation in lipid degradation results in disorders like MLD.

MLD is a lysosomal sulfatide storage disorder characterized by accumulation of sulfatide in the nervous system and other organs. The disease is caused by deficiency in the sulfatide degrading enzyme arylsulfatase A (ASA). MLD patients suffer from neurological symptoms and progressive demyelination. ASA(-/-) mice, the only animal model of MLD, in part displayed some, but less severe symptoms and no demyelination like MLD patients, thus resembling the earlier stages of human MLD. Since sulfatide storage is critical for MLD disease manifestations, it was hypothesized that increased sulfatide storage in ASA(-/-) mice might display the neuropathological symptoms of the disease. Hence, in order to increase sulfatide storage in ASA(-/-) mice, transgenic/ASA(-/-) [tg/ASA(-/-)] mice overexpressing galactosylceramide sulfotransferase (CST) under the control of PLP promoter were generated and analyzed. These tg/ASA(-/-) mice displayed a significant increase in sulfatide, in both central and peripheral nervous system. Animals older than one year displayed severe neurological defects like gait disturbances, hind limb paralysis and decreased nerve conduction velocity. Demyelination and hypertrophic neuropathy of peripheral nerves was prevalent in these mice, along with demyelination of the central nervous system. Biochemical analysis showed a decrease in MBP. Altogether these observations indicate that, increasing sulfatide storage resulted in neuropathological symptoms and demyelination akin to the advanced stages of MLD.

2. Introduction

The nervous system is composed of two major classes of cells, namely, neurons and glial cells. Neurons transmit action potentials through their axons and dendrites from different regions of the body to the brain and vice versa, whereas, glial cells are the supporting cells that perform a variety of functions like myelination, phagocytosis and maintenance of energy homeostasis. The number of glial cells far exceeds the number of neurons in the mammalian brain. During the development of the mammalian cortex, proliferating neuroepithelial cells from the ventricular and subventricular zone of the telencephalic brain give rise to neural and glial precursor cells (Doetsch et al., 1997). These cells in turn proliferate, migrate and differentiate to give rise to the complex interconnected neuroglial network.
Glial cells are classified based on their morphology and function into astrocytes, microglia, ependymal cells and oligodendrocytes in the central nervous system and Schwann cells in the peripheral nervous system.

2.1 Oligodendrocytes

Oligodendrocytes are cells of the central nervous system which generate myelin membranes. Although oligodendrocytes in general are myelin forming cells, a class of oligodendrocytes called satellite oligodendrocytes, are not involved in myelin synthesis, but maintain the microenvironment around neurons (Ludwin, 1997). During the development of the vertebrate central nervous system, the neural tube gives rise to neuroepithelial cells. Oligodendrocyte precursor cells (OPCs) are generated during late embryogenesis and early postnatal development in the ventricular regions of brain and spinal cord (Yu et al., 1994; Spassky et al., 1998; Timsit et al., 1992). These cells then migrate (Richardson et al., 2000) extensively before they differentiate into myelin-forming oligodendrocytes of the white matter. During the process of their generation, proliferation, migration and maturation different markers are expressed which play a crucial role in their development. The oligodendrocyte precursors express several different markers like platelet derived growth factor (PDGF) α-receptor (Pringle and Richardson, 1993), CNPase (Richardson et al., 2000), integrin receptors (Milner et al., 1996) and PSA-NCAM (Wang et al., 1994). The expression of these proteins helps in the proliferation and migration of oligodendrocyte precursors. During this stage of development, the OPCs are influenced by growth factors like platelet derived growth factor

(PDGF) and basal fibroblast growth factor (bFGF) (Gard and Pfeiffer, 1993; Hardy and Reynolds, 1993). PDGF and bFGF stimulate the proliferation of OPCs by binding to PDGF α-receptors and FGF receptors respectively. Extra-cellular matrix proteins like Tenascin-C (Bartsch et al., 1994) and Tenascin-R (Pesheva et al., 1997) also play a crucial role in the migration of OPCs. The OPCs get converted to progenitors, which have a bipolar morphology and then to pre-oligodendrocytes. During this stage of their development the pre-oligodendrocytes stop migrating and undergo morphological changes. They lose their bipolar morphology and develop a branched morphology. These pre-oligodendrocytes develop into immature oligodendrocytes. These immature oligodendrocytes undergo maturation to become mature non-myelinating oligodendrocytes. During this stage of maturation these cells express myelin basic protein (MBP), proteolipid protein (PLP), myelin associated glycoprotein (MAG) etc. which play a vital role in the synthesis of myelin membrane (Fig. 1). With the synthesis of myelin membrane, the mature oligodendrocytes acquire a differentiated morphology with extensive branching and interconnections to develop into a mature myelinating oligodendrocyte which can adhere and myelinate the axons. The ensheathment of myelin around axons increases the nerve conduction velocity by saltatory conduction of the action potential. Normally, the myelin sheath from a single oligodendrocyte can wrap around one or more axons (Baumann and Pham-Dinh, 2001).

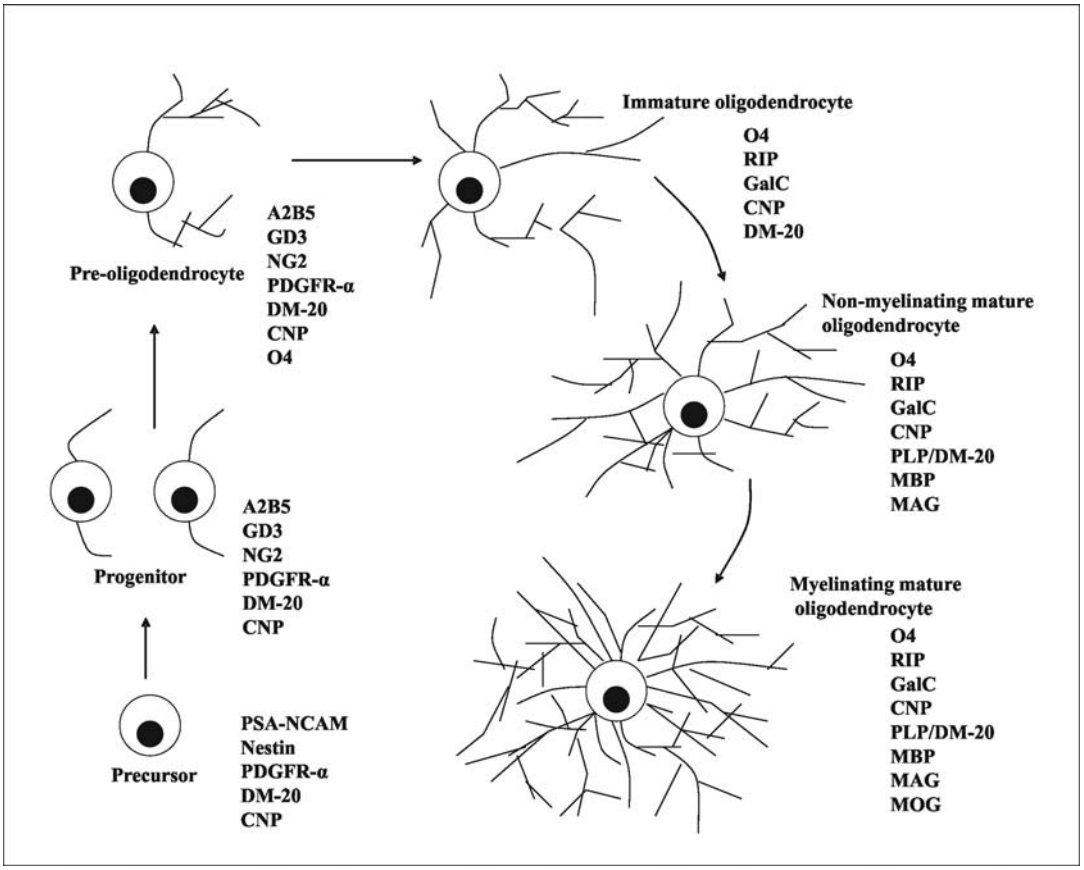

Figure 1: Illustration showing the developmental stages and markers expressed during oligodendrocyte development. Different markers are expressed on precursor, progenitor, immature and myelinating oligodendrocytes (Adapted from Baumann and Pham-Dinh, 2001).

2.2 Schwann cells

Schwann cells are the myelinating cells of the peripheral nervous system which ensheath the axons in the PNS. In vertebtrates, Schwann cells are derived from the neural crest and placodes of the head region during embryogenesis (Harrison, 1924). Schwann cells can be of two subtypes namely, ensheathing Schwann cells and myelinating Schwann cells. Both subtypes are derived from a common precursor. Ensheathing Schwann cells are associated with unmyelinated nerve fibers, providing ensheathment via membranous indentations on their surface. As the ensheathment provided by these Schwann cells is not necessary for nerve conduction, the exact function of these cells still remains unclear. Myelinating Schwann cells generate myelin and spirals around individual axons, so that unitary connection is established between the Schwann cell and the axon (Bung and Fernandez-Valle, 1995).

2.3 Neural cell adhesion molecule (NCAM) and Polysialic acid (PSA)

2.3.1 NCAM

NCAM is a cell adhesion molecule that belongs to the immunoglobulin super-family that plays a pivotal role in cell-cell interactions in various tissues. It is expressed mainly in the neural cells and skeletal muscle (Sanes et al., 1986). The diversity in NCAM functions is possible by generation of different isoforms, by alternative splicing of hnRNA from a single NCAM gene and by post-translational modifications. The 3 main isoforms in the brain are NCAM-120, 140 & 180 (Goridis et al., 1983; Gennarini et al., 1986). In the brain, NCAM-120 is expressed in oligodendrocytes (Bhat and Silderberg, 1986) and NCAM-140 & 180, in neurons. The extra-cellular domain of the polypeptide chain in all 3 isoforms consists of 5 immunoglobulin and 2 fibronectin type III like domains, respectively (Cunningham et al., 1987; Santoni et al., 1987). NCAM-120 is attached to the membrane by a glycosylphosphatidylinositol (GPI) anchor and lacks a transmembrane domain while NCAM-140 & 180 are transmembrane proteins, containing short or long cytoplasmic domains, respectively (Barthels et al., 1987; He et al., 1986; Hemperly et al., 1986). NCAM has been shown to participate in a number of developmental processes including cell migration, neurite outgrowth and synaptic plasticity (Crossin and Krushel, 2000; Ronn et al., 2000 and Schachner, 1997). NCAM carries out many of its functions by homophilic and heterophilic interactions with other NCAM molecules or with other cell adhesion molecules and receptors like L1 and fibroblast growth factor receptors and a variety of extra-cellular matrix components (Povlsen et al., 2003). Apart from its adhesive properties, NCAM influences the developmental events through its signalling properties. For example, NCAM-140 associates with Fyn kinase or acts as an alternative receptor for glial derived neurotrophic factor (GDNF) family of ligands and recruits focal adhesion kinase, a kinase known to participate in cytoskeletal rearrangements (Beggs et al., 1997; Paratcha et al., 2003).

2.3.2 Polysialic acid

Polysialic acid is a negatively charged, homopolymer of α2-8 linked sialic acid (N-acetyl neuraminic acid) residues attached post-translationally to NCAM (Finne et al., 1983). Besides brain, PSA is also expressed in heart and kidney (Finne et al., 1987; Roth et al., 1987). Two different sialyltransferases namely, STX (Nakayama et al., 1995) and PST (Eckhardt et al.,

1995) catalyze addition of PSA to NCAM in the trans-Golgi compartment (Scheidegger et al., 1994; Alcaraz and Goridis, 1991).

2.3.2.1 PSA synthesis

The three major building units of PSA are N-acetyl neuraminic acid (Neu5AC), 5-N-glycolylneuraminic acid (Neu5GC) and 5-deamino-3, 5-dideoxyneuraminic acid (2-keto-3-deoxynonulosonic acid, Kdn). The predominant building units of PSA in mammals are Neu5Ac and Kdn (Mühlenhoff et al., 1998). Condensation of N-acetyl mannose-6 phosphate (ManNAc-6-P) or mannose-6 phosphate (Man-6-P) with activated forms of pyruvate generates Neu5Ac or Kdn units. The free sialic acids are then converted to activated forms of CMP (cytidine monophosphate)-Sia, catalysed by the enzyme CMP-Sia synthetase. The activated CMP-Sia is then transported from the cytoplasm to the Golgi apparatus by a CMP-Sia antiporter. In the Golgi apparatus, sialic acid residues are transferred from CMP donors to proteins like NCAM by sialyltransferases like STX and PST (Varki et al., 1999). The free CMPs that are generated during the above reaction are transported back to the cytoplasm.
The developmental expression of STX and PST is tightly regulated, both PST and STX are expressed during embryonic stages (Ong et al., 1998) whereas, in the adult brain, PST expression persists only in regions displaying neurogenesis and plasticity and STX mRNA is almost not detectable (Livingston & Paulson, 1993; Hildebrandt et al., 1998). During the process of maturation of oligodendrocytes the expression of PSA-NCAM is downregulated due to a downregulation of PST mRNA (Stoykova et al., 2001).

2.3.2.2 Function

PSA promotes plasticity in cell-cell interactions during axonal migration, fasciculation and cell migration (Kiss et al., 1997; Rutishauser and Landmesser, 1996). Due to its size and negative charge PSA exhibits anti-adhesive properties, thereby inhibiting cell adhesion to other cells and extra-cellular matrix (Yang et al., 1992; Yang et al., 1994; Johnson et al., 2005). During spatial learning, which enhances synaptic plasticity, an increase in the number of PSA positive neurons is observed in hippocampus (Muller et al., 1996; Becker et al., 1996). Besides, it has been demonstrated that PSA is also required for long term potentiation (Cremer et al., 1994) and maintenance of circadian rhythm (Fedorkova et al., 2002). During the process of oligodendrocyte migration and differentiation oligodendrocytes are influenced

by a coordinated action of specific positive and negative signaling cues. While positive signals help the oligodendrocyte precursors to migrate and differentiate, negative signals prevent their premature differentiation. Among the different negative signals, polysialylated neural cell adhesion molecule (PSA-NCAM) is one such signal which is expressed in migratory oligodendrocyte precursors to facilitate their migration (Fig 1).

2.4 Myelin

In the CNS, oligodendrocytes synthesize a highly specialized plasma membrane called myelin. Myelin membrane wraps around the axons, acting as an insulator and enables saltatory conduction of nerve impulses thereby increasing the speed of transmission of action potential. Formation of myelin membrane is a tightly regulated developmental process involving synthesis of lipids and proteins and transport of these proteins or their mRNAs to the oligodendrocyte processes. The white matter in the CNS is made up of 40-50% of myelin on a dry weight basis. Myelin dry weight consists of 70% lipids and 30% proteins. This lipid-protein ratio is peculiar to myelin and is generally reverse in other cellular membranes (Baumann and Pham-Dinh, 2001).

2.4.1 Myelin lipids

The myelin lipids are enriched in cholesterol, forming a higher percentage of the total lipid composition. Phospholipids represent 40% of the total myelin and in general are similar in composition to the phospholipids of the plasma membrane. Sphingolipids like sphingomyelin and glycosphingolipids especially, galactocerebrosides, galactosylceramide (GalC) and sulfatide also form a part of the myelin membrane. GalC represents 20% of lipid dry weight in mature myelin. Glycosphingolipids are a subtype of glycolipids, synthesized from ceramide that carry a cerebroside side chain. Glycosphingolipids can be subdivided into cerebrosides, sulfatides, globosides and gangliosides. Several minor galactolipids like the sialylated gangliosides, GM1 and GM4, fatty esters of cerebroside, i.e., acylgalactosylceramides and galactosyldiglycerides also form a part of myelin membrane.

2.4.2 Myelin Proteins

Myelin is rich in a variety of proteins that are specific for myelin producing cells. The major proteins of myelin are myelin basic protein (MBP), proteolipid protein (PLP), myelin

associated glycoprotein (MAG) and CNPase. Other proteins like myelin oligodendrocyte glycoprotein (MOG), connexin-32 and myelin associated oligodendrocyte basic protein (MOBP) constitutes a very small percentage of the total myelin proteins.

MBP exists as several isoforms with molecular mass of the major isoforms being 21.5, 20, 18.5, 17 & 14 kDa in mouse. These isoforms are generated by alternative splicing of a single mRNA precursor (deFerra et al., 1985; Newmann et al., 1987). MBP is a basic hydrophilic membrane associated protein, expressed by oligodendrocytes and some cells of the haematopoetic system (Marty et al., 2002). Evidence from shiverer mutant mice, where the different isoforms of MBP are undetectable due to mutation in the MBP gene (Molineaux et al., 1986), indicates that MBP plays a major role in myelin compaction in the CNS (Roach et al., 1985).

Proteolipid proteins exists in two isoforms namely as a predominant, 30 kDa PLP and 25 kDa DM-20, produced by alternative splicing from a single gene (Nave et al., 1986; Morello et al., 1986). PLP is an integral membrane protein. mRNA of DM-20 can be detected in the CNS at a very early stage of development even before the onset of myelination (Ikenaka et al., 1992; Peyron et al., 1997; Timsit et al., 1992; Timsit et al., 1995), but in general in mouse brain PLP synthesis peaks a few days later than that of MBP synthesis. The period of active myelination in mouse brain is around 2-3 weeks postnatally. During this period, MBP synthesis reaches its peak at around 18 days when compared to PLP, which is 22 days. Analysis of PLP knock-out mice shows that PLP plays a role in stabilizing membrane junctions after myelin compaction (Boison et al., 1994; Boison et al., 1995).

Myelin associated glycoprotein (MAG) exists in two forms as L-MAG and S-MAG with molecular masses of 72 and 67 kDa, respectively. In the CNS, L-MAG is the major form during early myelinogenesis and S-MAG expression increases with maturation, so that in the adult, the two isoforms are expressed in equal amounts. In the PNS, S-MAG is the predominant isoform at all stages of development (Frail et al., 1985; Salzer et al., 1987). L-MAG is shown to be involved in the activation of Fyn kinase, which implicates the tyrosine phosphorylation cascade involved in myelinogenesis, maturation and differentiation of oligodendrocytes (Umemori et al., 1994). MAG is proposed to perform neuron-oligodendrocyte interactions through its sialic acid binding site at arginine-118 amino acid (Poltorak et al., 1987; Tang et al., 1997). MAG interacts with sialylated glycolipids like gangliosides or with sialylated proteins (Yang et al., 1996) and carry out these interactions. MAG is also shown to inhibit axon regeneration after lesion (Filbin, 1996; Qiu et al., 2000).

Analysis of myelin sheaths from MAG knock-out mouse showed that there was a delay in myelin compaction indicating that MAG might play a role in myelin compaction (Li et al., 1994; Montag et al., 1994).

2', 3-cyclic nucleotide 3-phosphodiesterase (CNPase) or RIP antigen (Watanabe et al., 2006) is a myelin-associated protein, expressed in oligodendrocytes and Schwann cells in the CNS and PNS, respectively. It exists in two isoforms, produced by alternate splicing, CNP1 and CNP2, with molecular masses of 46 kDa and 48 kDa, respectively. CNPase comprises 4% of the total protein present in myelin (Baumann and Pham-Dinh, 2001). Transgenic overexpression of CNPase in mice perturbs myelin formation and creates aberrant oligodendrocyte membrane expansion (Gravel et al., 1996).

2.4.3 Myelination in the CNS

The process of myelination progresses in a coordinated manner. Although the actual process of myelination is still not clearly understood, published reports show that it involves the following sequential steps like migration of oligodendrocytes towards axons, adhesion of oligodendrocytes processes with the axon and not with the dendrites and spiralling of these processes around axons with a predetermined thickness. In mouse, myelination starts at birth in the spinal cord and is complete by 45-60 days postnatally in brain. As the oligodendrocytes undergo differentiation from preoligodendrocytes to immature oligodendrocytes, they lose their capacity for migration and cell division. During this time, they synthesize myelin sheaths which express myelin specific genes like CNPase and Carbonic anhydrase II (CAII) (Sprinkle et al., 1989; Friedman et al., 1989; Butt et al., 1995). Axonal contact is vital for the survival of these immature oligodendrocytes (Burne et al., 1996). Axon-oligodendrocyte cross-talk is important for proper positioning of oligodendrocytes around unmyelinated axons and ensheathment of myelin around axons. Although it is still not clear which signaling cues help the oligodendrocytes to distinguish between axons which must be myelinated and those which should not be myelinated, reports suggest that the downregulation of Jagged1, a Notch receptor ligand, on axons, plays a role for oligodendrocytes to establish contact with axons and myelinate them (Schwab et al., 1989; Wang et al., 1998). Besides Jagged1, PSA-NCAM has been shown to negatively regulate myelination in the CNS. During development, axons express PSA-NCAM but later the axonal expression of PSA-NCAM goes down so that myelination occurs only on PSA-NCAM negative axons. Charles et al., (2000) showed that

myelination is controlled by both positive signals like electrical activity and negative signals like PSA-NCAM expression. Data from primary neuron-oligodendrocyte co-culture analysis from mice showed that PSA-NCAM level on axons is downregulated at the time of myelination. This was further confirmed by EndoN removal of PSA, which resulted in an increase in the number of myelinated internodes in these cultures. Removal of PSA in cultures treated with tetrotoxin, an action potential blocker, were unable to reverse the inhibition of myelination. Moreover, *in vivo* examination with optic nerve showed that the time of appearance of first MBP positive myelinated internodes coincided with the disappearance of PSA-NCAM on axons and later myelination occurred only on PSA-NCAM negative axons. Thus, these results show that downregulation of PSA-NCAM on axons is an important signal for myelination but removal of PSA-NCAM alone is not sufficient to promote myelination. Reports show that binding of adenosine from electrically active neurons to adenosine receptors on oligodendrocytes prevents oligodendrocyte proliferation and initiate differentiation. Adenosine acts as a potent neuron-glial transmitter that inhibits oligodendrocyte proliferation and stimulates differentiation and myelin formation (Stevens et al., 2002). Apart from neurons, astrocytes also play a role in myelination by aligning the oligodendrocytes with axons (Meyer-Franke et al., 1999). Upon axonal recognition, mature myelinating oligodendrocytes with flattened, extended myelin sheaths are formed (Bunge et al., 1962; Bunge, 1968). A single mature oligodendrocyte wraps around more than one axon with different diameters of myelin. Hence, the maintenance of myelin sheath thickness is an important step during myelination. Axons seem to play a role in this process by specifying the number of myelin lamellae formed by a single oligodendrocyte (Waxman and Sims, 1984). Although in the peripheral nervous system, the epidermal growth factor like ligand, neuregulin-1-type III, expressed on axons plays a role in Schwann cell differentiation and regulation of myelin sheath thickness, by binding to ErbB receptor tyrosine kinases on Schwann cells, its role in CNS is still an open question that remains to be answered (Nave and Salzer, 2006).

Despite complete ensheathment of axons with myelin, certain regions of axons called the nodes of Ranvier are not wrapped with myelin. The nodes of Ranvier are clustered with sodium channels in nodes and potassium channels in paranodes at regular intervals. As the myelin ensheathed regions of the axon membrane contain almost no sodium channels, they are not excitable; hence they have a low capacitance and a high resistance to current leakage. Thus, when an action potential is triggered at a node, the resulting current can be conducted to

the next node efficiently. Hence, the formation and maintenance of these nodes and the clustering of ion channels are one of the critical factors for the saltatory conduction of action potentials. Published reports show that signals from oligodendrocytes during their contact with axons generates the clustering of these ion channels (Kaplan et al., 1997).

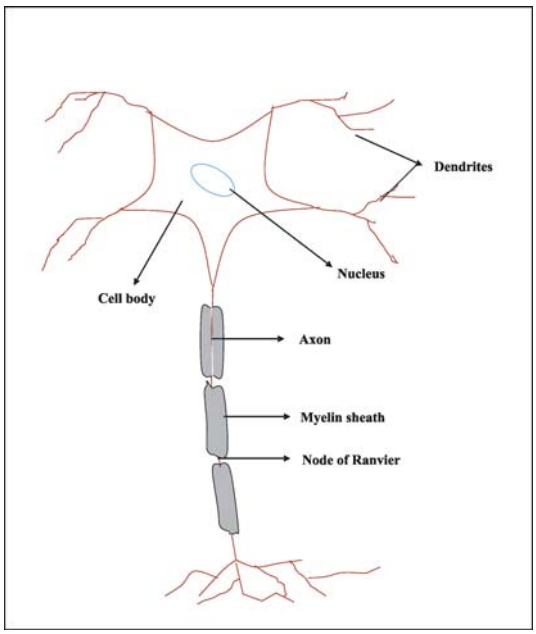

Figure 2: Illustration of neuron and myelin sheath. An illustration depicting the basic structure of neuron, myelin sheath and the nodes of Ranvier.

2.4.4 PSA and myelination

Charles et al., (2000) showed that PSA-NCAM is downregulated on axons before the onset of myelination. Oligodendrocyte precursor cells (OPCs) express PSA-NCAM, but as the OPCs undergo differentiation to become mature myelinating oligodendrocytes, PSA-NCAM is downregulated. Since PSA-NCAM is downregulated during early differentiation, the role played by PSA-NCAM in the process of myelination is still not clear. The question whether PSA-NCAM downregulation in oligodendrocytes, as in axons, is a necessary prerequisite for myelination still needed to be answered. Reports from Stoykova et al., (2001) show that the polysialyltransferase, PST, is responsible for the polysialylation of NCAM in oligodendrocytes. Hence, in order to address the question about the role played by PSA downregulation in oligodendrocytes on myelination, in this study, PST transgenic mice under the control of PLP, a marker for mature differentiated oligodendrocytes, promoter was

generated; so that, these mice sustain the expression of PST and the NCAM remain polysialylated even in mature differentiated oligodendrocytes.

2.4.5 Myelin disorders

The process of myelin formation and myelination is well synchronized that alterations in the synthesis or degradation of the myelin lipids and proteins leads to several myelin related disorders resulting in demyelination or dysmyelination or hypomyelination and uncompaction of myelin. The causes for these disorders could be due to a variety of factors like genetic, lesion, trauma, inflammation, malnutrition, viral infections, toxicity or improper metabolism of lipids and proteins. Among the several myelin disorders, leukodystrophies are a group of inherited disorders characterised by loss of myelin in CNS and PNS. Leukodystrophies can occur due to dysfunction in lipid metabolism as in metachromatic leukodystrophy, Krabbe's disease and adrenoleukodystrophy, or in protein metabolism as in Pelizaeus Merzbacher disease and Alexander's disease.

2.5 Metachromatic leukodystrophy (MLD)

Metachromatic leukodystrophy (MLD) is an autosomal recessively inherited lysosomal storage disorder caused by the deficiency of an enzyme Arylsulfatase A (ASA). ASA is an enzyme responsible for the degradation of sulfatide. Hence, the deficiency of this enzyme leads to storage of the sphingolipid sulfatide in nervous system and several other organs. The disease is characterized by progressive demyelination in both CNS and PNS, resulting in severe neuropathological symptoms in humans. The frequency of the disease is 1:40,000 to 1 in 100,000 newborns (von Figura et al., 2001).

2.5.1 Classification

MLD in human patients is classified depending on the age of onset into four forms of disease namely (a) late infantile, between 6 months and 4 years, (b) early juvenile, between 4 and 6 years, (c) late juvenile, between 6 and 16 years and (d) adult, older than 16 years. In all these forms, the disease is characterized by deficient ASA activity, decreased nerve conduction velocity, increased cerebrospinal fluid protein and increased excretion of urinary sulfatide. Besides these symptoms, ataxia, gait disturbance, progressive demyelination and optic

atrophy are the other manifestations of the disease. Table 1 indicates the characteristic features of different types of MLD.

Characteristics of late infantile, juvenile and adult forms of MLD

Table 1

Type	Age at onset (years)	Main clinical manifestations	Spinal fluid protein	Nerve conduction velocity	Urinary sulfatide excretion
Infantile	0.5–4	Gait disturbance, decreased tendon reflexes, mental regression, loss of speech, optic atrophy, ataxia, progressive spastic quadriparesis	Elevated	Slowed	Elevated
Early juvenile	4–6	Gait and postural abnormalities, emotional and behavioral disturbances, optic atrophy, progressive spastic quadriparesis	Elevated	Slowed	Elevated
Late juvenile	6–16	Behavioral abnormalities, poor school performance, language regression, gait disturbance, slowly progressive spastic tetraparesis	Elevated	Slowed	Elevated
Adult	>16	Mental regression, psychiatric symptoms, incontinence, slowly progressive spastic tetraparesis	Normal or elevated	Normal or slowed	Elevated

Adapted from The metabolic and molecular basis of inherited diseases: Metachromatic leukodystrophy, von Figura et al., 2001.

2.5.2 Pathology

The major hallmark of the disease is the progressive demyelination and deposition of metachromatic granules in central and peripheral nervous system. The metachromatic granules from MLD brain contain sulfatide amounting to 39% of their total lipid content. Electron microscopy of the storage granules shows characteristic prismatic and tuffstone like profiles and composite bodies containing lipofuscin. In the CNS, the amount of white matter is reduced, is firmer and show cavitation or spongiform degeneration in the affected areas, with accumulation of metachromatic granules in the oligodendrocytes, neurons and macrophages. Demyelination is observed in brain stem, spinal cord and cerebellum. The cerebellum is atrophic and shows prominent gliosis in demyelinated areas, with reduction in the number of Purkinje and granule cells. The PNS shows segmental demyelination with accumulation of metachromatic granules in Schwann cells and reduced myelin sheath thickness. Apart from the nervous system, storage of sulfatide is also observed in the visceral

organs like kidney, gall bladder, islets of Langerhans, anterior pituitary, adrenal cortex, testes and sweat glands.

In late infantile patients, the white matter sulfatide level is increased 3 to 4-fold, along with a marked decrease in myelin lipids like cholesterol and sphingomyelin. There is also a drastic reduction in cerebroside, hence, GalC:sulfatide ratio is reduced to one in late infantile form of MLD patients when compared to three in normal individuals (Harzer et al., 1987; Norton et al., 1982). In adults, the white matter sulfatide is only moderately increased when compared to normal white matter (Pilz and Heipertz, 1974) and contains more short chain and saturated and less unsaturated fatty acids (Malone et al., 1966). Moreover, sulfatide concentration is also increased in gallbladder, kidney and urine of MLD patients (von Figura et al., 2001).

2.6 Arylsulfatase A

Arylsulfatase A (ASA) is a cerebroside sulfatase found in lysosomes that cleaves the sulfate group in sulfatides, lactosylceramide 3-sulfate and seminolipids. Desulfation of sulfatide by ASA leads to the degradation of sulfatide to galactosylceramide (GalC). Arylsulfatases are expressed in all body tissues and fluids. During the period of myelination, ASA activity increases steadily with CST enzyme activity. After completion of myelination, CST activity is reduced whereas ASA activity is not.

The human ASA gene is located on chromosome 22 and consists of 8 exons. The gene is transcribed into a 2.1 kb mRNA, which in turn codes for the ASA precursor protein of 507 amino acids. Post-translational modifications take place in the endoplasmic reticulum, including the oxidation of thiol group to an aldehyde at the cysteine 69 amino acid of ASA protein. This oxidation generates a formylglycine residue at cysteine 69 position, which is important for ASA enzyme activity (Dierks et al., 1997). Within the lumen of the endoplasmic reticulum, the signal peptide is cleaved and N-oligosaccharide side chains are added at three potential N-glycosylation sites. After completion of protein folding, the enzyme is transported to the Golgi apparatus and recognized by lysosomal phosphotransferase as a lysosomal enzyme and mannose-6-phosphate residues are added to the N-oligosaccharide side chains. The addition of mannose-6-phosphate occurs in a two step reaction involving transfer of N-acetylglucosamine 1-phosphate from UDP-N-acetylglucosamine to mannose residues of N-linked oligosaccharides by a phosphotransferase (UDP-N-acetylglucosamine: lysosomal enzyme N-acetylglucosamine-phosphotransferase), followed by removal of N-

acetylglucosamine by N-acetylglucosaminidase, which generates mannose-6-phosphate residues on ASA. The mannose-6-phosphate residues are recognized by mannose-6-phosphate receptors and ASA is then transported in vesicles to lysosomes.
ASA is an acidic glycoprotein with low isoelectric point. The major substrates of ASA are sulfatide, galactosyl-3-O-sulfates (lactosyl ceramide 3-sulfate, seminolipid and lysosulfatide) and ascorbic acid-2-sulfate. Till date, more than 80 different mutations have been found in the ASA gene that causes MLD in humans (von Figura et al., 2001).

2.7 Cerebroside sulfotransferase (CST)

CST is a Golgi-associated sulfotransferase, whose activity has been demonstrated in brain, testis, kidney, liver, gastric mucosa, lung and endometrium of various mammals (Ishizuka, 1997). The major sulfoglycolipids synthesized by CST are sulfatide, seminolipid (3-O-sulfogalactosyl glycerolipid) and lactosylceramide 3-sulfate. The mouse CST gene is composed of 3 exons with exon 1 existing in 7 multiple forms at the 5'untranslated region contributing to tissue specific splicing of CST transcripts. The protein is made of 423 amino acids with a molecular weight of 48,995 daltons (Hirahara et al., 2000).

2.8 Sulfatide

Sulfatide is an acidic glycosphingolipid, whose sphingosine base is predominantly made up of C-18 sphingosine. It is a sulfatide ester of galactocerebroside with the sulfate joined by an ester linkage to the C-3 hydroxyl of galactose. Sulfatide accounts for 3-4% of myelin lipids in the nervous system (Norton and Poduslo, 1982). Maximum synthesis of sulfatide occurs during myelination and proceeds more slowly in the adult. Besides brain, sulfatide is abundant in the kidney (von Figura et al., 2001). Sulfatide synthesis begins with the addition of galactose residues to ceramides by UDP-galactose:ceramide galactosyltransferase (CGT), in the endoplasmic reticulum; resulting in the formation of Galactosylceramide (GalC). GalC is then transported from the endoplasmic reticulum to the Golgi apparatus where sulfate groups are added to it. This reaction is catalyzed by galactosylceramide 3'- sulfotransferase (CST), a Golgi enzyme, by transferring the sulfate from PAPS: 3'-phosphoadenosine 5'-phosphosulphate to GalC. PAPS, is a sulphonate donor, synthesized from the catalytic reaction of PAPS synthetase and ATP in the Golgi apparatus (Fuda et al., 2002).

A

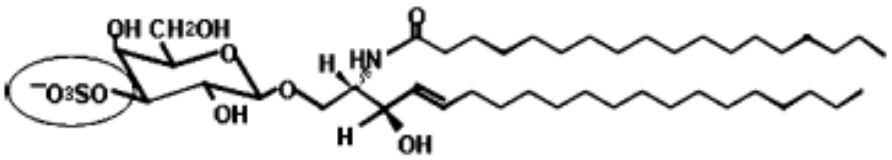

B

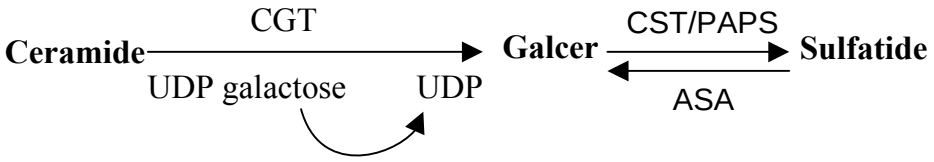

Figure 3: Sulfatide: structure, synthesis and degradation. A schematic diagram showing (A) sulfatide structure and (B) synthesis and degradation of sulfatide.

Sulfatide is transported from the Golgi apparatus to lysosomes, myelin membrane and plasma membrane in vesicles (Burkart et al., 1982). It is located on the outer leaflet of myelin membrane and is probably bound to MBP and PLP proteins by strong ionic interactions (von Figura et al., 2001). Sulfatide is first expressed when OPCs cease to proliferate and commence terminal differentiation. Analysis of CST knock-out [CST(-/-)] mice by Hirahara et al., (2004) show that there is a 2-3 fold enhancement in the number of terminally differentiated oligodendrocytes both in oligodendrocyte cultures and *in vivo,* indicating that sulfatide acts as a negative regulator of oligodendrocyte differentiation. Moreover, results from (Ishibashi et al., 2002; Honke et al., 2002; Marcus et al., 2006) show that CST(-/-) mice display abnormalities in paranodal junction formation and a decrease in Na^+ and K^+ ion channel clustering. These results show that sulfatide is essential for the maintenance of myelin, paranodal loops and clustering of sodium and potassium channels of the myelin membrane.

Sulfatide is also believed to be involved in active sodium transport, serving as a co-factor for Na/K-ATPase (Rintoul et al., 1989). Moreover, sulfatide also binds to various cellular adhesion molecules like laminin, selectin, thrombospondin and tenascin R (von Figura et al., 2001).

2.9 Animal model of MLD

An animal model for MLD, till date, is the ASA(-/-) mice deficient in ASA. The ASA(-/-) mice exhibit several characteristics of the human disease. These mice store sulfatide in the nervous system; in neurons, oligodendrocytes and Schwann cells, as well as in kidney and gall bladder (Hess et al., 1996). Mice between 6 and 12 months of age develop neuronal and glial degeneration of the acoustic ganglion, resulting in deafness. In older animals, 2 years of age, neuromotor alterations, ataxia, shorter gait and cerebellar deficits were observed (D'Hooge et al., 1999). Although the animals accumulate increasing amounts of sulfatide with age, they display less severe symptoms and their pathology did not reach the advanced stages of MLD, like slowed nerve conduction velocity, progressive hindlimb paralysis and progressive demyelination that are characteristics of the disease in human MLD patients. Thus their sulfatide storage pattern resembles that of human late infantile (early onset) MLD patients (Hess et al., 1996).

2.9.1 Improved animal model of MLD

Sulfatide storage is a critical criterion for the disease manifestation in human patients. Since the ASA(-/-) mouse show sulfatide storage similar to early phase of human MLD, in this study it was hypothesized that by increasing sulfatide storage in ASA(-/-) mice an improved animal model for human MLD could be generated that would display the neuropathology of late stages of the disease including progressive demyelination. The increase in sulfatide synthesis could be achieved either by overexpressing CGT or CST genes. Recent published reports (Fewou et al., 2005) showed that CGT transgenic mice demyelinate even with a functional ASA gene and do not show a net accumulation of sulfatide. Hence the increase in sulfatide synthesis was achieved by generating transgenic/ASA(-/-) [tg/ASA(-/-)] mice that would overexpress CST under the control of PLP promoter, so that these mice increase sulfatide storage in oligodendrocytes and Schwann cells. Hence, transgenic mice overexpressing CST in oligodendrocytes under the control of PLP-promoter was generated and bred with ASA(-/-) mice, to increase the sulfatide level. These mice were then analyzed in detail in the present study.

3. Materials and methods

3.1 Chemicals used

Unless otherwise stated chemicals were purchased from Serva (Heidelberg, Germany), Merck (Darmstadt, Germany), Fluka (Germany), BioRad Laboratories (Munich, Germany).

All cell culture solutions, buffers, DNaseI, antibiotics & horse serum are from Sigma (Deisenhofen, Germany), Invitrogen/Life technologies (Karlsruhe, Germany) & GibcoBRL (Karlsruhe).

In vitro transcription kit was from Roche (Basel, Switzerland) & Boehringer (Mannheim).

[α-^{32}P]-dCTP & [^{35}S]-Na_2SO_4 were obtained from Amersham (Buckinghamshire, UK).

Restriction enzymes, PCR reaction mix (Buffers, dNTPs, Taq polymerase enzyme, $MgCl_2$), RT-PCR kit, protein and DNA markers were from Fermentas (St.Leon-Rot, Germany).

3.2 Equipments and Materials used

Equipments and Materials	***Company***
ABI prism 310 genetic analyzer	Perkin Elmer
AIDA software	Raytest
Beckmann DU 640 spectrophotometer	Beckmann Coulter
Biomax MR film	Kodak
Block heater	Stuart Scientific
CAMAG automatic TLC sampler	CAMAG
Cell culture plates/flasks	Sarstedt
Centricon spin columns	Millipore
Centrifuge	
Eppendorf 5810R, 5417R and 5415 D	Eppendorf
Optima TLX ultracentrifuge	Beckmann Coulter
Ultracentrifuge L7-65	Beckmann Coulter
Sorvall GS3, JA-10 suppressed	Heraeus Sorvall
Cryostat CM 30	Leica
Digital balance	Typ 126MP; 1265-Sartorius

Electrophoresis apparatus-agarose gels	Hoefer Scientific Instruments
Electrophoresis apparatus for SDS-PAGE	BioRad
ELISA reader	BioRad
Film Developer Curix 60	Agfa
Freeze drier (LYO-VAC)	Amsco/finn-Aqua
Gel blot system	BioRad
Gel dryer	Savant
Haemocytometer	Hausser
Hi Trap Ni^{2+}-chelating column	Amersham Pharmacia
Homogeniser	Janke & Kunkel
HPTLC plates (Silica gel 60)	Merck
Hyper Cassette	Amersham
Ice machine AF–10	Scottsman
Imaging plates BAS IP MS 2325	Fuji Photo film
Laminar flow system-type CA/REV6	Clean Air
Magnetic stirrer	Janke & Kunkel
Micro pipettes	Gilson
Microscope Axiovert 100 M	Zeiss
Microwave oven	Sharp
PAPPEN	Dakocytomation
Pasteur pipettes	Assistent
Petri plates	Sarstedt
Pipettes (10µl, 200µl, 1000µl)	Heinrich EM
Pipette tips	Greiner
PEI TLC plates	Merck
pH-Meter (Digital-pH-Meter 646)	Knick
Phosphorimager ES 1000	Raytest
Scintillation counter Beckmann LS-6500	Beckmann
Shaking water bath	Köttermann
Speed vac SC-100	Savant
Sterile hood Labgrade class II, Typ A/B3	Nuaire
Super Frost Plus glass slide	Menzel-Glaser
Thermocycler T3	Biometra

Ultrasonicator	Branson Ultrasonic SA
UV hand lamp	Konrad Bender
Vortexer	Heidolph
Water purifier Milli-Q Plus	Millipore

3.3 Buffers and solutions

Table 2

Tris (hydroxyl methyl)-aminoethane buffered saline (TBS)	20 mM Tris-HCl, pH 7.4 150 mM NaCl
10x Phosphate buffered saline (PBS)	100 mM Na_2HPO_4/NaH_2PO_4, pH 7.4, 1.5 M NaCl, 25mM KCl
1x TAE	40 mM Tris-base, 20 mM acetic acid, 1 mM EDTA, pH 8
TNE	10 mM Tris-HCl, pH 7.4, 150 mM NaCl, 5 mM EDTA, 1 mM PMSF
20x SSC	3 M NaCl, 0.3 M Sodium citrate, pH 7.0
10x HEPES	100 mM HEPES, 20 mM EGTA, pH 7.4
SDS Blotting buffer	48 mM Tris-base, 39 mM Glycine, 0,037% SDS 20% Methanol
(4x) L4 DNA loading dye	0.25% Bromophenol blue, 30% Glycerol (100%), 100 mM Tris-HCl, pH 7
Lysis buffer	50 mM $MgCl_2$, 5 mM DTT, 1 mM PMSF, 0.5 mg/ml lysozyme, 1.7 U/ml DNase, 150 mM NaCl
Binding buffer	50 mM phosphate buffer, pH 8, 300 mM NaCl, 20 mM imidazole
Elution buffer	50 mM phosphate buffer, pH 8, 300 mM NaCl, 500 mM imidazole, 50 mM EDTA, pH 8
10x TE Buffer	100 mM Tris-HCl, pH 7.6, 10 mM EDTA
Ponceau S solution	0.2% Ponceau S, 3% Trichloroacetic acid
DEPC water	0.1% DEPC in ddH_2O. Mix it o/n at RT and then autoclave

4x Protein loading dye	8% SDS, 40% glycerol, 240 mM Tris-HCl, pH 6.8 4% Bromophenol blue, 4% β-mercaptoethanol
LB-Medium	10 g Bacto-Tryptone, 5 g Bacto-Yeast Extract 10 g NaCl in 1000 ml ddH_2O; pH 7.5; autoclave the solution
Agar plates	1.5% Agar in LB-Medium Autoclave. Cool the solution to 50°C and pour in Petri plates to dry
Antibiotics for selection	Ampicillin-100 µg/ml, Kanamycin-50 µg/ml To either LB medium or LB agar plates
SDS-PAGE running buffer	192 mM glycine, 25 mM Tris, 0.1% SDS, pH 8.3

3.4 Protease inhibitors

These inhibitors were added to buffers and solutions during protein preparations

2 mM PMSF in methanol

1 µg /ml Aprotinin

1 µg /ml Leupeptin

200 mM Pefabloc

5 mM EDTA

3.5 Animals and their genetic background

All animal experiments were approved by the local committee for animal welfare (Bezirksregierung Köln).

PLP-PST transgenic line - CBA x C57BL/6

PLP-CST transgenic line - CBA x C57BL/6 x 129Ola

ASA(-/-) mice - 129Ola

3.6 Chemical competent cells

Table 3

Strains	***Genotype***
BL-21	*E. coli* B F^- dcm ompT hsdS(r_B-m_B-) gal
XL1Blue	supE44 hsdR17 recA1 endA1 gyrA46 thi relA1 lac F'[$proAB^+$, $lacl^q$ lacZΔM15 Tn10 (tet^r)]

3.7 Antibodies, their source and dilutions used

Antibodies were used for Western blotting and immunofluorescence microscopy

Table 4

Antibody	***Source***	***Dilution used***
m735 (PSA), mouse monoclonal	Rita Gerardy-Schahn	3 µg/ml – Western, 1:500 – Immunofluorescence
MBP, rabbit monoclonal	Chemicon (Hofheim, Germany)	1:5,000 – Western, 1:200 – Immunofluorescence
Rabbit Fyn Mouse CNPase	Santacruz Biotechnology, USA	1:200 – Western 1:1,000 – Western
NCAM H28 (BSP2) – hybridoma cell culture supernatant	Rita Gerardy-Schahn	1:3 – Western, undiluted – Immunofluorescence
Rat ENCAM	BD Pharmingen, Germany	1:200 – Immunofluorescence
β-actin, mouse monoclonal GFAP, mouse monoclonal Mouse Na^+ Channel (PAN)	Sigma, (Taufkirchen, Germany)	1:4,000 – Western 1:2,000 – Western 1:500 – Immunofluorescence
Rabbit Paranodin	Arthur Butt	1 :1,000 – Immunofluorescence
Rabbit L-MAG	Arthur Butt	1:100 – Immunofluorescence
POD conjugated anti-mouse POD conjugated anti-rabbit Cy3 conjugated goat anti-	Jackson Laboratories, USA	1:5,000 – Western 1:10,000 – Western

rabbit ; Cy2 conjugated anti-rat ; Cy3 conjugated anti-mouse Cy2 conjugated anti-rabbit POD conjugated anti-rat		1:400 – Immunofluorescence 1:200 – Immunofluorescence 1:10,000 – Western
Alexa Fluor 594 anti-rat IgM Alexa Fluor anti-rat 488	Molecular Probes, Germany	1:200 – Immunofluorescence 1:400 – Immunofluorescence

3.8 Molecular Biology Methods

3.8.1 Genotyping

Metallic ear marks were used for labelling mice. One cm of mouse tail was cut and genomic DNA was extracted by incubating the tail with 750µl lysis buffer (10 mM Tris-HCl, 100 mM NaCl, 25 mM EDTA, pH 8, 1% SDS, 100 µg/ml proteinase K) at 56°C, o/n. 250µl of 6M NaCl was added to the lysed samples and incubated at 56°C for 5 min. The samples were centrifuged for 10 minutes at RT and 750µl of supernatant was collected and 500µl of isopropanol was added to the supernatant to precipitate the DNA. Genomic DNA was fished out with an yellow tip and immersed into 70% ethanol and allowed to air dry and was re-suspended in HPLC grade water.

3.8.2 Polymerase chain reaction (PCR)

For genotyping PLP-PST mice, PST sense and PST antisense primers were used. To genotype PLP-CST mice crossed with ASA(-/-) mice, CST1 sense, CST2 antisense, ASA sense, ASA antisense and ASA neo primers were used in one PCR reaction mix. PST sense and PST antisense primers were used to genotype PLP-PST mice.

PCR reaction mix

100-500 ng genomic DNA or 1.5 µl cDNA

2.5 µl of 10x PCR buffer

2.5 µl of 2 mM dNTPs

0.1 µl of 100 pmol/µl primers

5µl of 25 mM $MgCl_2$

1.5 µl of 1 U/µl Taq polymerase (for all PCR reactions) or 0.25 µl Phusion polymerase (MBP PCR). Volume was made up to 25 µl with HPLC grade water.

3.8.2.1 List of primers used for PCR reactions

Table 5

Primers	***Sequence***
ASA sense	5’ TAGGGTGGAAGTTACCCTAGA 3’
ASA antisense	5’ TGACCCAGGCCTTGTTCCCAT 3’
ASA neo	5’ GGAGAGGCTATTCGGCTATGAC 3’
PST sense	5’ CCATGCGCTCAATTAGAAAACG 3’
PST antisense	5’ GCTCTAGATTATTGCTTCATGCACT TTCC 3’
CST1 sense	5’ ATGACTCTGCTGCCAAAGAAGC 3’
CST2 antisense	5’ CCACCTTAGAAAGTCCCTAAGG 3’
MBP sense	5’ GCCTGGATGTGATGGCATCAC 3’
MBP antisense	5’ AGGTGCTTCTGTCCAGCCATAC 3’
β-actin sense	5’ TCCATCATGAAGTGTGACGT 3’
β-actin antisense	5’ GAGCAATGATCTTGATCTTCAT 3’
eEF2 sense	5’ GCCGAGCGTGCCAAGAAAGTAG 3’
eEF2 antisense	5’ AGCCTTGAGCAATGGCTTGCCC 3’
eIF1A sense	5’ TGGACGGTTGGAAGCAATGTGC 3’
eIF1A antisense	5’ TCAAGATGCCACTGTGTGGAGC 3’
eIF4A2 sense	5’ CGTGGGATTGACGTGCAACAAG 3’
eIF4A2 antisense	5’ ATTCAGCAACAGCGAGCACTGC 3’
eIF2 su 3 sense	5’ AACGATAGCAGAAAGGGGCACC 3’
eIF2 su 3 antisense	5’ TGGGGCCGATGTTTGTTCCAAC 3’
eIF4b sense	5’ CAACTGATGGGCTTGGGTGGTG 3’
eIF4b antisense	5’ CCGGAGAAGCGATTTGCTGTGC 3’
TGF-β III receptor sense	5’ ATGGCAGTGACATCCCACCA 3’
TGF-β III receptor antisense	5’ TCCGAAACCAGGAAGAGTCT 3’
SP6	5’ CTAGCATTTAGGTGACACTATAG 3’
T7	5’ TAATACGACTCACTATAGGG 3’

3.8.2.2 Genotyping of PLP-CST and PLP-PST mice

Table 6

Target	**Primers**	**PCR conditions**	**PCR products**
Mouse genomic DNA	CST1 sense, CST2 antisense, ASA sense, ASA antisense, ASA neo	94°C for 5min 94°C for 30 sec 56°C for 30 sec 72°C for 1 min (32 cycles) 72°C for 10 min	CST-transgene -1270 bp ASA wild-type - ~ 480 bp ASA knock-out - ~1100 bp
Mouse genomic DNA	PST sense, PST antisense	94°C for 5min 94°C for 30 sec 56°C for 30 sec 72°C for 1 min (32 cycles) 72°C for 10 min	PST-transgene - ~1100bp

The above PCR products from table 6 were analysed on a 1% agarose gel containing 0.5 µg/ml ethidium bromide.

3.8.2.3 PCR reactions for TGF-β III receptor, β-actin, elongation factors, initiation factors and MBP

Table 7

Target	**Primers**	**PCR conditions**	**PCR product**
cDNA	TGF-β-III sense, TGF-β-III antisense β-actin sense, β-actin antisense	94°C for 5min 94°C for 1min 56°C for 1 min 72°C for 1 min (30 cycles) 72°C for 10 min	TGF-β III receptor - 397 bp β-actin -153 bp

cDNA	eIF1A sense, eIF1A antisense eEF2 sense, eEF2 antisense eIF2 su 3 sense, eIF2 su 3 antisense eIF4A2 sense, eIF4A2 antisense eIF4b sense, eIF4b antisense	94°C for 5min 94°C for 1 min 56°C for 1 min 72°C for 1 min (25 cycles) 72°C for 10 min	eIF1A - 367 bp eEF2 - 276 bp eIF2 su 3 - 402 bp eIF4A2 - 269 bp eIF4b - 424 bp
cDNA	MBP sense, MBP antisense	94°C for 5min 94°C for 1min 60°C for 1 min 72°C for 1 min (32 cycles) 72°C for 10 min	MBP - 2032 bp

PCR reactions for TGF-β III receptor, β-actin, elongation and initiation factors were carried out separately in different reaction tubes. Except for MBP (which was run on a 1% gel), the other PCR products from table 7 were analysed on a 2% agarose gel containing 0.5 µg/ml ethidium bromide.

3.8.3 RT-PCR (Reverse transcription-polymerase chain reaction)

RT was done with RevertAid H minus first strand cDNA synthesis kit (Fermentas Life Sciences, Leon-Rot, Germany). To 5 µg of total RNA from wild-type CBAxBL/6x129Ola mouse, 1 µl of oligo $(dT)_{18}$ primers was added. Volume was made up to 12 µl with RNase-free DEPC-treated water. The mixture was incubated at 70°C for 5 min, chilled on ice and was briefly centrifuged. Four µl of 5x reaction buffer, 1 µl of ribonuclease inhibitor (20 U/µl) and 2 µl of 10 mM dNTP mix was added and the mixture was briefly centrifuged. The reaction mix was incubated at 37°C for 5 min and 1 µl of RevertAid H minus-MuLV reverse transcriptase (200 U/µl) enzyme was added and incubated at 42°C for 60 min. Reverse transcription reaction was stopped by incubating at 70°C for 10 min. PCR reactions for TGF-

β III receptor, elongation factors, initiation factors, β-actin and MBP, were carried out with 1.5 µl of the above synthesized cDNA (Table 7).

3.8.4 Spectrophotometric quantification of nucleic acids

Quantification of DNA/RNA can be done spectrophotometrically by measuring the absorbance. DNA/RNA absorbs light in ultraviolet range (200-400nm) with an absorption peak at 260nm and proteins have an absorption peak at 280nm. Hence, by measuring the absorbance at 260nm and 280nm and calculating the OD_{260}/OD_{280} ratio (Kalckar´s formula) the purity of the nucleic acid sample can be determined. The ideal ratio for a pure DNA or RNA preparation is 1.8 to 2.0; samples contaminated with protein's have a lower value. The concentration of DNA or RNA can be determined by Beer Lambert's law

$$E = \varepsilon c l$$

E = Extinction

ε = extinction coefficient [L mol^{-1} cm^{-1}]

c = concentration of sample [mol L^{-1}]

l = length of light pathway in centimetres [cm]

An OD_{260nm} measurement of 1.0 with l = 1 cm corresponds to approximately

50 µg/ml double stranded DNA

40 µg/ml single stranded DNA or RNA

33 µg/ml single stranded oligonucleotides

3.8.5 Restriction digestion

Restriction enzymes are endonucleases, which recognize specific, often palindromic sequences in double stranded DNA and cleave these sequences by hydrolysis of the phosphodiester bonds in DNA. Three kinds of restriction endonucleases designated Type I, Type II and Type III are currently known.

Of the 3 types, only Type II is used in molecular cloning. Typical Type II restriction enzymes recognize specific DNA sequences that are 4,5,6,8 or more nucleotides in length. The location of cleavage sites within a sequence differs from one enzyme to the other. Some enzymes cleave both strands exactly in the middle of the sequence creating fragments with blunt ends, while others cleave at similar locations which are some base pair's apart on the opposite strands of the DNA creating DNA fragments with single stranded termini (sticky ends). One

unit of restriction enzyme is defined as the amount of enzyme needed to hydrolyze 1µg λDNA at 37°C in one hour.

Restriction digestion of pBluescript SK(-) vector was done with *Eco*32I (*ECOR*V) restriction enzyme to generate blunt ends

Restriction reaction

5 µg DNA [pBluescript SK(-)] vector

2 µl 10x buffer R (10 mM Tris-HCl, pH 8.5, 10 mM $MgCl_2$, 100 mM KCl, 0.1 mg/ml BSA)

1 µl *Eco*32I (*ECOR*V), 10 U/µl, restriction endonuclease

Volume was made up to 20 µl with HPLC grade H_2O

The reaction mix was incubated for 4 hours at 37°C.

3.8.6 Ligation

Ligation is the generation of phosphodiester bonds between neighboring 3' hydroxyl and 5' phosphate ends of double stranded DNA. This reaction is catalyzed by an enzyme, DNA ligase. Typically T4 DNA ligase is used for ligation reactions and it requires ATP as a cofactor, which is hydrolyzed to generate the phosphodiester bonds. The amount of vector and insert ratio for optimal ligation can be calculated with the formula:

X ng insert = [(Y bp insert) x (50 ng vector)] / (total bp in vector)

Ligation reaction of MBP and pBluescript SK(-) vector cut with *Eco*32I (*ECOR*V) was carried out as given below

Ligation reaction of 20 µl volume

Vector-*Eco*32I cut blunt ended pBluescript SK(-)	1 µl
Insert-MBP (3 µg/µl)	15 µg
T4 DNA ligase(1 U/µl)	1 µl
10x ligase buffer	1 µl
HPLC grade H_2O	12 µl

The reaction was carried out at room temperature for 5 hours and the ligation mix was used for transformation into competent *E.coli* cells after the completion of the reaction.

3.8.7 Transformation

Transformation is a process where bacterial cells, (*E. coli*), take up free DNA from solution. Typically, bacterial cells are transformed with the ligated plasmid containing an antibiotic

selection marker gene, by either electroporation or through chemical transformation. During chemical transformation cells are heat shocked, then treated with the ligated plasmid and a high concentration of calcium ions. The calcium ions precipitate the DNA on the surface of the cell, where the DNA is forced into the recipient bacteria. This DNA then replicate by themselves, as extra chromosomal genomes. Transformed cells are selected by growing the cells in antibiotics. Only those cells containing the plasmid with the antibiotic gene are able to live and multiply.

One ng of ligated DNA was mixed with 100 µl of BL-21 competent cells in an eppendorf tube and incubated on ice for 30 min. Heat shock was given for 75 sec at 42°C in a heating block and the tube was cooled for 2 min on ice. 900 µl of pre-warmed LB medium was added to the tube and the transformation mix was shaken for 1 hour at 37°C. 100 µl and 500 µl of bacterial mix were spread on separate LB-ampicillin agar plates, spread previously with X-gal/IPTG mix for blue white screening.

3.8.8 Blue white colony screening

100 µl IPTG/X-gal mix for 1 LB-ampicillin plate
3 µl 1M IPTG
16 µl 40 mg/ml X-Gal
81 µl H_2O
The IPTG/X-Gal mix was spread on an LB-ampicillin plate and allowed to dry before the transformation mix was plated.

3.8.9 Agarose gel electrophoresis

Agarose gels were prepared by boiling agarose in TAE buffer, cooling the solution to 50°C and by adding (0.5 µg/ml) ethidium bromide, an intercalating agent of DNA. The gels were casted on trays with combs and DNA was loaded with (1x) L4 loading buffer and electrophoresis was carried out at 5-10 V/cm. As the DNA is negatively charged it migrates towards the positive anode and is separated based on its molecular weight (mobility is proportional to logarithm of molecular weight). DNA fragments of up to 1 ng concentration can be visualised under UV by exploiting the fluorescent properties of DNA-ethidium bromide complexes and their size is determined by running a DNA marker (λ/*Hind*III and λ/*EcoR*I/*Hind*III from Fermentas) alongside as standard.

3.8.10 Cycle sequencing

Cycle sequencing is a reaction, where, fluorescently-labelled dideoxy nucleotides of 4 different coloured dyes are used to label the products. As a result, the extension of the DNA is interrupted resulting in the formation of products of different lengths. Moreover, the reaction is linear and not exponential, because, only a single primer is used for the reaction. Hence, by loading the reaction mix into an automatic laser sequencer, the sequencer can read the different dyes as they pass the laser at the bottom of the gel, because the different fragments migrate towards the positively-charged pole at different rates, the shorter fragments migrate toward the bottom of the gel faster, so one can read it from bottom to top (5'->3'). The computer then compiles these data into the image of a gel. The colors are then read as bases to produce a chromatogram of the piece of DNA sequenced. The sequence can be taken right from the chromatogram with an extremely high level of accuracy, and the task is completed.

Cycle sequencing reaction was done with ABI PRISM Dye Terminator Cycle Sequencing Ready Reaction kit from ABI (Perkin Elmer) with AmpliTaq DNA Polymerase FS.

PCR reaction mix was prepared as given below:

0.5-0.8 µg	Template plasmid DNA (200 ng-1µg)
2 µl	Big Dye Terminator ready reaction mix
1 µl	Big Dye Sequencing buffer (5x)
3.2 pmol	T7 or SP6 primer

Volume was made up to 10 µl with HPLC grade H_2O

This was followed by a PCR reaction of 25 cycles as below

2 min	96°C Initial denaturation
10 sec	96°C Denaturation
5 sec	50°C Annealing
4 min	60°C Extension

The entire reaction was carried out in a 200 µl eppendorf tube. To precipitate the DNA for sequencing, 2 µl of 3M sodium acetate, pH 5.2 and 50 µl of 95% ethanol (stored at RT) was added to 10 µl of the above reaction mix. The mixture was vortexed briefly and centrifuged for 15 min, 15,000 rpm at RT. Supernatant was discarded and to the pellet, 250 µl of 70% ethanol (stored at RT) was added. The mixture was vortexed briefly and centrifuged for 15 min, 15,000 rpm at RT. After centrifugation, the DNA pellet was dried in a speed vac for 3 min or at RT for 5 min. 25 µl of HiDi Formamide was added to the dried pellet, vortexed and

centrifuged briefly. The DNA was denatured by heating the E-cup at 90°C for 2 min and cooled on ice for 5 min, vortexed and centrifuged briefly. Sequencing was done with ABIprism310 genetic analyzer and the sequencing data was analyzed with ABI Prism sequencing software.

3.8.11 Northern blot analysis

3.8.11.1 Isolation of RNA with TRIzol reagent

All solutions were treated with DEPC water to inactivate RNase activity. Total RNA was isolated from whole brain with TRIzol reagent (Invitrogen, Karlsruhe, Germany). Brain samples were frozen in liquid nitrogen and TRIzol reagent was added to it (1 ml TRIzol per 50-100 mg tissue). The samples were homogenized with a homogenizer (Ultra-turrax, Janke & Kunkel, Staufen, Germany) for 30 sec and incubated at RT for 5 min. 200 µl chloroform per 1 ml TRIzol was added and vortexed for 30 sec and incubated at RT for 3 min. After incubation, the samples were centrifuged at 12,000 x g for 15 min at 4°C. The supernatant was collected, 500 µl of isopropanol per ml of TRIzol was added and vortexed for 30 sec and incubated at RT for 10 min. After incubation, the samples were centrifuged for 10 min at 12,000 x g, 4°C. The supernatant was discarded and the pellet was washed with 1 ml of 75% ethanol (pre-cooled at 4°C) and centrifuged at 12,000 x g for 10 min at 4°C.The pellet was air dried and was re-suspended in DEPC water and incubated at RT for 10 min, followed by incubation at 65°C for 15 min.

3.8.11.2 Northern blotting of RNA

20 µg of total RNA was mixed with corresponding volume of 2x RNA loading dye (MBI Fermentas, Germany). The samples were denatured by heating at 65°C for 10 min, incubated on ice for 5 min (to remove secondary structures) and were separated on a 1% denaturing agarose gel containing 20 mM MOPS, pH 7.0, 5 mM sodium acetate, 1 mM EDTA and 2.2 M formaldehyde. The separated RNA was transferred to a Hybond N^+ nylon membrane (Amersham Pharmacia) with 20x SSC buffer.

3.8.11.3 Preparation of DNA templates

Mouse PST cDNA (1.09 kb) was obtained by restriction digestion of pBluescript vector with *Hind*III/*Xba*1 enzymes. CST coding region was amplified by doing a PCR with CST1 sense and CST2 antisense primers. The products were gel purified with Qiagen gel purification kit and the DNA concentration was estimated by running on an agarose gel with λ *Hind*III marker as standard.

3.8.11.4 Synthesis of [α-^{32}P]-labelled CST/PST probes and detection of CST and PST mRNA

Radiolabelled DNA probes were synthesized in an eppendorf tube by mixing 25 ng of DNA with 5 µl random primers. The volume was made up to 50 µl with double distilled water and was incubated at 95°C for 5 min and at RT for 10 min. 10 µl of labelling buffer (5x), [α-^{32}P]-dCTP and 2 µl of Klenow enzyme (1 U/µl) was added to the above tube and incubated at 37°C for 10 min. Labelled probes were purified with G-50 sephadex column (Amersham Pharmacia) by centrifugation at 3000 rpm for 5 min (RT). 2 µl of the probe was taken in a scintillation vial to measure the incorporated radioactivity. The labelled DNA fragments were denatured at 100°C for 5 min followed by incubation on ice for 5 min.

Membranes were pre-hybridized for 1 hour at 42°C with hybridization solution (0.2 ml hybridization solution per cm^2 of the membrane) containing formamide, 20x SSC, 1 M Tris-HCl, pH 7.5, 50x Denhardt´s reagent, 50% dextran sulfate, in the presence of, 100 µg of heat denatured salmon sperm DNA per ml of hybridization solution. Hybridization was carried out overnight at 42°C with 2 million cpm/ml hybridization solution of [α-^{32}P]-dCTP labelled mouse CST or PST DNA. After hybridization, membranes were washed twice for 10 min at RT with 2x SSC, 0.1% SDS and twice for 20 min at 65°C with 0.2x SSC, 0.1% SDS. After washing, membranes were sealed in plastic bags and exposed to a phosphorimager screen (Fuji/Raytest, Straubenhardt, Germany) for a few hours at RT followed by exposure to an x-ray film at -80°C.

3.8.12 Generation of PLP-CST and PLP-PST transgenic constructs

CST cDNA (1270 bp) was amplified from postnatal day 18 mouse brain by RT-PCR with CST1 sense and CST2 antisense primers. The PCR product was ligated into pCR4-TOPO

(Invitrogen) vector followed by subcloning into the *Eco*RI site of pcDNA3.1-zeo (Invitrogen) vector, resulting in the plasmid pcDNA3.1-zeo-CST (Eckhardt et al., 2002).The plasmid was then cut with *Pme*I restriction enzyme and cloned into the PLP-promoter cassette. PST cDNA (1095 bp) was cloned into the *Pme*I site of the PLP-promoter cassette (Fewou, 2005). The PLP-promoter cassette (a gift from W. Macklin, Cleveland Clinic Foundation, Ohio) is derived from PLP gene sequence. The cassette contains the PLP-promoter, transcription start site, exon 1, intron 1 and 37 bp of exon 2 intact.

3.8.13 Generation of PLP-CST and PLP-PST transgenic mice

Generation of PLP-PST transgenic mice, refer (Fewou, 2005). In order to generate PLP- CST transgenic mice, vector sequences were removed from the pcDNA3.1-zeo-CST plasmid by digesting the DNA with *Not*I and *Apa*I restriction enzymes followed by agarose gel purification. Pronuclear injection into fertilized eggs from F2 C57BL/6×CBA mice was performed at the Karolinska Center for Transgene Technologies (Stockholm, Sweden). Founder mice were identified by Southern blotting of *Sty*I digested genomic tail DNA using a [^{32}P]-labelled CST cDNA probe. Four transgenic founder mice were identified. Two male founder mice with a high transgene copy number were infertile. The other two (female) transgenic founder mice (tg2639 and tg2645) were bred with ASA(-/-) mice. Genotyping of the mice was done by PCR on genomic mouse tail DNA with CST1 sense and CST2 antisense primers.

3.9 Biochemical Methods

3.9.1 Protein precipitation (Wessel and Flügge, 1984)

Protein precipitation was done with a mixture of chloroform:methanol:water. To 100 µl protein solution, taken in an eppendorf tube, 400 µl methanol was added and vortexed for 30 sec and centrifuged for 1 min at 9000 x g (RT). To the above tube, 100 µl of chloroform was added. The tube was then vortexed and centrifuged as above. To the protein containing mix, 300 µl ddH_2O was added and the whole mixture containing water was vortexed for 1 min and centrifuged for 5 min at 9000 x g (RT). Two phases were formed and the protein is normally in the interphase. The upper phase was discarded without the interphase and to the remaining solution, 300 µl methanol was added and vortexed for 1 min and centrifuged at 9000 x g for

10 min (RT). After centrifugation, the supernatant was discarded, the pellet was air dried and was resuspended in Laemelli sample buffer (4% SDS, 0.5% bromophenol blue, 1% β-mercaptoethanol, 0.5% glycerol, 0.5 M Tris-HCl, pH 6.8) for SDS-PAGE or stored at -20°C. (Depending on the initial volume of the protein solution, the entire protocol was scaled up).

3.9.2 Protein quantification

Protein estimation was done with BioRad Dc assay kit. This assay is based on the Lowry assay (Lowry et al., 1951). Five different concentrations (0.125, 0.25, 0.5, 1 and 2 mg/ml) of bovine serum albumin (BSA) were used as a standard for the protein estimation of the sample. The BSA standards were solubilized in the same buffer as the sample. The entire assay was carried out in a 96 well plate in triplicates of the standard, sample and negative control (5 µl/well), pipetted into each well. 20 µl of Dc assay reagent A (20 µl of Dc assay reagent S per ml of reagent A). 200 µl of Dc assay reagent B was added into each well and the plate was incubated in dark for 5 min and then scanned with a BioRad plate reader, at 655nm. Protein concentration of the sample was determined in µg/µl.

3.9.3 Sodium dodecyl sulfate polyacrylamide gel electrophoresis (SDS-PAGE)

Proteins are charged due to the acidic and basic amino acids and in PAGE, the migration depends on the protein charge. In SDS-PAGE, proteins are separated by their molecular mass. Negatively charged SDS molecules bind along the polypeptide chain and confers a negative charge to the polypeptide chain. During electrophoresis, migration distance of the reduced SDS-protein complex is proportional to its molecular mass and not dependent on protein charge. Separating gels of different percentages and stacking gels were prepared as given below.

Reagents for SDS-PAGE separating gel

Total volume: 10 ml

Table 8

Ingredients	***Percentage of Gel***				
	6%	***7.5%***	***10%***	***12.5%***	***15%***
H_2O	5.79 ml	5.42 ml	4.79 ml	4.17 ml	3.54 ml
40% Acrylamide	1.50 ml	1.88 ml	2.50 ml	3.13 ml	3.75 ml
1.5M Tris-HCl, pH 8.8	2.50 ml	2.50 ml	2.50 ml	2.50 ml	2.50 ml
10% SDS	0.10 ml	0.10 ml	0.10 ml	0.10 ml	0.10 ml
10% APS	0.10 ml	0.10ml	0.10 ml	0.10 ml	0.10 ml
TEMED	0.01 ml	0.01 ml	0.01 ml	0.01 ml	0.01 ml

Reagents for 5% SDS-PAGE stacking gel

Table 9

Ingredients	***Volume for 10 ml***
H_2O	6.04 ml
40% Acrylamide	1.25 ml
0.5 M Tris-HCl, pH 6.8	2.50 ml
10% SDS	0.10 ml
10% APS	0.10 ml
TEMED	0.01 ml

50-100 µg of the protein samples to be analyzed from brain or myelin or cell homogenates were denatured by heating in one fourth the volume of 4x Laemmli sample buffer. For detection of NCAM-PSA by Western blotting, the protein samples were denatured at 60°C for 5 min. For detection of other proteins by Western blotting, the protein samples were denatured at 95°C for 5 min. After a brief centrifugation, depending on the molecular weight of the protein analysed, the samples were loaded onto SDS-PAGE of 7.5% or 10% or 12.5% gels, in an apparatus containing running buffer in both chambers. A constant voltage of 80 V was applied to the gel until the loading dye (bromophenol blue) entered the separating gel.

Then the voltage was increased to 120 V until the dye reached the bottom of the gel and proteins were then blotted onto nitrocellulose membranes.

3.9.4 Silver Staining

Silver staining is the most sensitive method for permanent visible staining of proteins in polyacrylamide gels. This sensitivity, however, comes at the expense of high susceptibility to interference from a number of factors. Precise timing, high-quality reagents and cleanliness are essential for reproducible and high-quality results. In silver staining, the gel is impregnated with soluble silver ions and developed by treatment with formaldehyde, which reduces silver ions to form an insoluble brown precipitate of metallic silver. This reduction is promoted by protein.

Fixing solution I

30% ethanol

10% acetic acid

60% ddH_2O

Fixing solution II

30% ethanol

0.5 M sodium acetate

0.2% sodium thiosulfate

100% with ddH_2O

Staining solution

0.1% silver nitrate (from 30% stock)

Developing solution

2.5% sodium carbonate in ddH_2O and 2.5% sodium carbonate in 0.15% of 37% formaldehyde in ddH_2O

Neutralising solution

5% and 1% acetic acid in ddH_2O

Procedure

The gel was transferred to fixing solution I and was left overnight or for a minimum of 20 min and replaced with fixing solution II for 20 min, washed thrice with ddH_2O. The gel was then stained for 20 min with silver nitrate solution and washed once with ddH_2O for 2 min and rinsed with 2.5% sodium carbonate. The gel was developed with sodium carbonate-

formaldehyde mix and the reaction was stopped with 5% acetic acid. The gel was left in 1% acetic acid with 0.05% glycerol. Finally, the gel was placed o/n in water containing 0.05% glycerol mix before drying.

3.9.5 Western Blotting

Mouse brains were homogenised with a homogeniser in TBS buffer, pH 7, with protease inhibitors and 2 mM EDTA. The crude homogenate was lysed with 1% Triton X-100 for 30 min on ice and then centrifuged at 15,000 x g, 4°C, 15 min. Protein estimation was done with the BioRad Dc assay kit and 50-100 µg protein was loaded on an SDS-PAGE of different percentages (7.5-12.5%). The proteins were transferred onto a nitrocellulose membrane (pore size-0.45 µm; Schleicher & Schuell, Dassell, Germany) in a semi-dry blotting apparatus at a constant current of 0.8 mA/cm^2 of membrane. After blotting, the membrane was stained with Ponceau S (Roth, Karlsruhe, Germany) (to ensure the homogeneous transfer of proteins onto the membrane) and washed with TBS buffer. Non specific binding sites were blocked by incubating the membrane with 3% skimmed milk powder in TBS containing 0.05% tween-20 (TBS-T) for 1 hour at RT or o/n at 4°C. After blocking, the membrane was incubated with primary antibody diluted in blocking solution for 1 hour at RT and washed thrice with TBS-T for 10 min each at RT, to remove any unbound antibodies. The membrane was then incubated with corresponding secondary antibody, diluted in blocking solution for 1 hour at RT or o/n at 4°C and washed thrice with TBS-T for 10 min each at RT. Bound antibodies were visualised with ECL system (Amersham Pharmacia) according to the manufacturers protocol or with indigenous ECL system.

3.9.6 Preparation of indigenous ECL solution for detecting peroxidase conjugated secondary antibodies

Solution A: 250 mM luminol (Fluka, 09253) in DMSO (MW; 177.16) i.e., 5 g in 112 ml DMSO solution. This solution was stored as 2 ml aliquots at –80°C.

Solution B: 90 mM coumaric acid (Fluka, 28200) in DMSO (MW: 164.16) i.e., 1 g in 67 ml DMSO solution. This solution was stored as a 1 ml aliquot in eppendorf tubes at -80°C.

Solution C : 1 M Tris, pH 8.5.

For 20 ml: 200 µl of solution A was added to 89 µl of solution B. To this mixture, 2 ml of solution C was added and the volume was made up to 20 ml with ddH_2O.

For detecting the peroxidase conjugated antibody -
6.1 µl of 30% hydrogen peroxide was added to 20 ml of solution C, mixed well and added to the membrane and incubated for 1-5 min depending on the signal intensity of the protein.

3.9.7 Coomassie staining

Table 10

Staining solution	***Wash solution 1***	***Wash solution 2***
1% (w/v) Coomassie blue – 35051	-------	-------
40% (v/v) Methanol	50% (v/v) Methanol	10% (v/v) Methanol
10% (v/v) Acetic acid	10% (v/v) Acetic acid	10% (v/v) Acetic acid
50% (v/v) Water	40% (v/v) Water	80% (v/v) Water

3.9.8 Lipid analysis of total brain and sciatic nerve

Lipids were isolated as described (Van Echten-Deckert, 2000 and Yaghootfam et al., 2005). Total brain or a pair of sciatic nerves were homogenized with a homogenizer (Ultraturrax, Janke & Kunkel, Staufen, Germany) in TBS, pH 7.4 (PLP-CST mice) or in 1:2 chloroform:methanol (PLP-PST mice). The crude homogenate was ultra-centrifuged (Beckmann Coulter) at 50,000 rpm in TLA-110 rotor for 60 min. The supernatant was discarded and the pellet was homogenized with (1:2) chloroform:methanol (v/v). Lipids were extracted at 56°C for 4 h with continuous stirring. The extract was filtered through a glass fibre wading to remove insoluble material and the filtrate was dried under N_2 gas at 54°C. The dried lipid was re-extracted with 1:1 chloroform/methanol (v/v), filtered and dried as above. After extraction, the samples were treated with 100 mM NaOH in methanol for 2 hours at 37°C, followed by reverse phase chromatography with RP18 column. The lipid was finally re-suspended in 1:1 chloroform:methanol (v/v).
Lipid samples were loaded on a HPTLC silica gel 60 plates (Merck, Darmstadt, Germany) using an automatic TLC sampler (CAMAG, Berlin, Germany) and developed by thin layer chromatography (TLC) using chloroform:methanol:water (60:27:4, v/v/v, to resolve sulfatide and galactocerebroside lipds extracted from PLP-CST mice) or (55:45:10, v/v/v, to resolve the gangliosides from PLP-PST mice) as developing solvents. Lipids were visualised by

spraying cupric sulphate in aqueous phosphoric acid on the TLC plates, followed by incubation at 180°C for 7 min or for 10 min (to visualise gangliosides) (Yao J.K et al., 1985). Stained plates were scanned and lipids were quantified by densitometry using AIDA software (Raytest, Straubenhardt, Germany).

3.9.9 Isolation and purification of PAPS synthetase

PAPS synthetase enzyme was cloned into an expression vector. The bacterial culture grown overnight was pelleted down and lysed with 10 ml of lysis buffer containing 10 mM imidazole by incubating on ice for 1 hour. After incubation, the lysate was freeze-thawed thrice in liquid N_2-RT, and then by thawing under warm running water. The lysate was then incubated on ice for 30 min followed by ultracentrifugation at 25,000 rpm for 30 min at 4°C.
A Hi trap Ni^{2+}chelating column was washed with 5 ml of ddH_2O, 1 ml 0.1 M nickel sulphate and 5 ml of ddH_2O. The column was equilibrated with 5 ml of binding buffer at a flow rate of 100 ml/h. After equilibration, the supernatant was loaded onto the column.
The flow through from the column was collected and was added onto the column again. The column was washed with 10 ml of binding buffer at a flow rate of 50-100 ml/h. The protein was eluted with 5 ml of elution buffer. The eluates were collected as 500 µl fractions and O.D at 280nm was measured spectrophotometrically. The fractions containing the protein were pooled and were concentrated by adding equal volume of 10 mM Tris-HCl (pH 7)-50% glycerol mix and centrifuging with Centricon spin columns at 4°C as per the manufacturers instructions.

3.9.10 [^{35}S]-PAPS-synthesis

[^{35}S]-labelled 3'-phosphoadenosine-5'-phosphosulfate ([^{35}S]-PAPS) was synthesized using recombinant murine PAPS synthetase and [^{35}S]-sulfate in a reaction mixture containing reaction buffer (150 mM Tris-HCl, pH 8.0, 50 mM KCl, 15 mM $MgCl_2$, 3 mM EDTA, 45 mM DTT), 200 mM ATP, 3.25 µCi [^{35}S]-Na_2SO_4, 0.5 U/µl pyrophosphatase and murine PAPS synthetase.
PAPS reaction
50 µg PAPS synthetase
15 µl reaction buffer
1.3 µl [^{35}S]-Na_2SO_4

3.2 µl pyrophosphatase

2 µl ATP

Volume made up to 100µl with ddH_2O

The reaction was carried out at 37°C for 3 hours and stopped by incubating the reaction mix at 95°C for 5 min, followed by centrifugation at 14,000 x g for 5 min at RT. The radiolabelled PAPS was loaded on a PEI TLC plate (Merck, Germany). [^{35}S]-labelled sulfate was loaded as a control. The plate was developed with 0.9 M LiCl and visualised with a phosphorimager screen. The incorporation of radiolabel was calculated with a scintillation counter.

3.9.11 Cerebroside Sulfotransferase Assay

Whole brain from PLP-CST transgenic and wild-type mice were dissected and briefly homogenized in TBS containing 100 mM PMSF and 20 µg/ml aprotinin. The homogenates were adjusted to a protein concentration of 10 mg/ml. Initially, GalC (4 mg/ml) and 1% Triton X-100 were dried in an eppendorf tube. The assay was started by addition of 10 µl of the homogenate to 40 µl reaction mixture containing 100 mM Tris-HCl (pH 7.0), 20 mM $MgCl_2$, 2.5 mM ATP and 50 µM [^{35}S]-PAPS (~3.7 MBq/µmol) and incubation at 37°C for 2 hours. After incubation, the reaction was stopped by adding 1 ml of chloroform:methanol (2:1, v/v) and 200µl of 150mM NaCl. The mixture was vortexed and centrifuged at 14,000 x g for 5 min at RT. The organic phase was collected and was washed once with methanol:150 mM NaCl:chloroform (48:47:3, v/v/v) and dried in a speed vac concentrator (Savant). The dried samples were re-suspended in 20 µl chloroform:methanol (2:1, v/v), loaded on a silica gel 60 HPTLC plate (Merck, Germany) and developed with chloroform:methanol:H_2O (65:25:4, v/v/v) as solvent system. The radioactive sulfatide was visualised with a phosphoimager screen (Raytest, Straubenhardt, Germany) and quantified using AIDA software (Raytest). For quantification, the AIDA values obtained with AIDA software were subtracted from the background and this value, AIDA value-background, was then expressed as arbitrary units for each of the sample. These arbitrary units were then used as a measure to express the CST activity of each sample.

3.9.12 Myelin preparation

All solutions used for the preparation contained 1 mM PMSF, 20 µg/ml aprotinin as protease inhibitors and the entire preparation was carried out at 4°C. All centrifuge tubes and rotors

were pre-cooled. The principle of the method relies on the low density of myelin compared to other cellular membranes due to its high lipid content. Hence, myelin can be isolated as a band between 5% and 30% sucrose. The contaminating axonal membrane (axolemma) can be removed by several osmotic shocks and sucrose gradient.

Myelin was isolated from forebrains of 2-month-old transgenic and wild-type mice, at different time points as described (Norton and Poduslo, 1973). Briefly, brains were homogenised in 8 ml 10.5% (w/v) sucrose-water using an Ultra-turrax homogenizer and centrifuged at 17,000 x g for 45 min at 4°C. The supernatant was discarded and the pellet was re-suspended in 9 ml 30% (w/v) sucrose-water and transferred to a 12 ml ultracentrifuge tube. The myelin-30% sucrose solution was overlaid with 3 ml 5% (w/v) sucrose-water and centrifuged at 68,000 x g for 50 min at 4°C. Myelin was recovered carefully from the 30% / 5% inter-phase into a new tube and was subjected to hypo-osmotic shock by washing twice with water and centrifugation at 68,000 x g for 50 min at 4°C, followed by a second sucrose gradient (30%-5%) and centrifugation at 68,000 x g for 50 min at 4°C. The purified myelin was again washed twice with water and was re-suspended in water and stored in aliquots at -80°C.

In order to determine the total amount of myelin in the brain, the purified myelin was lyophilized and the dry weight was determined. For protein assays and Western blotting, myelin samples were solubilized in 1% SDS. Protein concentrations were determined using the BioRad DC protein assay (BioRad, München, Germany).

3.9.13 Preparation of detergent resistant membrane fractions

Detergent (Triton X-100) resistant myelin membranes (DRM) were isolated as described (Krämer et al., 1999). Briefly, myelin (500 µg protein) of total brain was solubilized in TNE (10 mM Tris-HCl, pH 7.4, 150 mM NaCl, pH 7.4, 5 mM EDTA, 1 mM PMSF) with 2 % Triton X-100. The extract was incubated on ice for 30 min with vortexing every 5 min. One volume of 80% sucrose (in TNE) was added, overlaid with a step gradient of 30% and 5% sucrose (in TNE). The sucrose gradient was centrifuged at 35,000 rpm with a Beckman SW41 rotor for 16 h at 4°C. One ml fractions of the sucrose gradient were recovered from the top of the gradient.

3.10 Cell Culture

3.10.1 Preparation of mixed glial cell culture from brain

Newborn mice were genotyped and cultures from transgenic and wild-type mice were prepared separately**.** Mixed cultures were prepared from the forebrains of postnatal day 1 or 2 mice. The cerebral hemispheres were removed and transferred to cold Hank's balanced salt solution (HBSS) and were cut into small pieces. Finely cut tissue was dissociated in 1% trypsin (Sigma) for 12 min at room temperature. The tissue homogenate was mixed with 7 ml HBSS (Sigma) and centrifuged at 600 x g for 10 min at 4°C. The supernatant was removed and the pellet was further dissociated with addition of 0.05% DNase (Sigma, bovine pancreas) solution. Flamed Pasteur pipettes (first with a large (1 mm), then with a medium (0.5 mm) and finally with a small opening) were used, to pipette repeatedly, to remove any clumps. The dissociated cells were washed with HBSS as describe above. The pellet was re-suspended in DMEM containing 10% horse serum, 2 mM Glutamine, 100 U/ml penicillin and 100 U/ml streptomycin. Finally the cells were seeded in poly-L-lysine (sigma, MW >300,000) coated tissue culture flask and maintained in the same medium (DMEM + 10% horse serum) described above for 8-10 days in a humidified incubator at 37°C, in the presence of 5% CO_2.

3.10.2 Preparation of primary oligodendrocyte cell culture

Primary oligodendrocyte cultures are prepared from confluent glial cultures. After 8 to 10 days, when glial cell culture reached confluence, microglial cells were dislodged by tapping the culture flask 3-4 times and the medium was removed and the flask was washed once with 10 ml cold HBSS, followed by addition of fresh cold medium (DMEM containing 5% horse serum). Oligodendrocyte precursor cells grown on top of the astrocytes monolayer were shaken off by harsh shaking for 20-30 sec. The medium was collected and the cells were centrifuged at 600 x g for 5 min at RT. The supernatant was removed and the pellet was re-suspended in DMEM containing 5% horse serum. The cells were seeded on a Petri dish for 30 min, to allow the remaining microglia to attach to the dish. The non-adherent oligodendrocytes containing medium was collected and centrifuged at 600 x g for 5 min at RT. The pellet was re-suspended in SATO medium (DMEM supplemented with 10 µg/ml insulin, 0.1 mM putrescine, 0.2 µM progesterone, 0.5 µM triiodothyronine, 0.22 µM sodium selenite, 0.1 mg/ml apo-transferrin, 520 nM L-thyroxine, 25 µg/ml gentamycin, 2 mM L-

glutamine, 100 µg/ml penicillin, 100µg/ml streptomycin) with 1% horse serum and the cells were seeded on poly-L-lysine coated glass cover slips at a density of 3-4×10^4 cells/12 mm cover slip and grown in SATO medium.

3.10.3 Immunofluorescence of primary oligodendrocyte culture

Cover slips containing primary oligodendrocytes were collected at different days (day1 to day 4), were fixed in 4% paraformaldehyde in PBS for 10 min at room temperature. Non-specific binding sites were blocked for 30 min in 0.2% gelatin in PBS and cells were permeabilized with 0.3% Triton X-100. Cells were incubated with rabbit anti-MBP antibody (1:200), diluted in 0.2% gelatin in PBS. In some experiments, cells were additionally stained for PSA using mouse monoclonal antibody 735 (1:50 of 1 mg/ml) ((Frosch et al., 1985), rabbit anti L-MAG (1:100) (kind gift from, A. Butt), rat monoclonal antibody H28 NCAM (hybridoma cell culture supernatant) and rat monoclonal IgM ENCAM (1:100). Primary antibodies were detected with anti-rat IgM-Alexa Fluor 594 (1:200), anti-rabbit Ig- Alexa Fluor 488 (1:400) (Molecular probes), anti-rabbit Ig-Cy2 (1:200), anti-rabbit Ig-Cy3 (1:400), anti-mouse Ig-Cy3 (1:400) and anti-rat Ig-Cy2 (1:400) (Jackson Immunoresearch / Dianova, Hamburg, Germany) in blocking solution. Nuclei were stained with DAPI. Specimens were mounted in Kaiser's gelatin and analyzed with an Axiovert 100M microscope (Carl Zeiss, Jena, Germany).

3.11 Immunohistochemistry

3.11.1 Immunofluorescence of brain and optic nerve cryosections

Whole brains and eye with optic nerves of PLP-PST transgenic and wild-type mice were removed, immediately frozen in cold isopentane and stored at -80°C. Coronal or sagittal cryosections were cut at 10 µm thickness on a cryostat at -20°C by mounting the tissue with Tissue-Tek OCT (Sakura Finetek, Europe) and post fixed in 4% paraformaldehyde in PBS for 10 min at RT. Cryosections were stored with desiccant at -80°C. Sections were permeabilized with 0.3% Triton X-100 and non-specific binding sites were blocked with 1% BSA, 5% FCS, in PBS for 1 hour at RT. PSA and MBP were stained with antibodies 735 (Frosch et al., 1985; mouse IgG; gift of Rita Gerardy-Schahn, Medizinische Hochschule Hannover, Germany) (1:500) and rabbit MBP antiserum (Chemicon, Hofheim, Germany) (1:200) in blocking solution. Primary antibodies were visualized with anti-mouse Ig-Cy2 (1:200) and anti-rabbit

Ig-Cy3 (1:300) conjugate in blocking solution. Nuclei were counter stained with DAPI. Sections were mounted in Kaiser's gelatin (Merck, Darmstadt, Germany) and examined with a Zeiss Axiovert fluorescence inverted microscope attached to an Axiocam camera. Photographs were taken with the Axiovision program (Carl Zeiss, Jena, Germany).

3.11.2 Cryoprotection of brain tissue

Mice were perfused with 5 ml PBS followed by 50 ml 4% PFA-PBS. The brains are dissected out from the animal and post fixed o/n in 4% PFA, followed by incubation in 5% sucrose-PBS for 1 hour, 15% sucrose-PBS for 5 hours (or until the brain sinks to the bottom), 20% sucrose, o/n. The tissue was then removed and immersed into cold isopentane kept on dry ice for 5 sec and put into a pre-cooled tube and stored at -80°C until further use.

3.11.3 In situ Hybridisation

In situ hybridisation was performed either on paraffin sections or on cryosections (10 µm thickness). For cryosections, total brain was dissected from mice and was immersed into cold isopentane, kept on dry ice, before transferring the tissue to -80°C.

3.11.3.1 Preparation of probe

cRNA probes for MAG was synthesised from cDNA (1997 bp) cloned into pCR Blunt II TOPO vector (clone ID IRAM p995E019Q obtained from RZPD, Berlin, Germany). MBP cRNA probes were prepared from mouse brain RNA, by reverse transcribing the RNA and amplifying the cDNA with MBP sense and antisense primers. The above MBP PCR product (2032 bp) was run on a 1% agarose gel and the band corresponding to the size of MBP was cut and purified with Qiagen gel purification kit, according to the instruction of the manufacturer and was cloned into pBluescript SK(-) vector (Stratagene) by blunt end ligation with *Eco*32I. Positive colonies were selected and plasmid DNA was isolated with Qiagen plasmid purification kit. MAG/MBP antisense and sense probes were transcribed with T7 or SP6 RNA polymerase and digoxigenin-RNA labelling kit according to the instruction of the manufacturer (Roche Molecular Diagnostics, Mannheim, Germany).

1 µg linearised plasmid

2 µl Digoxigenin-RNA labelling mix

2µl 10x Transcription buffer

2 µl RNA Polymerase (T7 or SP6)

The volume is made up to 20 µl with DEPC H_2O

The reaction mix was mixed, centrifuged briefly and incubated for 3 hours at 37°C. Template DNA was removed with 2 U RNase free DNaseI (10 U/µl, Roche, Germany) and incubation at 37°C for 15 min. After incubation, 0.8 µl of 0.5 M RNase free EDTA and 1.2 µl DEPC water was added to stop the reaction. $1/10^{th}$ volume of 3 M sodium acetate and 2 volume cold 100% ethanol was added to the cRNA's and precipitated o/n at -80°C, followed by centrifugation at 15,000 rpm, 60 min, 4°C. The pellet was washed once with cold 70% ethanol, air-dried and re-suspended in 24 µl DEPC H_2O.

3.11.3.2 Determination of cRNA probe dilution

MBP, MAG-sense and antisense cRNA probes were serially diluted (1:20, 1:200, 1:2,000, 1:20,000 and 1:200,000) in DEPC treated water. A cRNA probe whose concentration was already determined was used as a control. 1 µl from each of the above dilutions from MAG, MBP cRNA and 1 µl of control cRNA was spotted onto a Hybond N^+ nylon membrane. The membrane was baked for 30 min at 120°C and washed for 1 min with washing buffer and incubated for 30 min with blocking solution. The membrane was then incubated for 30 min with anti-digoxigenin antibody (1:10,000) diluted in blocking solution, washed twice for 15 min each with washing buffer to remove any unbound antibody and then incubated for 2 min in AP buffer. The membrane was developed o/n with NBT/BCIP in AP buffer.The dilutions of the digioxigenin labelled cRNA's were determined visually by comparing the signal intensity of the different dilutions with the control cRNA.

3.11.3.3 Preparation of tissue

In situ hybridisation was carried out as described by Baader et al. (1998). Paraffin sections were dehydrated by immersing in xylol thrice for 10 minutes each followed by immersion in 100% propanol, thrice, 5 min each. The sections were rehydrated by immersing in 96% propanol, 90% propanol and in 75% propanol once, 5 min each and then in 50% propanol for 2 min and washed for 5 min once with PBS-DEPC. The sections were fixed with 4% PFA for 90 min (cryosections were thawed at room temperature for 30 min before fixation). After fixation, the slides were washed twice with PBS-DEPC for 5 min. The sections were permeabilized with Proteinase K for 4 min, followed by washing for 5 min once with PBS-

DEPC. A second permeabilization with 0.25% Triton X-100 was performed for 4 min followed by washing 3 times with PBS-DEPC. The sections were incubated in 0.2 M HCl for 8 min, in 0.1 M TEA for 10 min and then in 2x SSC at 50°C for 10 min.

3.11.3.4 Hybridization

Hybridization was performed with digoxigenin-labelled sense and antisense cRNA riboprobes for MAG and MBP in hybridization buffer (50% formamide, 1x Denhardt's solution, 0.1% SDS, 0.25 mg/ml ssDNA, 10% dextran sulphate and 10% hybridization salt solution (3 M NaCl, 0.1 M PIPES, 0.1 M EDTA) and 4 M DTT. The digoxigenin-labelled cRNA's were diluted in 1x SSC-DEPC

Dilutions of digoxigenin-labelled cRNA's

MBP sense-1: 200	MAG sense-1: 200
MBP antisense-1: 600	MAG antisense-1: 200

The probes were heated for 5 min at 80°C, cooled on ice for 5 min and incubated with the sections o/n at 70°C in a humid chamber (the sections containing the probe were covered with GeneFrame (Abgene, Surrey, UK)). After incubation, to remove any unbound and non-specific probes, the sections were washed with 2x SSC, 5min, 60°C; 2x SSC, 30 min, 60°C; 50% formamide in 1x SSC, 20 min, 60°C; 0.1x SSC, 45 min, 70°C.

3.11.3.5 Detection

The sections were incubated with MAB buffer (100 mM Maleic acid, pH 7.5; 150 mM NaCl) for 5 min at RT. Non specific binding sites were blocked with 10% blocking reagent (Roche Diagnostic GmbH, Germany) in MAB buffer for 1 hour at RT and incubated o/n with anti-digoxigenin alkaline phosphatase (AP) Fab-Fragment antibody (1:5,000 dilution, Roche Diagnostic GmbH, Germany) at 4°C in a humid chamber. Excess antibody was removed by washing with MAB buffer, five times, 1 hour each and then with AP buffer (100 mM Tris-HCl, pH 9.5; 100 mM NaCl, 50 mM $MgCl_2$) for 5 min, RT. Detection was done by incubating in the dark with 200 µl NBT/BCIP (Roche Diagnostic GmbH, Germany)/10 ml AP buffer at RT. For MBP and MAG mRNA detection, incubation was done for 5 hours and 16 hours, respectively.

Stained sections were washed with ddH_2O and mounted using Kaiser's gelatin. Number of positive cells from wild-type and PLP-PST transgenic mice were counted and difference of means was tested with Student's t- test.

3.12 Apoptosis assay (TUNEL assay)

Parasagittal cryosections of brains from 14-day-old transgenic PLP-PST and wild-type mice were used for performing an apoptosis assay. The assay was carried out with BrdUTP-FragEL^{TM} DNA Fragmentation Detection kit (Merck Biosciences, Darmstadt, Germany), as per the manufacturers instruction. This assay is based on the principle that TdT binds to the free 3'-OH group of fragmented DNA generated in apoptotic cells and catalyzes the addition of biotin labelled and unlabelled deoxynucleotides. Biotinylated nucleotides are detected using a streptavidin-horseradish peroxidase conjugate and addition of diaminobenzidine (DAB) results in the formation of an insoluble coloured substrate at the site of DNA fragmentation. The cryosections were fixed in 4% PFA and permeabilized with 20 µg/ml proteinase K. Endogenous peroxidases were inactivated with 30% H_2O_2 diluted in methanol. The labelling reaction was carried out with BrdU labelled dUTPs and TdT enzyme. The enzymatic reaction was detected using anti BrdU-biotin/streptavidin conjugate and DAB as substrate.

3.13 Preparation and immunofluorescence staining of teased sciatic nerve fibres

PLP-CST mice were sacrificed and sciatic nerves were collected from the hind limbs and transferred to cold PBS on ice. The sciatic nerve was transferred to a super frost glass slide and with a very fine forceps one end of the nerve was held and single nerve fibres (teased fibres) were obtained by pulling the other end of the sciatic nerve with another fine forceps. The teased fibres were air dried overnight at room temperature. After drying, the slides were used immediately for immunostaining or stored at -80°C until further use.

The slides were thawed at room temperature (if stored at –80°C) and bordered with PAPPEN. The teased fibres were fixed by adding ice-cold acetone for 10 min at RT and washed twice with PBS for 10 min each at RT. The fibres were permeabilized with 0.5% Triton X-100 and washed thrice with PBS, 10 min each at RT. Non specific binding sites were blocked with 5% FCS/1% BSA in PBS for 30 min at RT. Na^+ channel and paranodin stainings were done with mouse anti-sodium channel PAN and rabbit anti-paranodin antibodies in blocking solution for

1 hour at RT. Unbound primary antibodies were washed thrice with PBS, 10 min each (RT). Primary antibodies were detected with anti-mouse Ig-Cy2 and anti-rabbit Ig-Cy3 antibodies. Unbound secondary antibodies were washed twice with PBS, 10 min each (RT). Nuclear staining was done by incubating the preparation for 1 min at RT with PBS-DAPI (1:500) (Sigma). The stained fibres were mounted using 50% glycerol in 1x PBS and Kaiser‘s gelatin bordering the cover slips.

3.14 Rotarod assay

Rotarod assay is a motor activity analysis, which tests for balance and co-ordination in mice. The mice are placed on a rotating rod and the cumulative falls/minute or the time the mouse remained on the rod is calculated. The assay was done as described (Kuhn et al., 1995) with modifications. The mice were acclimatized with the rotarod for 3 days by placing them on the rotating rod (3 rpm) for 10 sec. On the fourth day, mice were tested for 1 min at 3 rpm [5-11 months old mice; number of mice tested - 8 tg/ASA(-/-) and 8 ASA(-/-)] or 1.3 rpm [21-24 months old mice; number of mice tested - 10 tg/ASA(-/-), 8 ASA(-/-), 10 tg (ASA(+/-), 6 wt/ASA(+/-)] and the number of falls / min was recorded. The cumulative number of falls per min was calculated and differences of means were tested for statistical significance using Student’s t-test.

3.15 Electrophysiological investigations

Electrophysiological investigations were performed by Dr. Carsten Wessig (University of Würzburg) as described previously (Zielasek et al., 1996). Motor nerve conduction of sciatic nerves and EMG of intrinsic foot muscles were studied in anaesthesia. In brief, CMAP was recorded with two needle electrodes in the foot muscles after distal stimulation of the tibial nerve at the ankle and proximal stimulation of the sciatic nerve at the sciatic notch. EMG of foot muscles was assessed for spontaneous activity. Statistical analysis was performed using Student's t-test.

3.16 Preparation of avertin (anaesthetic)

40x stock of avertin -1 g, 2, 2, 2-tribromoethanol (Fluka) in 1 ml tertiary amyl alcohol (Fluka). Dilute to 2.5% avertin (100 µl 40x stock + 3.9 ml 0.9 % NaCl).

3.17 Perfusion of mice

Mice were anaesthetised by injecting intra-peritoneally with 700-800 µl of 2.5% avertin solution. The abdominal region of mice was cut in the form of a 'T' from middle abdomen to cervix and at the caudal edges to both sides. The peritoneum below the lower thoracic aperture, diaphragm and thoracic cage were opened. Mice were then perfused by cutting the right atrium and then by inserting a sharp needle (26G X ½'') into the left ventricle, first with warm (37°C) 100 mM phosphate buffer [100mM potassium dihydrogen phosphate (K_2HPO_4) and 100mM disodium hydrogen phosophate (Na_2HPO_4)] for 15 min and then with warm (37°C) 6% glutaraldehyde in 100 mM phosphate buffer for 30 min. The fixed animals were post fixed in 3% glutaraldeyde in 100 mM phosphate buffer and stored at 4°C until further use.

3.18 Electron microscopy and alcian blue staining

Electron microscopy and alcian blue stainings were performed by Prof. Renate Lüllmann-Rauch & Kerstin Khalaj Hedayati (University of Kiel). 7-months and 18-months-old PLP-CST mice were anaesthetised and perfused intracardially with 6% glutaraldehyde or 25% Bouin's solution. Alcian blue staining of vibratome sections, toluidine blue staining of semi-thin sections and electron microscopy of ultra-thin sections were done as described recently (Wittke et al., 2004).

4. Results

4.1 Analysis of PLP-PST transgenic mice

As the oligodendrocytes undergo differentiation, the expression of PST is downregulated in adult mice, resulting in the downregulation of polysialylated NCAM. In order to understand how PSA downregulation is important for oligodendrocyte differentiation and myelin formation, transgenic mice was generated by overexpressing PST under the control of PLP promoter, so that these mice sustain polysialylation and do not downregulate PSA on NCAM in oligodendrocytes.

4.1.1 Generation of PLP-PST transgenic mice

The transgenic construct was generated by ligating the 1.08 kb murine PST cDNA into the *Pme*I site of the PLP promoter cassette (gift from Dr.Wendy Macklin). The PLP promoter cassette consists of the 5'-flanking region containing the PLP promoter, first exon, first intron and the splice acceptor site of exon 2 of the mouse PLP gene. The ATG start codon in the cassette was mutated; so that, translation would take place from the start codon of the cDNA construct (Fig. 4A). Several transgenic mice were generated and identified by Southern blotting of mouse tail genomic DNA which was digested with *Acc*I restriction enzyme. PST cDNA was used as a probe to identify the transgene. Of the several transgenic mice identified, two transgenic mice lines, tg281 and tg246 were established and maintained on a mixed C57BL/6×CBA genetic background. tg246 line carried a higher copy number of the transgene in their genome when compared to the tg281 line. Generation and identification of the transgenic mice by southern blotting were done by Dr. Simon Fewou (Fewou, 2005).

4.1.2 Expression level of PST mRNA

The expression level of both endogenous and transgenic PST mRNA was investigated by performing a Northern blot analysis (Fig. 4B). Total RNA from transgenic and wild-type litter mates, postnatal day 1 (P1) and 7-months-old mice, was isolated, blotted onto a Hybond N^+ nylon membrane and detected with [α-^{32}P]-dCTP labelled PST specific cDNA probe. The transgene mRNA expression was upregulated in the transgenic animals between P1 and 7-months and the endogenous mRNA expression was downregulated in the wild-type animals. Transgene expression in the tg246 line was higher than the tg281 line. To get a signal of the endogenous PST mRNA in adult wild-type and transgenic animals, the membrane was

overexposed. As a result of this overexposure, the endogenous PST mRNA signal in the 7-months-old mice from tg246 line is not clearly visible.

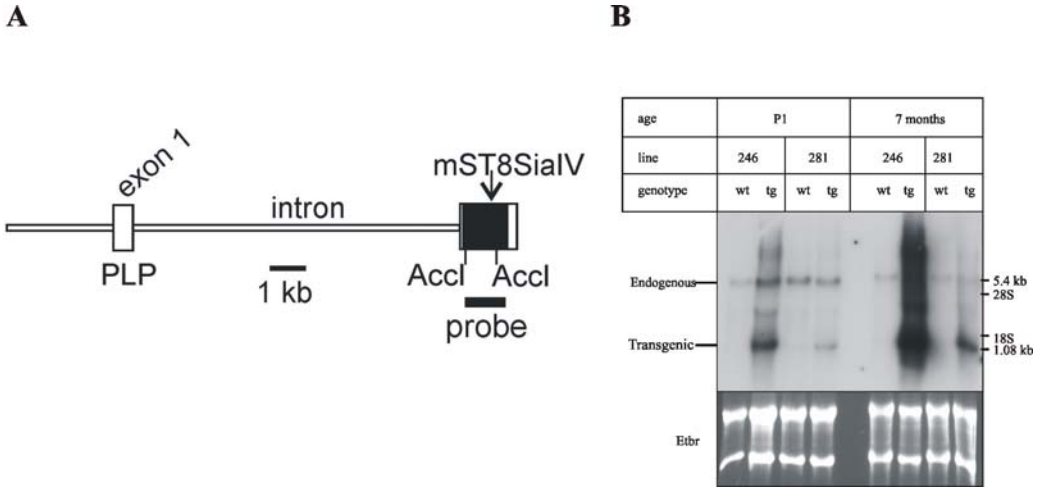

Figure 4: PLP-PST transgenic construct and Northern Blot analysis of PST mRNA expression. (A) Represents a schematic diagram of the PLP-PST transgenic construct (Fewou, 2005). (B) PST mRNA expression of postnatal day 1 (P1) and 7-months-old wt and tg mice from lines, tg246 and tg281, were analysed by Northern blot analysis. 10 µg/lane of total RNA from brain was separated on an agarose-formaldehyde gel and transferred to a Hybond N^+ nylon membrane and detected with PST specific probe. The wild-type and transgenic PST mRNA were detected and their molecular weights (transgene - 1.08 kb; endogenous - 5.4 kb) are indicated in the figure. 7-months-old mice had a stronger transgene expression than 1-day-old mice. Transgene expression in tg246 line was higher than the tg281 line. Ethidium bromide staining was used to control for equal loading of lanes.

4.1.3 PSA is expressed in the white matter of PST transgenic mice

PSA expression in 4-months-old adult transgenic mice was examined by immunofluorescence staining of sagittal and coronal cryosections of brain and optic nerve, respectively. Double staining of cryosections was carried out with MBP and PSA antibodies. In the brain of wild-type mice, PSA expression was restricted to the subventricular zone around the lateral ventricles and no expression was detected in the white matter regions of corpus callosum (Fig. 5A), cerebellum [Fig. 6A (b)] or optic nerve (Fig. 7A). In contrast, in the transgenic mice, PSA was strongly expressed in the white matter tracts of corpus callosum (Fig. 5E), cerebellum [Fig. 6A (e)] and optic nerve (Fig. 7E, I). Double staining with PSA and MBP antibodies showed co-localization of PSA with MBP indicating the presence of PSA in myelin [Fig. 6A (f)]. Higher magnification of microscopic pictures of cerebellum, indicated only partial co-localization of PSA with MBP [Fig. 6B(c)]. The wild-type animals showed no co-localization of PSA with MBP [Fig. 6A (c) and 7D].

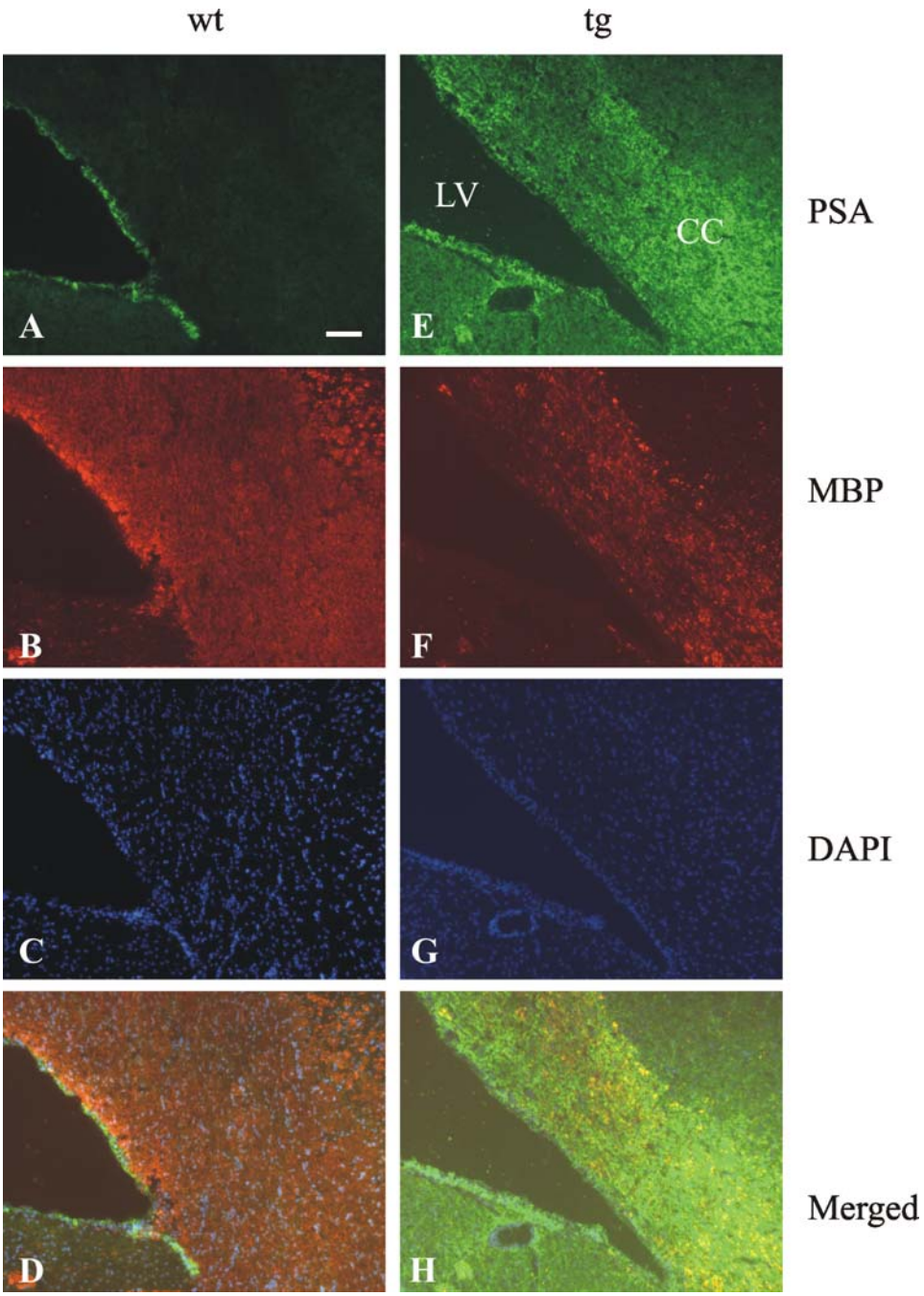

Figure 5: Immunofluorescence staining of parasagittal brain cryosections from PLP-PST mice. Parasagittal cryosections of brain from 4-months-old wt and tg mice were prepared and immunofluorescence double staining with PSA and MBP antibodies was carried out. (A, B, C & D) are stainings of wt brain and (E, F, G & H) are of tg brain. Nuclear staining was done with DAPI (C & G). In the tg brain LV-lateral ventricle and CC-corpus callosum, stained strongly for PSA when compared to the wt mice, where staining was restricted to the subventricular zone with no staining in corpus callosum. (D & H) merged pictures of PSA and MBP stainings. Scale bar 100µm (A-H).

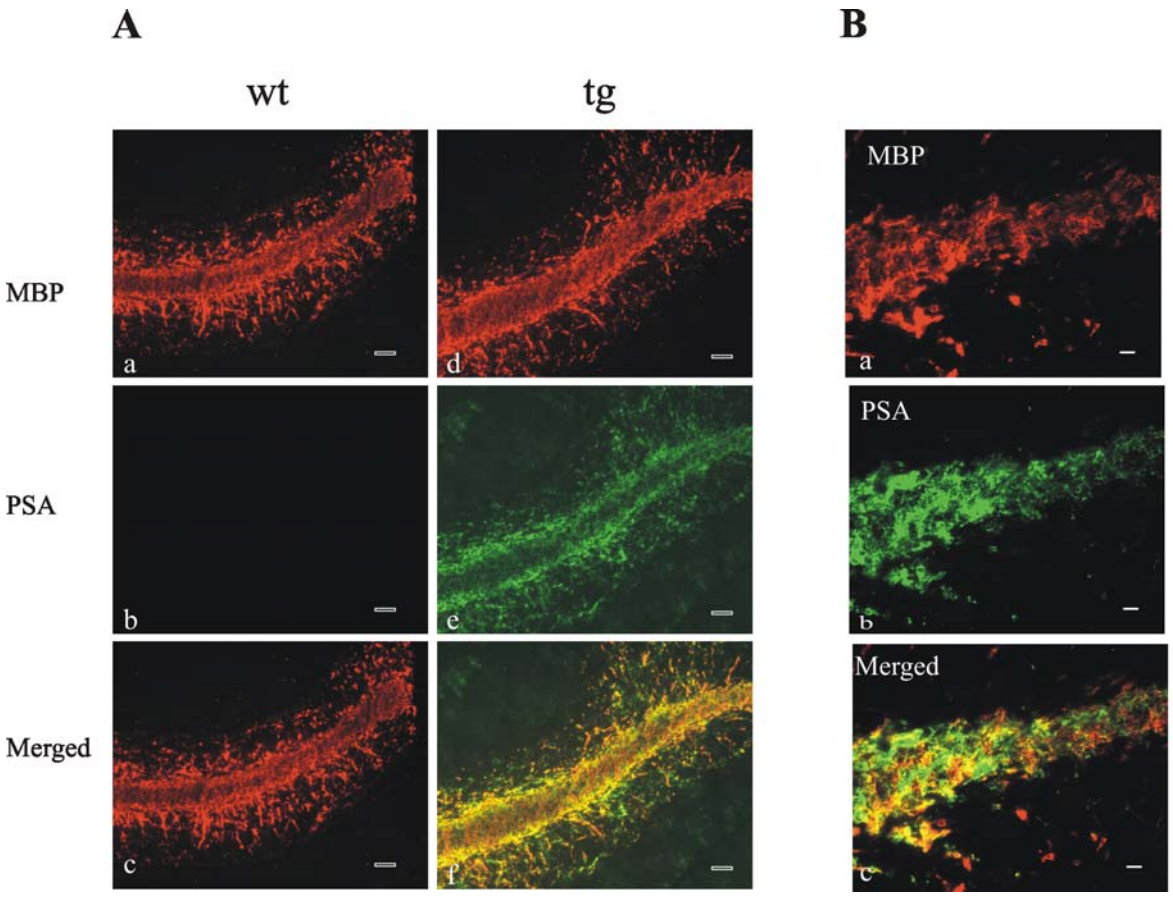

Figure 6: PSA expression in cerebellum of PLP-PST mice. Parasagittal cryosections of brain from 4-months-old tg and wt mice were cut and stained for PSA and MBP. (A) Lower magnification of the cerebellar tracts from wt (a, b & c) and tg (d, e & f) mice for MBP (a & d); PSA (b & e) and merged (c & f) stainings. (B) Higher magnification pictures of cerebellum from transgenic mice stained for MBP (a), PSA (b) and merged (c) taken with an Axiovert mcroscope, showing partial co-localization of PSA and MBP in cerebellum. Scale bars: 50 µm [A (a-f)] and 10 µm [B (a-c)].

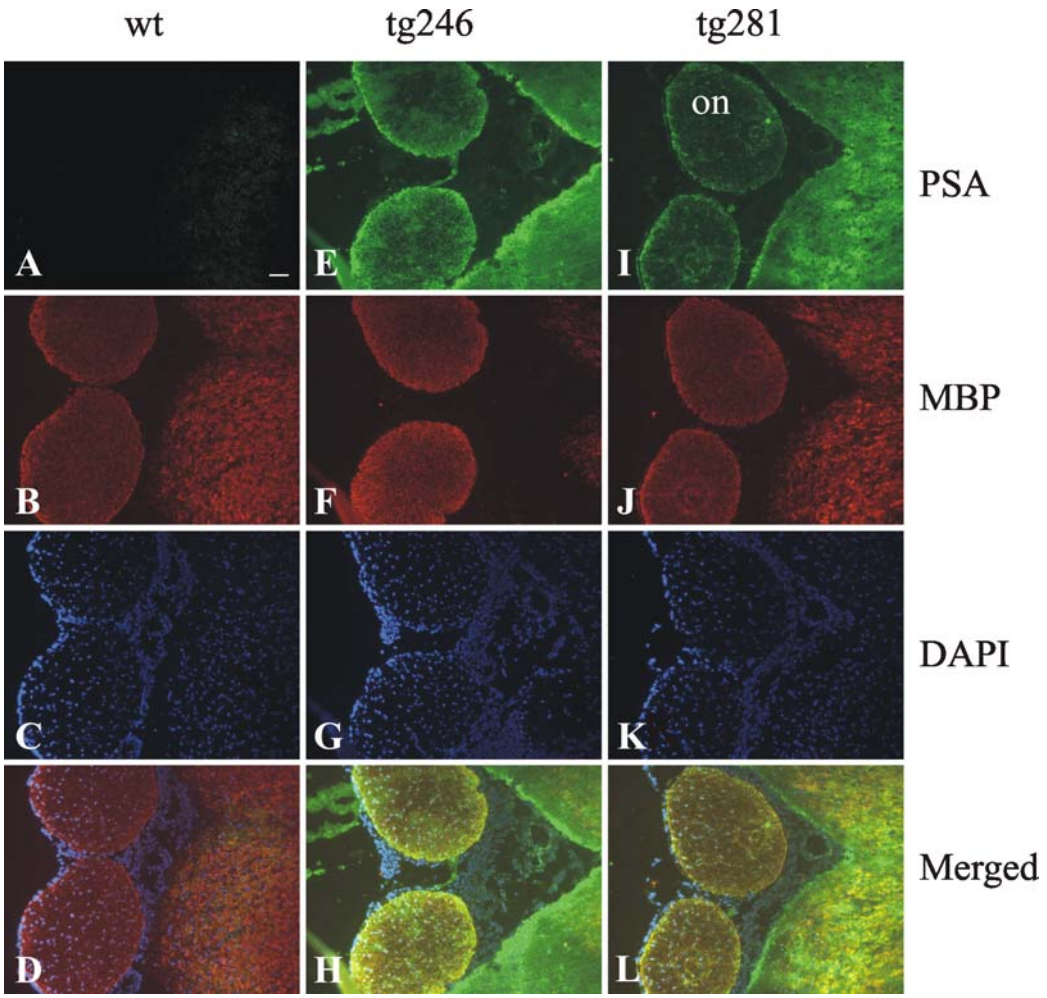

Figure 7: PSA expression in optic nerve of PLP-PST mice. Coronal cryosections of optic nerve from 4-months-old tg and wt mice were cut and stained for PSA and MBP. (A, B, C & D)-wt; (E, F, G & H)-tg mice from tg246 line; (I, J, K & L)-tg mice from tg281 line. (A, E & I)-PSA staining; (B, F & J)-MBP staining. Nuclear staining was done with DAPI (C, G & K); (D, H & L) are merged pictures of PSA and MBP stainings. on-optic nerve. Scale bar: 50µm (A-L).

4.1.4 Overexpression of PST leads to a decrease in the number of mature oligodendrocytes

The transgenic overexpression of PST leads to a decrease in myelin content and MBP gene expression (Fewou, 2005). These results led to the hypothesis that the decrease in myelin and MBP level could be due to several possibilities namely (a) decrease in the number of oligodendrocyte precursor cells (b) decrease in the number of mature differentiated oligodendrocytes (c) apoptosis of mature oligodendrocytes or (d) reduced synthesis of myelin. Hence, to understand and verify which of the hypothesis is valid, an *in situ* hybridization was performed on parasagittal cryosections of brains from 1-week-old transgenic and wild-type littermates, with digoxigenin-labelled PDGF α-receptor, (PDGF α-receptor is a marker for oligodendrocyte precursor cells), PLP (Fewou, 2005), MAG and MBP (Fig. 8A) (markers for

differentiated oligodendrocytes) cRNA probes. Counting the number of PDGF α-receptor positive cells in the forebrain by Dr. Simon Fewou did not show any significant difference in the cell number between transgenic and wild-type mice. However quantification of PLP positive cells showed a significant decrease in the transgenic mice when compared to wild-type mice (Fewou, 2005). Since PLP is also expressed in a subpopulation of OPCs the reduction that was observed could be due to a reduction in this subpopulation of OPCs or could be a general reduction in differentiated oligodendrocytes. Hence, to verify this, the number of mature oligodendrocytes was quantified by counting the number of MAG positive cells in the forebrain regions (corpus callosum) of both transgenic and wild-type animals (Fig. 8B). Counting the number of MAG positive cells also indicated a reduction in the number of cells in transgenic mice when compared to wild-type animals, which points towards a decrease in differentiated oligodendrocytes upon PST overexpression. For quantification, MBP positive cells were not considered, as MBP is expressed even in the branches of differentiated oligodendrocytes, distinguishing the cell body from the branches of fully differentiated oligodendrocytes is difficult.

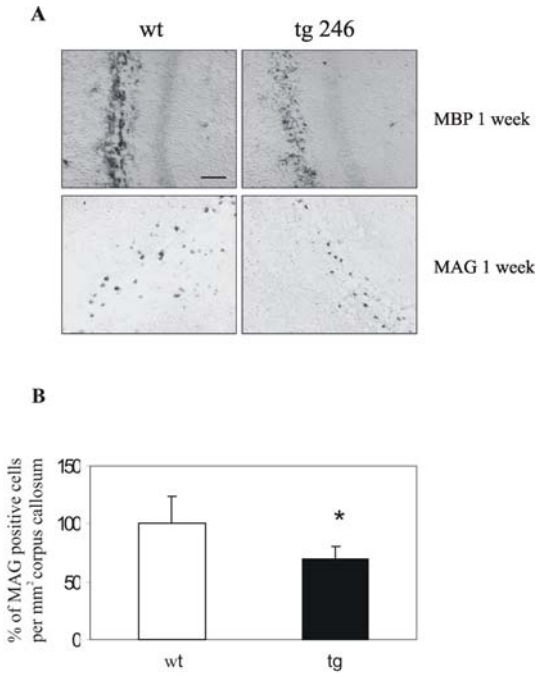

Figure 8: *In situ* hybridisation of 1 week old PLP-PST mice brain. *In situ* hybridization was performed on cryosections of brain from 1-week-old wild-type and PLP-PST transgenic mice (tg246 line). *In situ* hybridization was done with DIG-labelled cRNA probes for MBP and MAG. n=3 animals per genotype were used for the analysis. (A) MBP and MAG positive cells from the corpus callosum region of the brain were documented. (B) Number of MAG positive cells was counted for both transgenic and wild-type animals and the percentage of MAG positive cells was calculated. Shown are the mean ± SD (n=3). (* $p<0.05$ determined by Student's t-test). Scale bar: 100µm (A).

4.1.5 Effect of transgenic over expression on oligodendrocyte cell death

In order to rule out that the decrease in mature oligodendrocyte number is due to apoptosis of oligodendrocytes, a TUNEL assay was carried out on the coronal cryosections from 14-days-old transgenic (Fig. 9B & C) and wild-type (Fig. 9A) mice. After staining, the sections were evaluated under a microscope. Few TUNEL positive cells were detected in both transgenic and wild-type mice; otherwise, there was no significant difference in the TUNEL staining between the transgenic and wild-type mice.

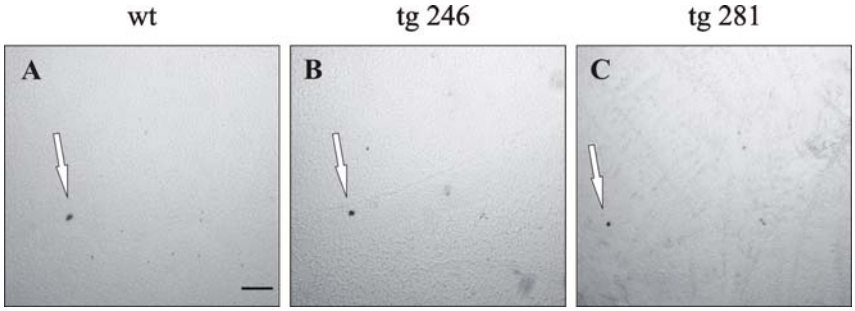

Figure 9: TUNEL assay to detect apoptosis in PLP-PST mice. TUNEL staining of parasagittal cryosections from forebrain of 14-days-old mice from wt-wild-type, tg246-transgenic tg246 line and tg281-transgenic tg281 line. A few TUNEL positive cells (indicated by an arrow) were detected in wild-type and transgenic animals, but there was, however, no increase in the number of apoptotic cells in transgenic mice when compared to wild-type mice. Scale bar: 100µm (A-C).

4.1.6 Overexpression of PST does not alter the ganglioside composition in transgenic mice

Gangliosides are oligosialylated glycosphingolipids carrying strings of sialylated oligosaccharide side chains. To investigate the possibility of alterations in ganglioside composition due to PST overexpression, total brain lipids were isolated, alkaline hydrolyzed and resolved on a HPTLC plate (Fig. 10). Analysis of the different gangliosides namely, GM1a, GD1a, GD1b, GT1b, led to the observation that there was no significant difference in the ganglioside composition between transgenic and wild-type mice.

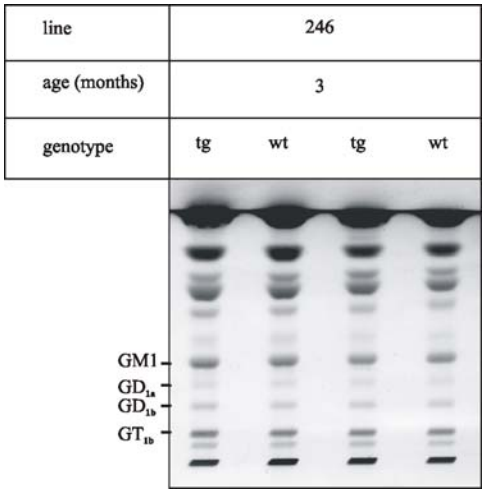

Figure 10: TLC analysis of gangliosides in PST transgenic mice. Effect of PST overexpression on sialylated gangliosides was analysed by TLC. Total brain lipids from 3-months-old tg246-transgenic line 246 and wt-wild-type mice were separated in (55:45:10) chloroform:methanol:water, solvent system. TLC analysis was done with 3 animals per genotype. Ganglioside mix (GM1a, GD1a, GD1b, and GT1b) and sphingomyelin from bovine brain were used as standards. Figure shows the lipid profile from two tg and two wt animals.

4.1.7 In vitro culture of PST overexpressing oligodendrocytes

To examine the influence on morphology and differentiation of oligodendrocytes due to PST overexpression, mixed glial cell cultures were prepared from the forebrain of newborn mice and maintained for 8-10 days in DMEM containing 10% horse serum. The mixed glial cell culture is composed of astrocytes, forming an astrocyte monolayer, microglia and oligodendrocyte progenitors. The microglia and oligodendrocyte progenitors, which grow on top of the astrocytic monolayer, were removed by shaking the flask. Oligodendrocyte progenitor cells are separated from microglia by incubating the oligodendrocyte progenitor/microglia cell mixture on a plastic Petri plate. Microglia remained attached to the Petri plate and the oligodendrocyte progenitors remained in the medium. These undifferentiated oligodendrocyte progenitors in the medium were collected and were then differentiated in SATO medium, containing 1% horse serum, fixed and collected for immunofluorescence staining with ENCAM and MBP antibodies, between 1 and 4 days of culture (Fig. 11 & 12). MBP was used as a marker for mature differentiated oligodendrocytes. Day 1 or day 2 cultures from transgenic and wild-type mice were less differentiated when compared to day 3 or day 4 cultures, which were characterized by extensive branching and interconnections in oligodendrocytes. In cultures from transgenic mice, positive PSA staining was observed in both immature (Fig. 11A & E) and mature oligodendrocytes (Fig. 12A & E) with no staining in the cultures from wild-type mice (Fig. 11I, M & 12I, M). The number of MBP positive cells at each day of culture was counted by fluorescence microscopy. Several

different random fields of view were selected for counting and the percentage of MBP positive cells was calculated as a function of time (Fig. 13A). Analysis of the data showed no significant difference in the percentage between transgenic and wild-type cells, indicating no change or delay in the process of *in vitro* differentiation due to PSA overexpression. However, the morphology of the differentiated transgenic oligodendrocytes was comparatively less mature than that of wild-type cells. The transgenic oligodendrocytes were less branched, 33.5 ± 10.3 (mean ± SD) branches, with fewer processes and membranous extensions when compared to wild-type oligodendrocytes, which had 58 ± 25 (mean ± SD) branches (Fig. 13B). Analysis of cell soma diameter indicated no significant difference between the cultures from tg and wt mice. Although PSA staining in the culture from tg mice showed PSA localisation in the branches, membranous extensions of oligodendrocytes, there was also PSA staining in the perinuclear region and around the cell body [Fig. 11 (A, E) & 12 (A, E)]. Co-staining of PSA with Golgi marker, giantin (1:200) in cultures from tg mice showed no co-localization in the less mature oligodendrocytes (Fig. 15A-D), whereas there was partial co-localization in mature (Fig. 15E-H) differentiated oligodendrocytes.

In mature oligodendrocytes, normally, PSA-NCAM is localised in the plasma membrane, but, since the mature oligodendrocytes from transgenic mice showed PSA staining in the perinuclear region and also partial localisation of giantin and PSA, the possibility of mislocalisation of NCAM (carrier of PSA) or other glycoproteins like L-MAG, a marker for differentiated oligodendrocyte, around the perinuclear region was analysed. In order to analyse the above possibility, immunofluorescence double staining of PSA with NCAM (Fig. 16A-H) and L-MAG antibodies (Fig. 14A-D) and double staining for NCAM and L-MAG (Fig. 17A-H) was performed. Analysis of NCAM and L-MAG stainings from the cultures of both transgenic and wild-type mice showed that both the proteins were normally distributed in the plasma membrane, membranous extensions of mature oligodendrocytes and there was no alteration in their distribution between cultures from transgenic and wild-type mice. Double staining of oligodendrocytes from transgenic mice with NCAM and PSA antibodies, showed co-localization of NCAM and PSA in the membranous extensions. However, in the perinuclear region, NCAM showed only a weak staining when compared to the strong PSA staining. Besides, there was no co-localisation of NCAM and PSA in the perinuclear region (Fig. 16E-H). Thus, these observations suggest the possibility of other proteins carrying PSA apart from NCAM in the mature oligodendrocytes from transgenic mice.

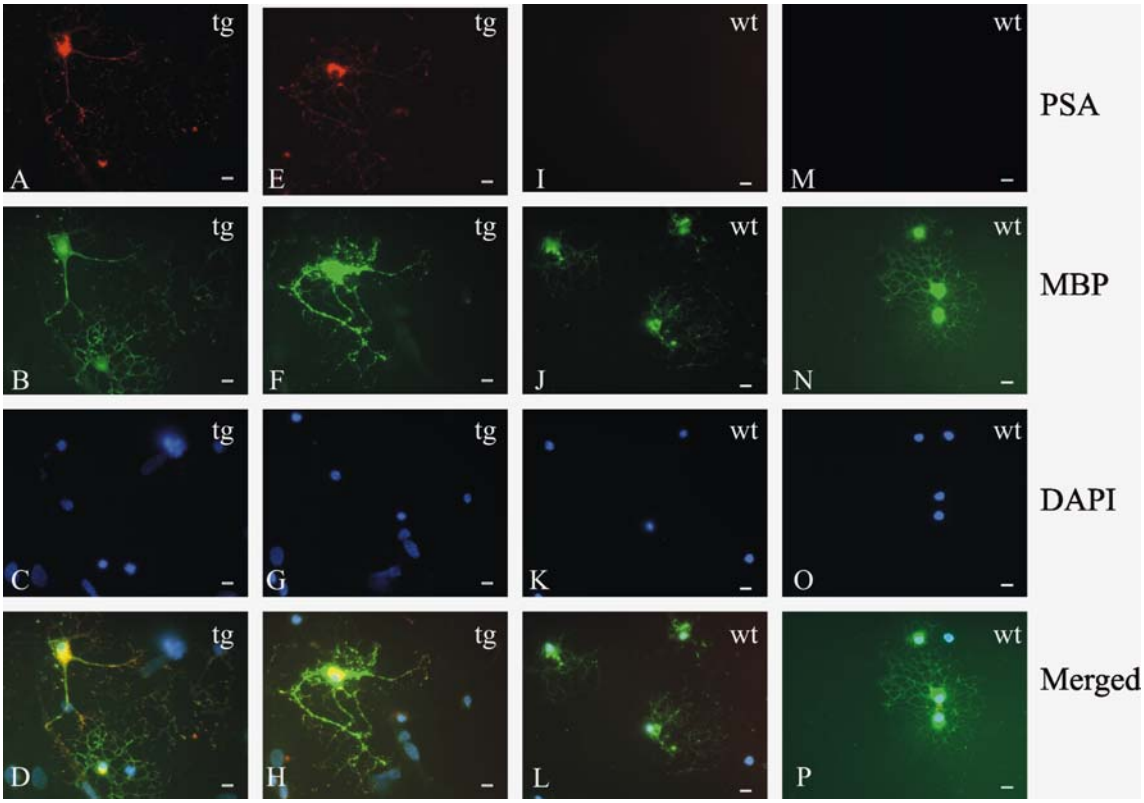

Figure 11: PSA and MBP expression in immature oligodendrocytes. Primary oligodendrocyte culture from tg and wt animals was co-stained for PSA (A-M) and MBP (B-N). (A-D & E-H) and (I-L & M-P) represent the different morphologies of tg and wt oligodendrocytes. These cultures from tg and wt mice represent immature oligodendrocytes. Nuclear staining was done with DAPI (C, G, K & O). (D, H, L & P) are the overlap stainings of PSA, MBP and DAPI. Scale bar: 50µm (A-P).

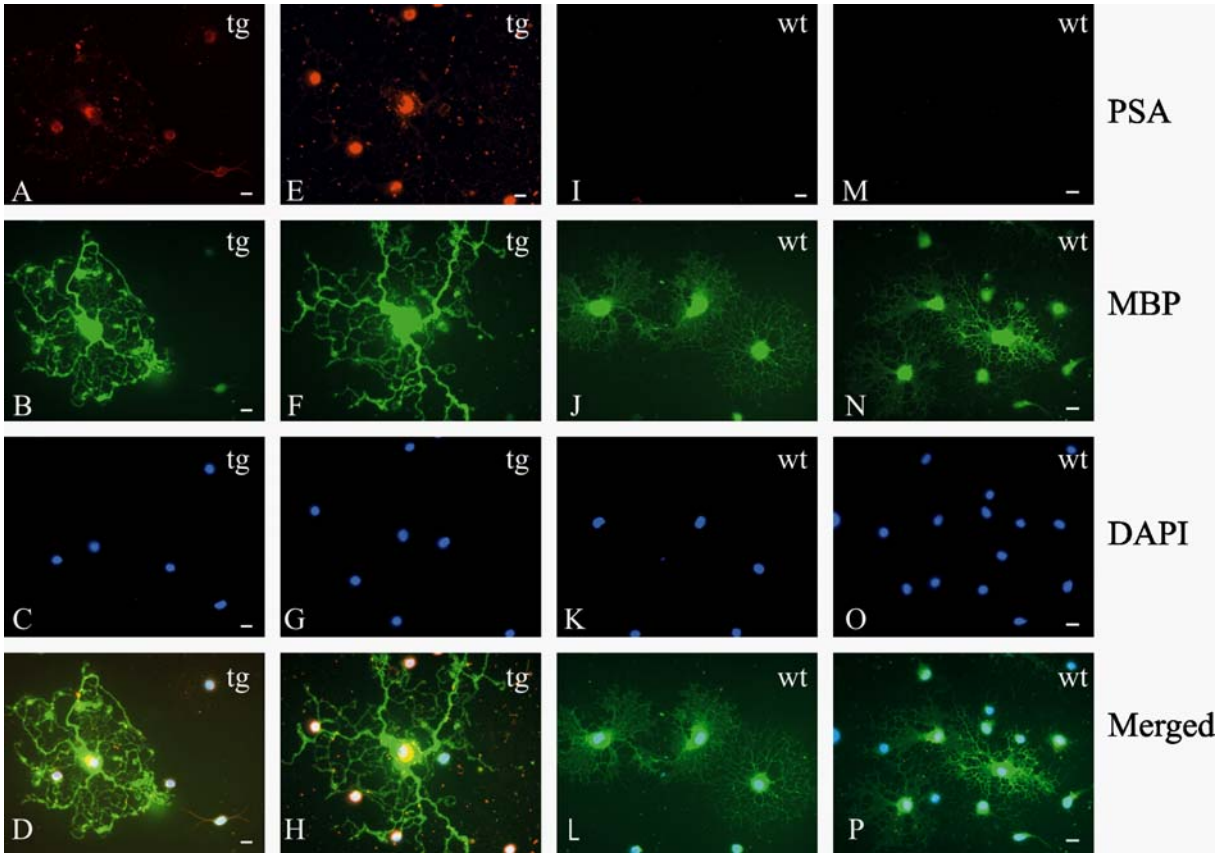

Figure 12: PSA and MBP expression in mature oligodendrocytes. Primary oligodendrocyte culture from tg and wt animals was co-stained for PSA (A-M) and MBP (B-N). (A-D & E-H) and (I-L & M-P) represent the different morphologies of tg and wt oligodendrocytes. PSA staining is perinuclear in the oligodendrocytes from tg mice. The wt oligodendrocytes are more branched and well interconnected with neighbouring oligodendrocytes when compared to tg oligodendrocytes, which show less extensive branching and membrane sheaths. Nuclear staining was done with DAPI (C, G, K & O). (D, H, L & P) are the overlap stainings of PSA, MBP and DAPI. Scale bar: 50µm (A-P).

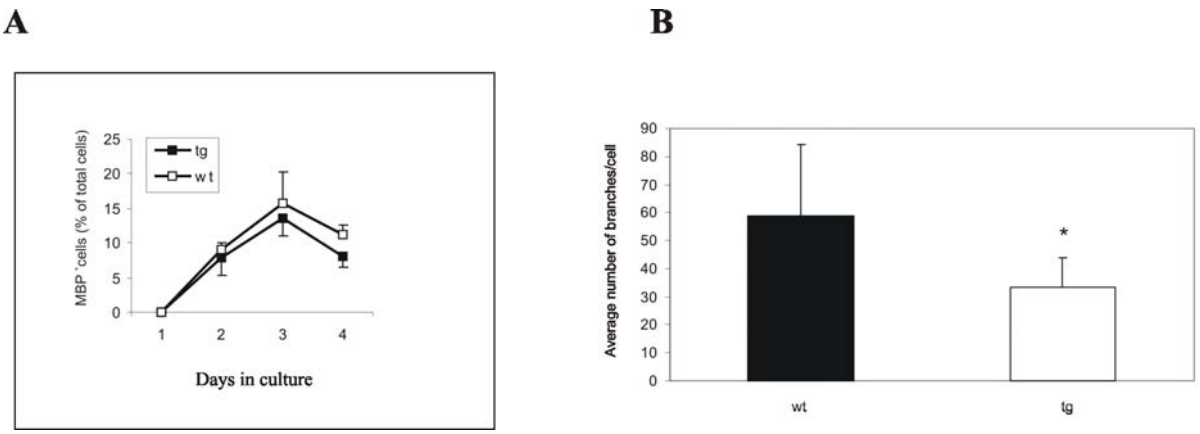

Figure 13: Quantification of MBP positive oligodendrocytes and branches from primary culture. Primary oligodendrocyte culture was prepared and the number of MBP positive oligodendrocytes was calculated and plotted as a function of time from wt and tg PLP-PST mice (A). Cells were counted from 3 separate culture preparations of tg and wt mice (n=3). Both weakly labelled immature and mature oligodendrocytes were included in the count. For each time point, cells were counted on 4–6 random fields of view and 400-600 cells were counted and documented. Nuclear staining was done with DAPI. (B) Quantification of branches from oligodendrocyte cultures prepared from tg and wt mice. Number of branches in MBP positive cells of day 4 cultures from tg and wt mice were counted (n=15 cells per genotype; * $P<0.05$, determined by Student's t-test). Branches longer than the cell soma diameter were counted for quantification. The average number of branches in cultures from wt mice were, 58 ± 25 branches (mean ± SD) and in cultures from tg mice were 33.5 ± 10.3 branches (mean ± SD). The average cell soma diameter of cultures from wt mice were, 14 ± 2 µm (mean ± SD) and in cultures from tg mice were, 15 ± 6 µm (mean ± SD). Quantification of branches and cell soma diameter was done with axiovision software from Carl Zeiss microimaging GmbH.

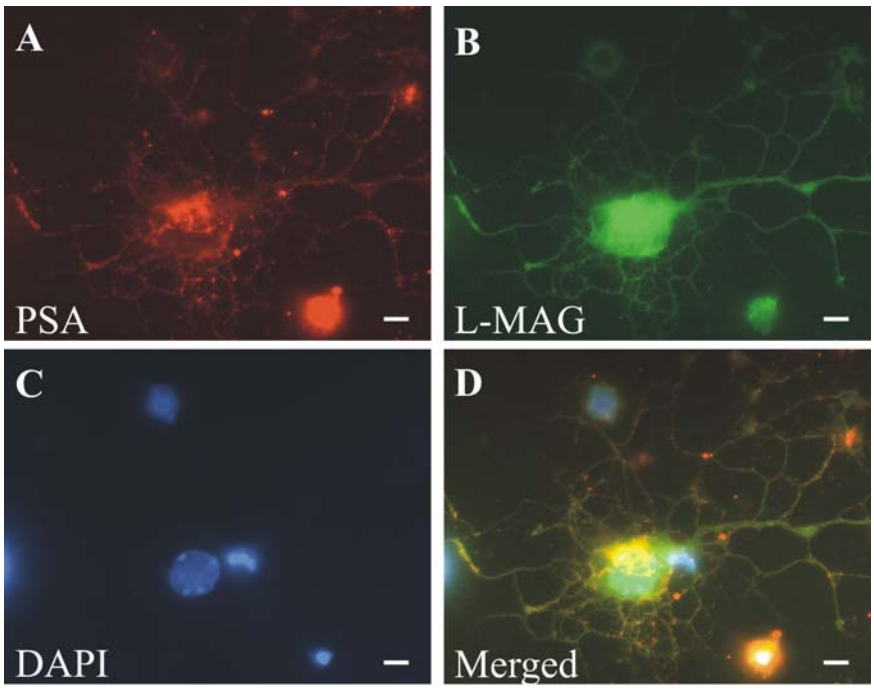

Figure 14: Co-staining of oligodendrocytes from transgenic mice for PSA and L-MAG. Oligodendrocyte cultures from tg mice were stained for (A) PSA and (B) L-MAG. (C) Nuclear staining was done with DAPI. (D) Merged picture of PSA, L-MAG and DAPI staining. Scale bar: 5µm (A-D)

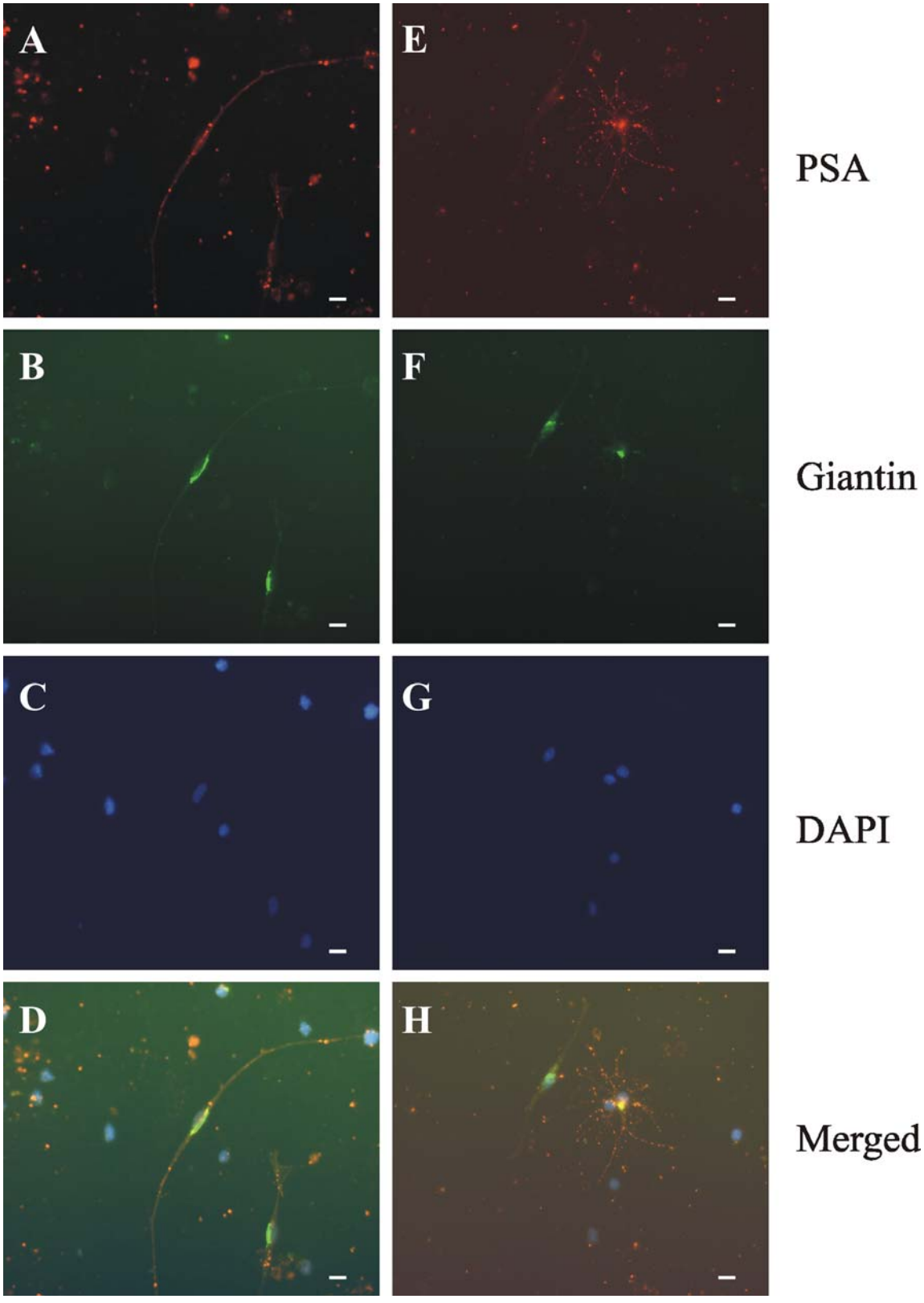

Figure 15: Immunofluorescence staining of oligodendrocytes from tg mice, for PSA and giantin. Double staining of primary oligodendrocyte cultures from tg mice was performed for PSA (A & E) and giantin (B & F), a Golgi apparatus marker. Nuclear staining was done with DAPI (C & G). (D & H) represent the merged stainings of DAPI, PSA and giantin. (A, B, C & D) shows an example of less differentiated oligodendrocytes and (E, F, G & H) shows an example of more differentiated oligodendrocytes. Scale bar: 10µm (A-H).

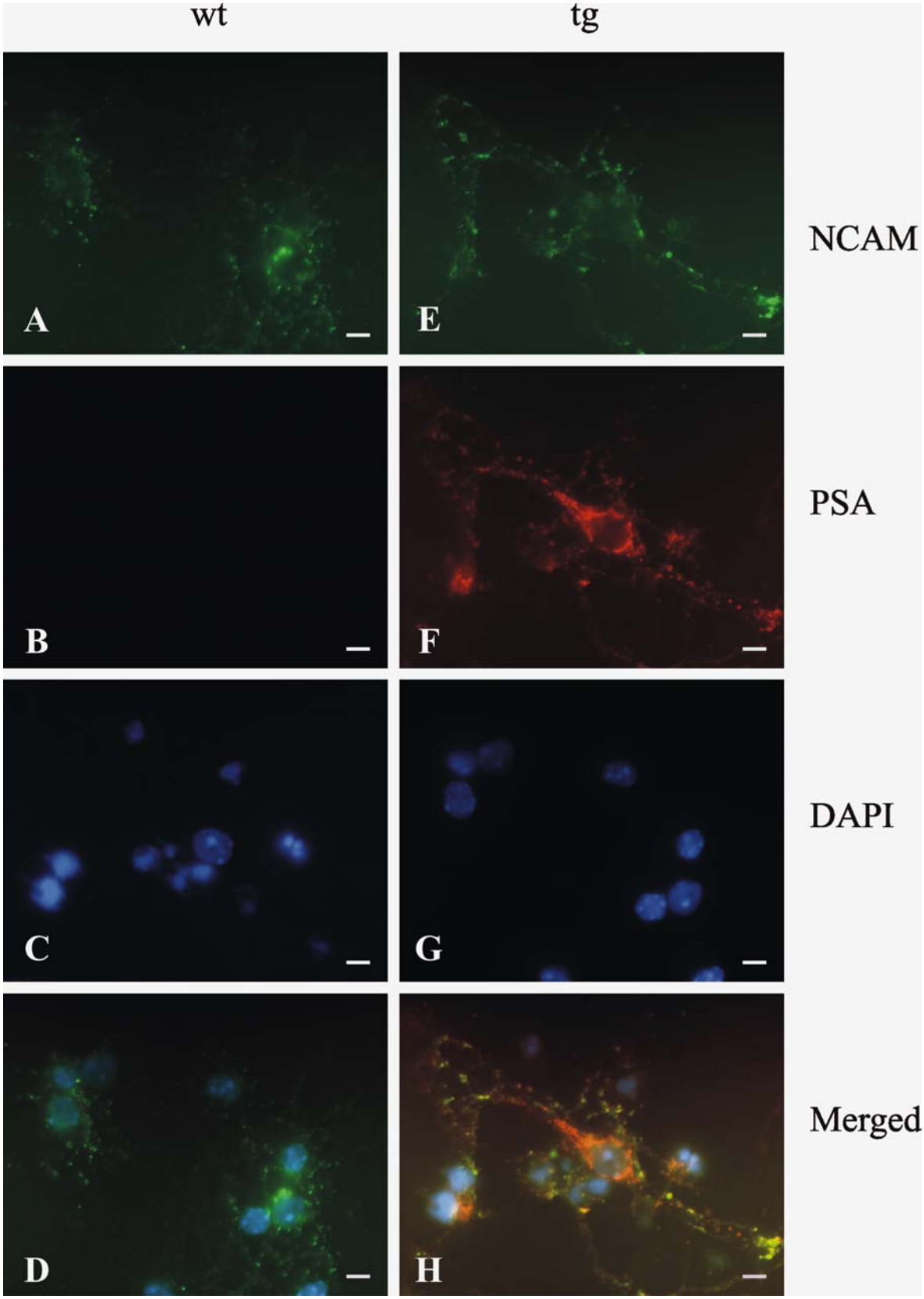

Figure 16: Co-staining of oligodendrocyte culture with NCAM and PSA antibodies. Oligodendrocyte cultures were prepared from wt (A-D) and tg (E-H) mice and were stained for NCAM (A & E) and PSA (B & F), to analyse the distribution of NCAM in the cultures from both tg and wt mice, respectively. Nuclei were stained with DAPI (C & G). (D & H) represent the merged pictures of NCAM, PSA and DAPI. Scale bar: 5µm (A-H).

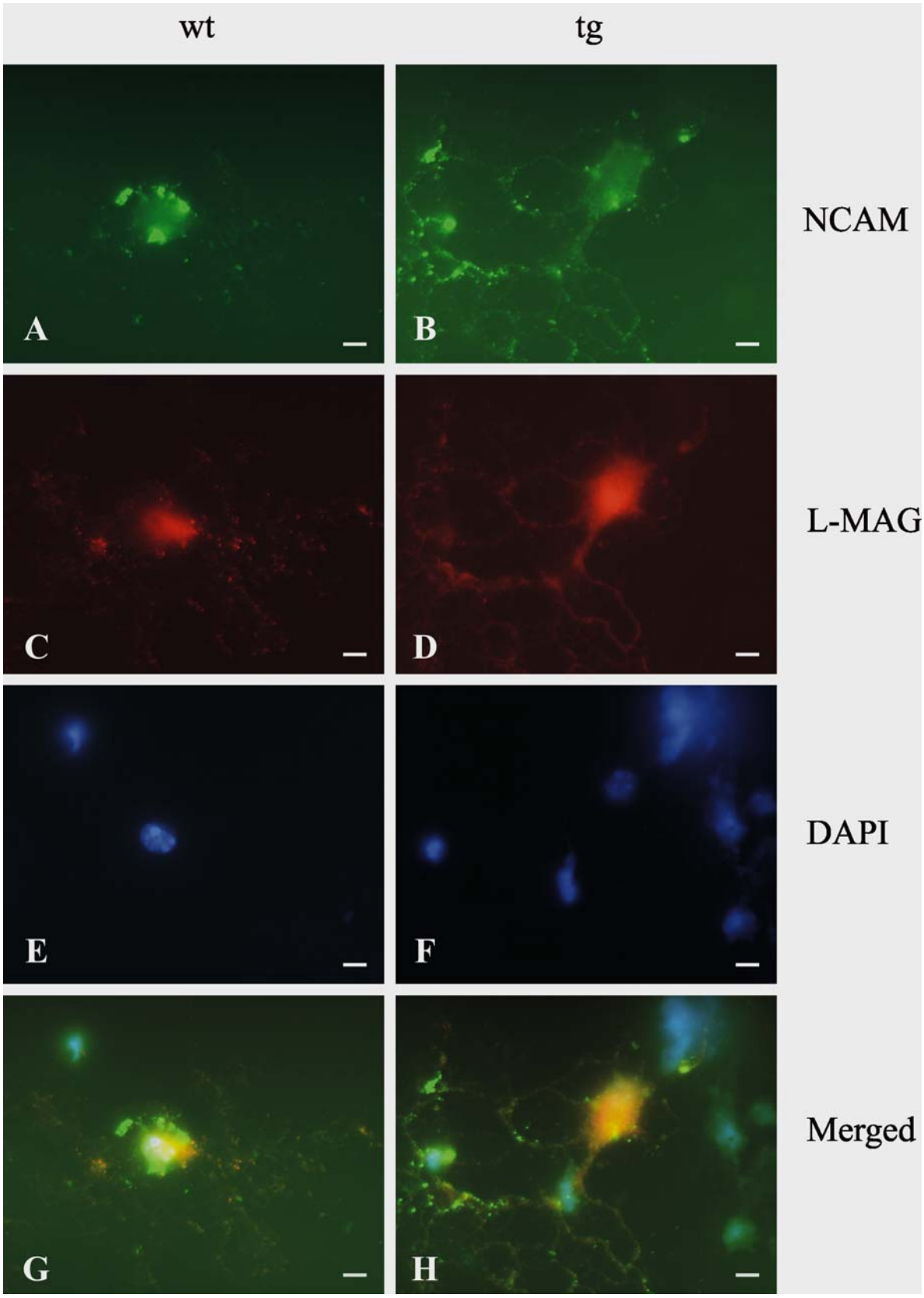

Figure 17: Immunofluorescence co-staining of oligodendrocyte cultures with NCAM and L-MAG antibodies. (A, C, E & G) represent the culture from wt mice and (B, D, F & H) represent the culture from tg mice, stained for NCAM (A & B) and L-MAG (C & D). DAPI was used to stain the nuclei (E & F). (G & H) represent the overlap of NCAM, L-MAG and DAPI stainings. Scale bar: 5µm (A-H).

4.2 Analysis of PLP-CST mice

Metachromatic leukodystrophy is a lysosomal sulfatide storage disorder caused by the deficiency of sulfatide degrading enzyme ASA, resulting in the accumulation of sulfatide in the nervous system and other organs. The manifestations of the disease include various neuropathological symptoms including demyelination. Till date, ASA(-/-) mice is the only animal model for this disease. Though ASA(-/-) mice displays similar symptoms to MLD, the symptoms are less severe than the patients. Moreover, these mice also do not display demyelination that is characteristic of the disease. Since accumulation of sulfatide is a critical factor for the neuropathological symptoms, including demyelination, it was hypothesized that an increase in sulfatide accumulation in ASA(-/-) mice would result in the display of symptoms akin to MLD. Hence, in order to increase sulfatide synthesis in oligodendrocytes and Schwann cells, transgenic mice overexpressing CST under the control of PLP promoter was generated and bred with ASA(-/-) mice, so that one of the offsprings from this breeding, tg/ASA(-/-) mice, would show an increase in sulfatide synthesis in myelinating cells.

4.2.1 Generation of PLP-CST transgenic mice

The transgenic construct was generated by ligating the 1.3 kb murine CST cDNA into the *Pme*I site of the PLP promoter cassette. The PLP promoter cassette consists of the 5'-flanking region containing the PLP promoter, first exon, first intron and the splice acceptor site of exon 2 of the mouse PLP gene. The ATG start codon in the cassette was mutated; so that, translation would take place from the start codon of the cDNA construct (Fig. 18A).

Four transgenic founder mice of the mixed C57BL/6×CBA genetic background were generated and identified by Southern blotting of mouse tail genomic DNA which was digested with *Sty*I restriction enzyme. CST cDNA was used as a probe to identify the transgene. Two males with high copy number were infertile and the other two female founder mice were used for establishing two mice lines namely tg2645 and tg2639. Generation of transgenic mice and identification of transgenic founder mice by Southern blotting was performed by Dr. Simon Fewou. tg2645 carried a higher copy number of the transgene when compared to tg2639. The two founder mice tg2645 and tg2639 were bred with ASA(-/-) mice. The offsprings from this breeding were of the mixed C57BL/6×CBA×129Ola genetic background and were of the following four genotypes - tg/ASA(-/-), tg/ASA(+/-), ASA(-/-) and ASA(+/-). Mice of all the four genotypes were used for further analysis.

4.2.2 Northern blot analysis of CST transgene expression

Northern blot analysis of brains from 14-months-old animals, from both lines tg2645 and tg2639, was carried out to detect the CST transgene expression (Fig. 18B). Total RNA from ASA(+/-), tg/ASA(+/-), ASA(-/-) and tg/ASA(-/-) mice was isolated and transferred onto a Hybond N^+ nylon membrane and probed with [α-^{32}P]-dCTP labelled CST cDNA probe. The CST mRNA expression in the transgenic mice on an ASA(+/-) and ASA(-/-) background, from both lines, was several fold higher when compared to the mRNA from ASA(+/-) and ASA(-/-) mice. The expression level of the tg2645 line was higher when compared to the tg2639 line.

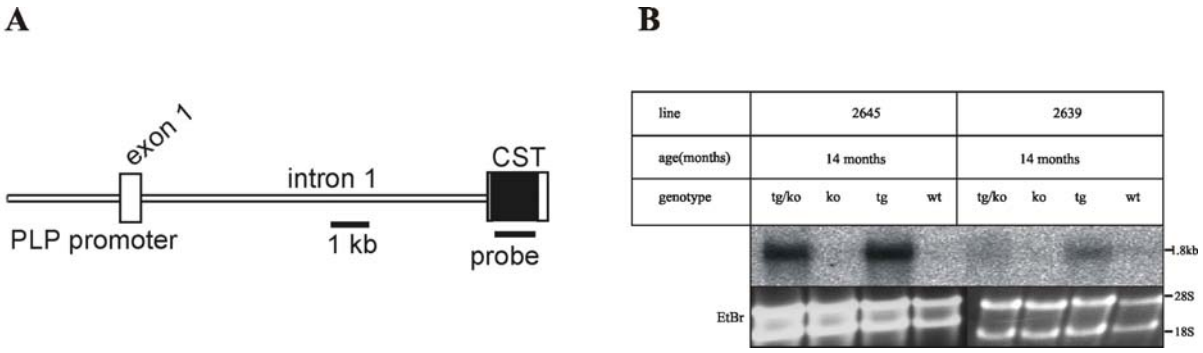

Figure 18: PLP-CST transgenic construct and Northern blot analysis of CST transgene expression. (A) Schematic representation of PLP-CST transgenic construct. (B) Expression of endogenous and transgene CST was analysed by Northern blot analysis. Total RNA from brain of 14-months-old tg/ko-tg/ASA(-/-), ko-ASA(-/-), tg-tg/ASA(+/-), wt-ASA(+/-) mice from both the transgenic lines, tg2645 and tg2639, was isolated and 10 µg/lane was loaded on an agarose gel containing formaldehyde. The size of the CST mRNA (1.8 kb) is indicated in the figure. The transgene expression in the tg2645 line was stronger than the tg2639 line. The endogenous mRNA signal was weak when compared to the transgene signal. Ethidium bromide staining served for equal loading of the lanes. Radioactivity was visualized with a phosphorimager screen.

4.2.3 Purification of PAPS synthetase and synthesis of [^{35}S]-labelled PAPS

The CST mRNA expression in the PLP-CST mice was higher when compared to the ASA(+/-) and ASA(-/-) mice. Hence, to compare the correlation between CST mRNA expression and CST enzyme activity, a sulfotransferase assay was carried out. In order to carry out this assay, PAPS, a sulfonate donor was needed. Hence, murine PAPS synthetase, the enzyme needed to synthesise PAPS, cDNA was cloned into an expression vector and transformed into BL21 competent cells by Mandy Ruf, so that these bacteria express recombinant PAPS synthetase enzyme, which can be isolated and purified, for synthesising radiolabelled PAPS.

The bacterial cells were lysed and the crude homogenate from bacteria expressing recombinant PAPS synthetase was purified on a nickel chelating column and the different eluted fractions from the column were pooled. To the pooled fraction, Tris-glycerol buffer was added and the mixture was concentrated with Centricon spin columns. The concentrated protein was resolved on an SDS-PAGE to identify the fractions containing PAPS synthetase. In the lane for pooled concentrated fractions, Ps1 and Ps2, a polypeptide of ~66 kDa, corresponding to PAPS synthetase was observed and in the lane for flow through glycerol fractions, Gs1 and Gs2, no protein was observed (Fig. 19A).

The purified PAPS synthetase was used in a reaction, containing [^{35}S]-labelled sulfate, to synthesize radiolabelled PAPS. The synthesized PAPS was verified by loading it on a PEI-TLC plate, with [^{35}S]-labelled sulfate as control. PAPS migrates slightly higher when compared to radiolabelled sulfate donor as shown in figure (Fig. 19B).

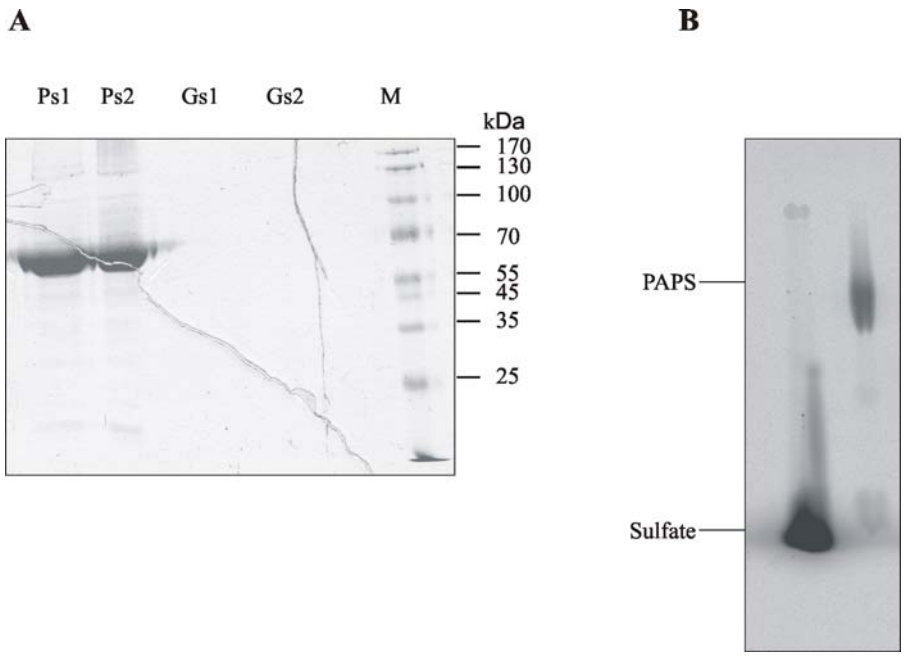

Figure 19: PAPS synthetase purification and [^{35}S]-radiolabelled PAPS synthesis. (A) Purification of PAPS synthetase. PAPS synthetase was purified on a HiTrap Ni^{2+}chelating column. Eluted fractions containing protein were pooled and Tris (pH 7)-glycerol buffer was added to it. The protein fractions were concentrated by centrifugation with Centricon spin column. Ps1 and Ps2 represents the pooled eluted fractions from the column after concentration, containing PAPS synthetase (~66 kDa), Gs1 and Gs2 represent the flow through glycerol fractions after concentration. (B) TLC analysis of [^{35}S]-radiolabelled PAPS. Radiolabelled PAPS was synthesized with the purified PAPS synthetase, [^{35}S]-labelled sulfate and ATP in a reaction buffer at 37°C for 3 hours. Purity of the synthesized PAPS was verified on a PEI-TLC plate with [^{35}S]-labelled sodium sulfate as standard and 0.9M lithium chloride as developing solvent. The radioactivity was visualized on a phosphorimager screen.

4.2.4 Increase in CST enzyme activity in PLP-CST transgenic mice

To examine whether the CST transgene overexpression leads to an increase in CST activity, CST activity was compared between transgenic and wild-type mice by performing a sulfotransferase assay. Brain homogenates from 3-weeks and 3-months-old mice from wild-type and tg2639 line and 4-6 months old mice from wild-type and tg2645 line were analyzed. After completion of the reaction, the reaction mix was analysed on a HPTLC plate. [^{35}S]-sulfatide was visualized by exposing the HPTLC plate to a phosphorimager screen and the product, sulfatide, was quantified densitometrically with AIDA software (Fig. 20A). Analysis of the data showed an increase in CST enzyme activity by nearly 60-fold in the tg2639 line and to about 200-fold in the tg2645 line when compared to wild-type controls (Fig. 20B).

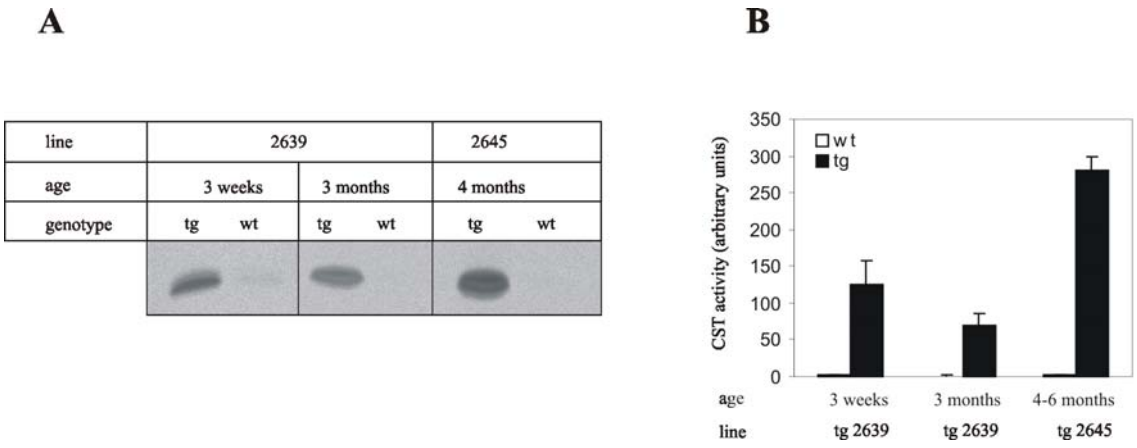

Figure 20: CST enzyme activity assay. Brain homogenates of 3-weeks and 3-months-old wt and tg mice (line tg2639) and 4-6 months-old wt and tg mice (line tg2645) were used to perform a radioactive CST assay. (A) The product of the assay, [^{35}S]-labelled sulfatide, was resolved on a HPTLC plate with (60:27:4) chloroform:methanol:water as solvent system and detected on a phosphorimager screen. The sulfatide signal from wild-type mice was very weak when compared to that from tg mice (~ 2 arbitrary units for wild-type animals). (B) HPTLC plates were scanned densitometrically to calculate the CST activity in arbitrary units. wt-ASA(+/-), tg-tg/ASA(+/-).

4.2.5 CST overexpression in ASA(-/-) mice leads to an increase in sulfatide accumulation

To analyse whether CST overexpression leads to changes in the lipid compositon in the PLP-CST mice, lipid analysis of total brain and sciatic nerve was performed. Lipids from total brain of 7-months (tg2639 and tg2645 line) and 17-months (tg2645 line) or 18-months (tg2639 line) old ASA(+/-), tg/ASA(+/-), ASA(-/-) and tg/ASA(-/-) mice (Fig. 21A & B) and sciatic nerve of 18-months-old (tg2639 line) ASA(-/-) and tg/ASA(-/-) (Fig. 23A) mice were extracted and analyzed by TLC. In order to quantify the sulfatide and GalC concentrations, sulfatide and GalC standards (0.5 µg, 1 µg, 2 µg, 4 µg and 8µg) were loaded along with the

brain lipids from 7-months and 18-months-old mice or sulfatide, GalC and cholesterol standards for sciatic nerve lipids from 18-months-old mice. A standard curve was generated and sulfatide, GalC concentration of the brain lipids or sciatic nerve lipids was calculated from the standard curve and then normalised to milligram wet brain weight for brain lipids or normalised to cholesterol in case of sciatic nerve lipids.

Quantification of brain lipids from 7-months-old mice, showed 1.7-fold increase in sulfatide levels in the tg/ASA(-/-) mice when compared to ASA(-/-) mice or ASA(+/-) mice (Fig. 22A) and there was no significant increase in sulfatide levels in the ASA(-/-) mice when compared to the ASA(+/-) mice. Despite no significant reduction in the GalC levels in both tg/ASA(-/-) and ASA(-/-) mice (Fig. 22B), the GalC:sulfatide ratio in both tg/ASA(-/-) and ASA(-/-) was significantly reduced when compared to the ASA(+/-) mice (Fig. 22C). The reduction in GalC:sulfatide ratio in ASA(-/-) mice was in accordance to results reported previously by Yagoothfam et al., (2005).

In 17-18 months old animals sulfatide accumulation increased in tg/ASA(-/-) mice (nearly 1.4 fold more) when compared to ASA(-/-) mice (Fig. 22D). However, the relative sulfatide increase in 17-18 months old tg/ASA(-/-) mice, when compared to ASA(-/-) mice, was less than that of 7-months-old animals, possibly indicating demyelination in these mice. Though the GalC levels in 18-months-old tg/ASA(-/-) mice was decreased when compared to ASA(-/-) mice the reduction was not significant (Fig. 22E) The GalC:sulfatide ratio of 17-18 months old tg/ASA(-/-) mice was significantly reduced when compared to ASA(-/-) mice (Fig. 22F). The tg/ASA(+/-) mice from both age groups showed no significant difference in the sulfatide level when compared with the ASA(+/-) control mice. For data analysis lipid data from 7-months-old animals from both the lines (2 animals per line per genotype) were combined.

The sciatic nerves from the 18-months-old tg/ASA(-/-) mice showed a significant increase (nearly 1.5 fold) in sulfatide level (Fig. 23B) indicating sulfatide accumulation in the peripheral nervous system of these mice. The GalC:sulfatide ratio was also significantly reduced in the the tg/ASA(-/-) mice when compared to ASA(-/-) mice (Fig. 23D) A significant reduction in the GalC:sulfatide ratio in brain and sciatic nerve of tg/ASA(-/-) mice indicates alterations in lipid metabolism due to sulfatide accumulation.

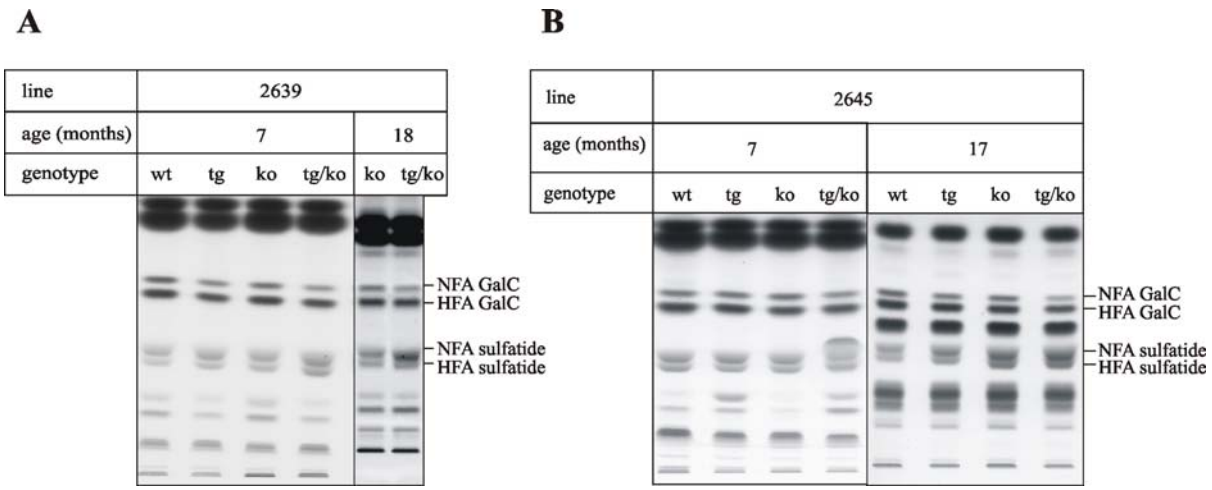

Figure 21: TLC representation of total brain lipids from PLP-CST mice. Total brain lipids were extracted and separated on HPTLC plates from wt, tg, ko and tg/ko mice. (A) 7-months and 18-months-old mice from tg2639 line. (B) 7-months and 17-months-old mice from tg2645 line. Alkaline hydrolysis, to remove phospholipids, was carried out for all the age groups except for 17-months-old mice. NFA-non-hydroxy fatty acid, HFA-hydroxy fatty acid, GalC-galactosylceramide. wt-ASA(+/-), tg-tg/ASA(+/-), ko-ASA(-/-), tg/ko-tg/ASA(-/-).

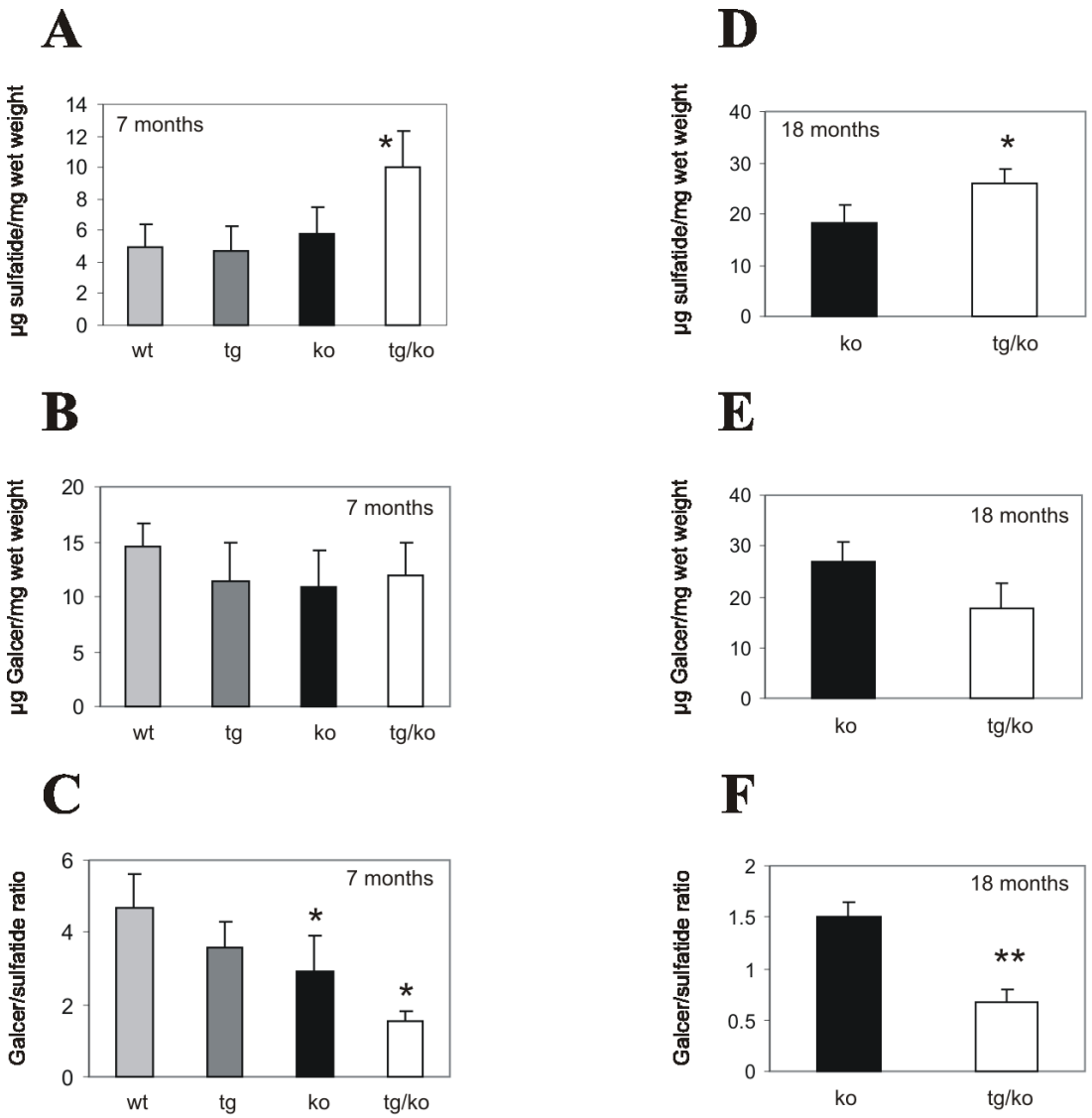

Figure 22: Quantification of brain lipids from PLP-CST mice. Brain lipids from 7-months (tg2639 + tg2645 lines; n = 4 per genotype) and 18-months (tg2639 line; n = 3 per genotype) old wt, tg, ko and tg/ko mice were run on a HPTLC plate. Total sulfatide (A & D), GalC (B & E) values were determined by scanning the HPTLC plates and analyzing them densitometrically. GalC:sulfatide ratio (C & F) was calculated from the densitometric data. For quantification, sulfatide and GalC standards (0.5 µg, 1 µg, 2 µg, 4 µg and 8µg) were loaded along with the brain lipids from 7-months and 18-months-old mice. A standard curve was generated and sulfatide, Galcer concentration of the brain lipids was calculated from the standard curve and then normalised to milligram wet brain weight. (* P< 0.05, ** P< 0.005 determined by Student's t-test). wt-ASA(+/-), tg-tg/ASA(+/-), ko-ASA(-/-), tg/ko-tg/ASA(-/-).

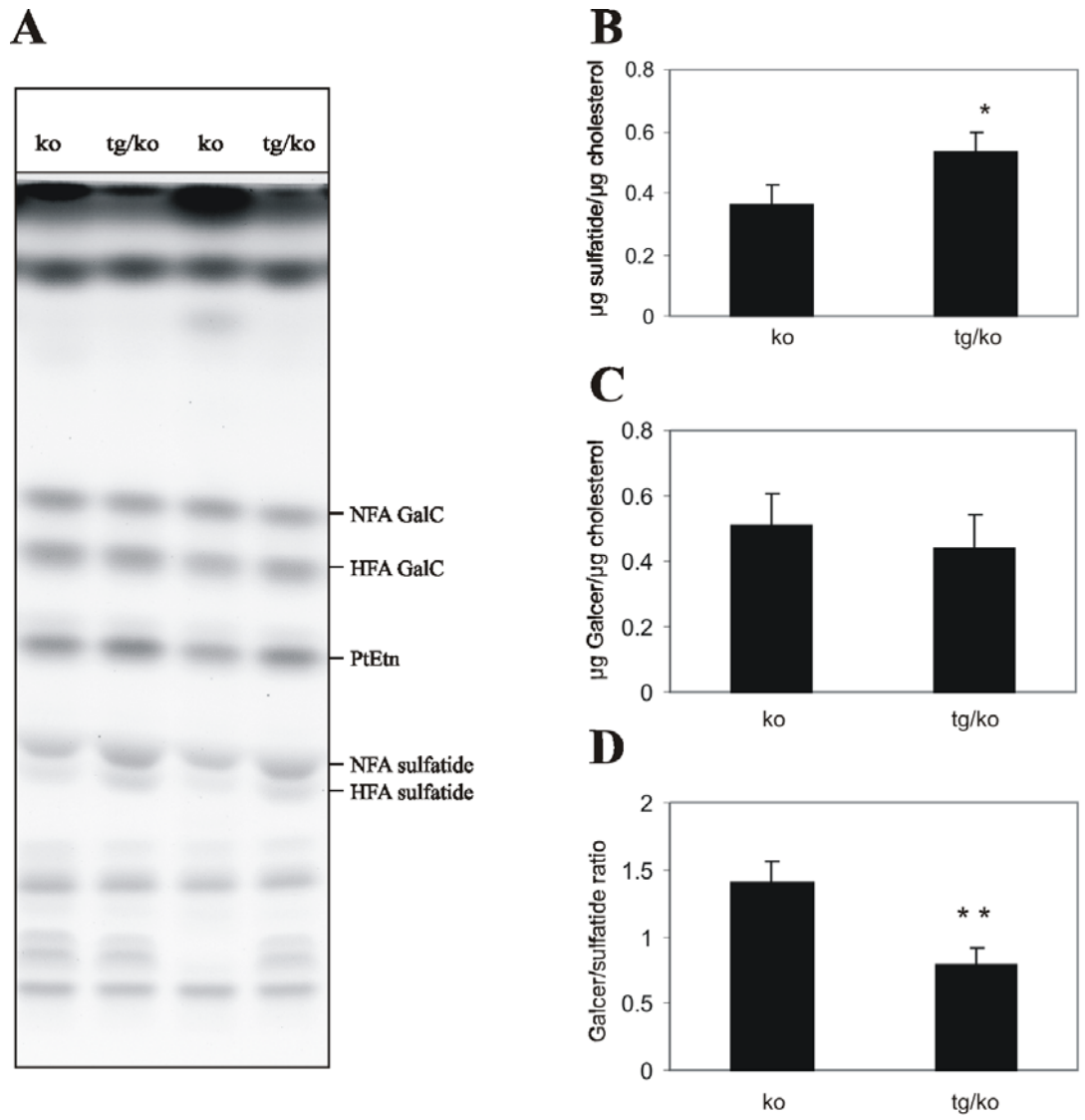

Figure 23: Analysis and quantification of lipids from sciatic nerves of PLP-CST mice. (A) Lipids were extracted and separated on a HPTLC plate from sciatic nerves of 18-months-old ASA(-/-) and tg/ASA(-/-) mice (tg2639 line). Lipids were normalized to cholesterol, for equal loading, scanned and analyzed densitometrically to determine sulfatide (B), GalC (C) values and GalC:sulfatide ratio (D) was calculated (n = 3 per genotype) (* P< 0.05, ** P< 0.005 determined by Student's t-test). wt-ASA(+/-), tg-tg/ASA(+/-), ko-ASA(-/-), tg/ko-tg/ASA(-/-).

4.2.6 Behavioural abnormalities, hind limb paralysis and motor co-ordination deficits in older tg/ASA(-/-) mice

The behaviour of tg/ASA(+/-) mice that were less than 6-months of age and those that were even older than 18-months, was not different from that of the ASA(+/-) controls. Similarly there was no difference in the behaviour of tg/ASA(-/-) within one year of age, when compared to ASA(-/-) controls. However, tg/ASA(-/-) mice older than one year showed some behavioural changes. These mice when suspended by their tail clasped their hind limbs and folded them towards their body (Fig. 24B), indicating hind limb weakness and paralysis in

these mice. In contrast, tg/ASA(+/-), ASA(+/-) and ASA(-/-) (Fig. 24A) mice spread their hind limbs apart. Moreover, older tg/ASA(-/-) mice developed a progressive hind limb paralysis when compared to the ASA(-/-) controls (Fig. 24C). Motor co-ordination abilities of tg/ASA(-/-) mice were tested by performing a rotarod analysis. The experiment was performed with ASA(+/-), tg/ASA(+/-), ASA(-/-), tg/ASA(-/-) mice of different age groups. The experiment was conducted by training the mice for three days on a rotarod and on the fourth day the performance was assessed by recording the number of cumulative falls/minute for each mouse. Analysis of the data indicated no significant difference in the performance of mice that were less than 11-months-old (Fig. 24D). However, older tg/ASA(-/-) mice (21-24 months) was unable to remain on the rod and fell more often than the ASA(-/-) control mice (Fig. 24E). The reason for the poor performance of the tg/ASA(-/-) could be due to hind limb weakness and paralysis of these mice.

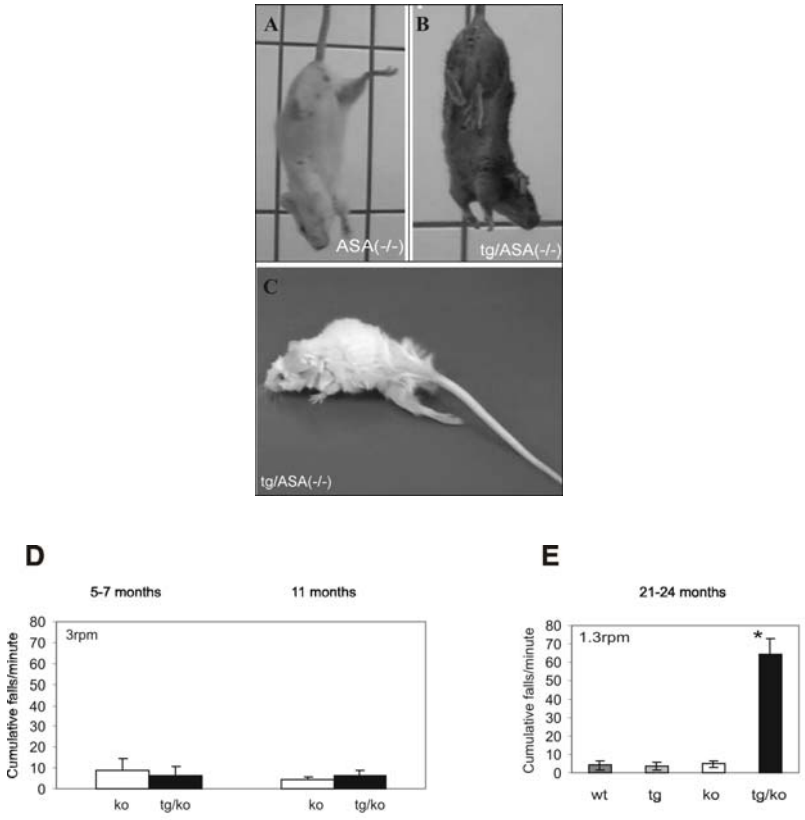

Figure 24: Behavioural analysis of PLP-CST mice. Detection of hind limb weakness (B) tg/ko mouse clasped their hind limbs and folded them towards their body when suspended by their tail when compared to (A) ko mice, which stretched their hind limbs. (C) tg/ko mice when placed on a table showed hind limb weakness and progressive hind limb paralysis. Rotarod analysis was performed on ko, tg/ko, wt and tg animals to analyze their motor co-ordination behaviour by calculating the number of cumulative falls/min. Rotarod analysis of mice up to 11-months-old, ko and tg/ko was performed at 3 rpm (D) and 21-24 months old; ko, tg/ko, wt and tg mice was performed at 1.3 rpm (E). In 11-months-old mice, there was no significant difference in the performance between tg/ko and ko mice (D). When 21-24 months old mice were compared, the performance of tg/ko mice was poor and the mice fell more often from the rod due to hind limb weakness and paralysis when compared to ko mice. There was no significant difference in the performance between the ko, tg and wt animals (E) (* $P<0.05$, determined by Student's t-test). wt-ASA(+/-), tg-tg/ASA(+/-), ko-ASA(-/-), tg/ko-tg/ASA(-/-).

4.2.7 Decrease in myelin basic protein (MBP) expression in tg/ASA(-/-) mice

The effects of increased sulfatide accumulation on myelin and astrogliosis was investigated by performing a Western blot analysis on the brain of ASA(+/-), tg/ASA(+/-), ASA(-/-) and tg/ASA(-/-) mice. Effects on myelin was investigated by analyzing different myelin proteins like MBP, Fyn, CNPase (Fyn and CNPase, only on older mice) and the effects on astrogliosis with GFAP (only on older mice), an astrocyte marker. When 7-months-old mice, were analyzed, there was no significant difference in the MBP level among the different genotypes (Fig. 25A). However, 17-18 months old, tg/ASA(-/-) mice, showed a significant reduction in the MBP level when compared to ASA(-/-), tg/ASA(-/-) and ASA(+/-) mice, from both the transgenic lines, tg2645 (Fig. 25C) and tg2639 (Fig. 25B). No alteration in MBP level was found in 17-18 months old ASA(-/-) mice when compared to wild-type mice. This observation is in accordance with the result obtained previously (Yaghootfam et al., 2005). Thus, a decrease in MBP level in the older tg/ASA(-/-) mice correlates well with demyelination in these mice (Fig. 25B & C). No significant difference was observed in the protein expression level of Fyn, CNPase and GFAP among the four genotypes.

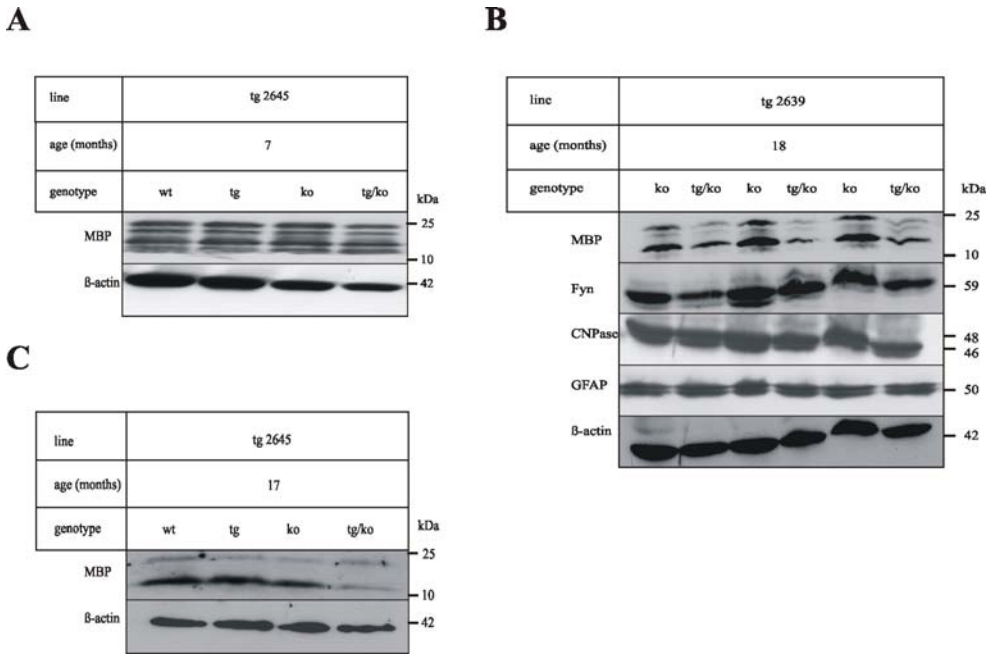

Figure 25: Western blot analysis of brain from PLP-CST mice. 50 µg protein from total brain homogenate was loaded on an SDS-PAGE to analyze the expression of different proteins by Western blotting. (A) Analysis of MBP expression in 7-months-old wt, tg, ko and tg/ko mice. (B) Analysis of MBP, Fyn, CNPase, and GFAP in 17-months-old mice from tg2639 line (n=3) and (C) MBP expression in 18-months-old mice from tg2645 line (n=1). β-actin served to control protein loading. wt-ASA(+/-), tg-tg/ASA(+/-), ko-ASA(-/-), tg/ko-tg/ASA(-/-).

4.2.8 Decrease in nerve conduction velocity in tg/ASA(-/-) mice

Electrophysiological analysis was performed by Dr. Carsten Wessig (University of Würzburg) in sciatic nerves of 21-24 months old PLP-CST mice. tg/ASA(-/-) mice showed a significant decrease in nerve conduction velocity when compared to ASA(-/-) mice. There was no difference in the electrophysiological recordings between the tg/ASA(+/-) and ASA(+/-) mice. Moreover, the F-wave latency (the total time taken for the conduction of a signal, from the region of stimulus in a skeletal muscle to the dorsal root ganglion and back from the dorsal root ganglion to the region of stimulus) was significantly increased in tg/ASA(-/-) mice when compared to ASA(-/-) controls. The compound muscle action potential (CMAP) amplitude in tg/ASA(-/-) mice was significantly reduced (Table 11). The tg/ASA(-/-) mice also showed spontaneous muscle activity in the foot muscles as recorded by electromyography, indicating axonal degeneration in tg/ASA(-/-) mice. No spontaneous activity could be detected in the controls.

Analysis of nerve conduction in sciatic nerve

Table 11

Genotype	***ASA(+/-)***	***tg/ASA(+/-)***	***ASA(-/-)***	***tg/ASA(-/-)***
Age (months)	23 ± 1[a] (n = 3)	22 ± 0 (n = 3)	24 ± 0 (n = 3)	23 ± 1 (n = 5)
NCV (m/s)	42.9 ± 0.5	48.0 ± 0.1	46.6 ± 1.1	28.2 ± 6.4[b]
F-wave latency (ms)	4.7 ± 0.1	5.0 ± 0.3	5.7 ± 0.5[b]	7.6 ± 1.3[b]
CMAP amplitude (mV)	10.9 ± 4.7	16.1 ± 4.0	6.9 ± 3.5	6.3 ± 4.3
Spontaneous activity	0/3[c]	0/3	0/3	5/5

[a]mean ± SD

[b]difference to ASA(+/-) is statistically significant (t-test, $p<0.05$)

[c]number of mice showing spontaneous activity/number of mice examined

4.2.9 Axonal degeneration and demyelination in the nervous system of tg/ASA(-/-) mice

To understand the effects of increased sulfatide storage on myelin, electron microscopic studies were performed by Prof. Lüllmann-Rauch (University of Kiel), in the brain, spinal cord and *N. phrenicus* (peripheral nerve) of 17-18 months old tg/ASA(-/-), ASA(-/-), tg/ASA(+/-) and ASA(+/-) mice. The analysis indicated axonal degeneration, uncompacted

thin myelin formation and demyelination in central and peripheral nervous system in tg/ASA(-/-) mice (Fig. 26D and Fig. 27D & H) when compared to ASA(-/-) mice (Fig. 26C and Fig. 27C & G). Alteration or deformation in the myelin structure was not observed in the tg/ASA(+/-) mice (Fig. 26B and Fig. 27B & F) when compared to ASA(+/-) mice (Fig. 26A and Fig. 27A & E). Altogether, the electron microscopic data indicates demyelination in tg/ASA(-/-) mice in central and peripheral nervous system when compared to ASA(-/-) mice.

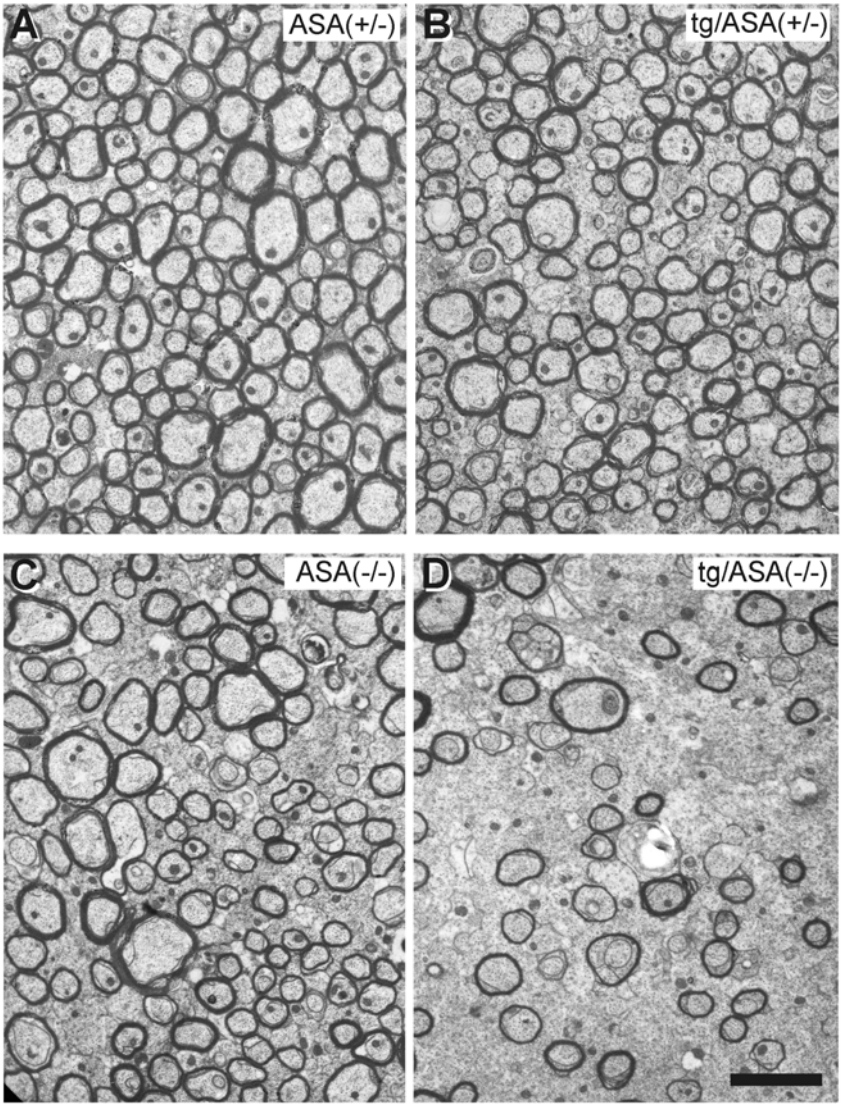

Figure 26: Electron microscopic analysis of corpus callosum from PLP-CST mice. Electron microscopy was performed on corpus callosum of (A) ASA(+/-), (B) tg/ASA(+/-), (C) ASA(-/-)**,** (D) tg/ASA(-/-) mice. The tg/ASA(-/-) electron microscopic picture show several axons with reduced myelin thickness, an indication of demyelination in these mice. (Pictures for electron microscopy were taken by Prof. Lüllmann-Rauch).

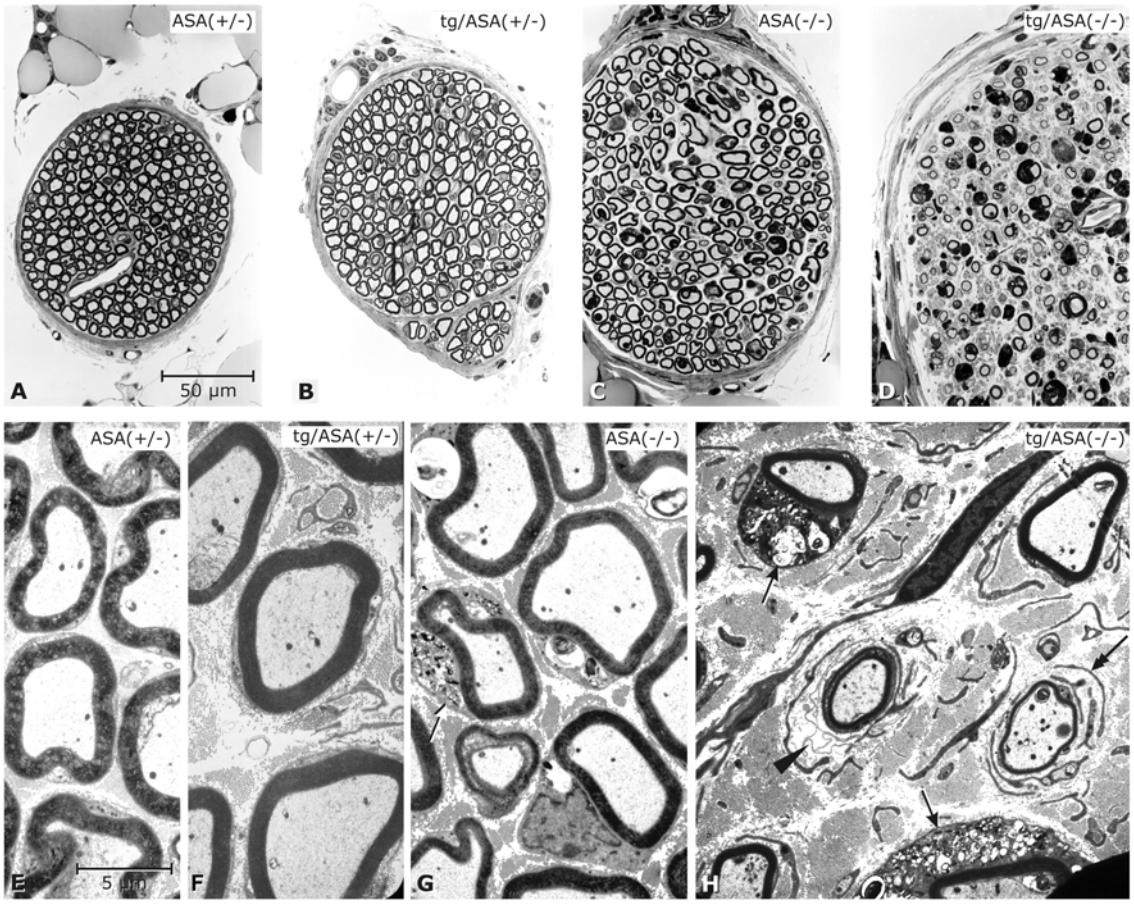

Figure 27: Electron microscopic analysis of *N.phrenicus* from PLP-CST mice. Electron microscopy was performed on *N. phrenicus* (peripheral nerves). (A-D) are lower magnification (50µm) pictures and (E-H) are higher magnification (5µm) pictures of the nerve. (A & E)-ASA(+/-)**,** (B & F)-tg/ASA(+/-)**,** (C & G)-ASA(-/-) and (D & H)-tg/ASA(-/-) mice. (Pictures for electron microscopy were taken by Prof. Lüllmann-Rauch). Scale bars: 50 µm (A-D) and 5 µm (E-H).

4.2.10 Effects of sulfatide accumulation on elongation and initiation factors and TGF-β III receptor

Mutations in elongation factors lead to hypomyelination disorders like vanishing white matter disease (van der Knapp et al., 2002). Hence, in order to investigate whether demyelination due to sulfatide accumulation in tg/ASA(-/-) mice, alters expression of elongation factors and other genes like TGF-β III receptor, a semi quantitative RT-PCR was done on ASA(+/-), tg/ASA(+/-), ASA(-/-) and tg/ASA(-/-) mice. Total RNA was isolated from brain and cDNA was synthesized by performing a reverse transcription reaction on the isolated total RNA. This cDNA was then used for carrying out PCR reactions as described for different elongation factors, initiation factors (eEF2, eIF2, eIF4A2, eIF4b) (Fig. 28A) and TGF-β III receptor (Fig. 28B). β-actin was used for normalizing the mRNA expression level. Analysis of the data

indicated that there was no alteration in the mRNA expression level of elongation factors, initiation factors and TGF-β III receptor.

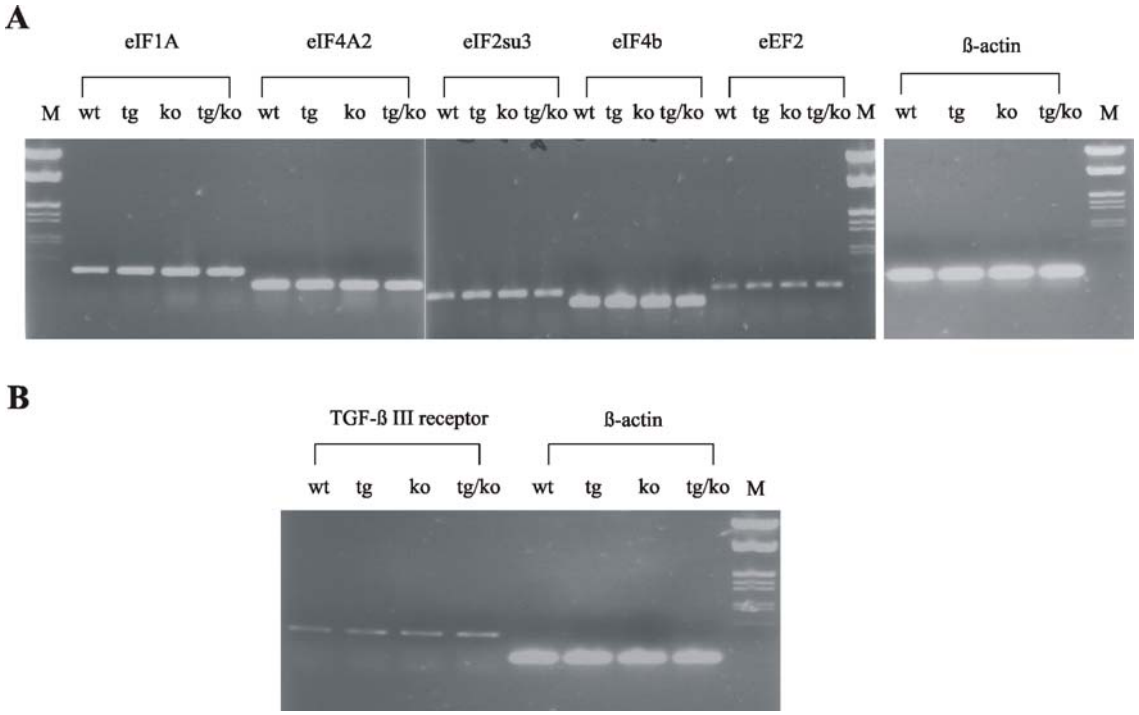

Figure 28: mRNA expression of elongation factors, initiation factors and TGF-β III receptor in PLP-CST mice brain. Brain mRNA was extracted from 17-months-old wt, tg, ko and tg/ko mice. RT-PCR analysis was performed, after reverse transcription, with specific primers. (A) mRNA expression of different elongation and initiation factors (eEF2, eIF2, eIF4A2, eIF4b) and β-actin as normalisation control for mRNA expression of elongation and initiation factors. (B) RT-PCR analysis of TGF-β III receptor with β-actin as normalisation control. M-DNA marker, λ phage DNA cut with *Hind*III/*Eco*RI restriction enzymes. wt-ASA(+/-), tg-tg/ASA(+/-), ko-ASA(-/-), tg/ko-tg/ASA(-/-).

4.2.11 Analysis of axonal nodes and paranodes in tg/ASA(-/-) mice

Electron microscopic analysis of tg/ASA(-/-) mice indicated demyelination and irregular ensheathment of myelin around axons. Electrophysiological studies showed a decrease in the nerve conduction velocity in these mice. Reports from CST knock-out mice indicated that sulfatide is necessary for maintenance of ion channels and formation of paranodal junctions and lack of sulfatide results in redistribution of sodium and potassium channels (Honke et al., 2002; Ishibashi et al., 2002). Hence, in order to investigate the effects of sulfatide accumulation on the nodal and paranodal regions of the axonal membrane, teased fibres of sciatic nerves from ASA(+/-), tg/ASA(+/-), ASA(-/-) and tg/ASA(-/-) were prepared and immunofluorescence staining of paranodin, a paranodal marker (Fig. 29A, D, G & J) and Na^+ channel, a nodal marker (Fig. 29B, E, H & K) was carried out and analysed by fluorescence

microscopy (Fig. 29A-L). Observations of nodes and paranodes indicated no significant alteration in the distribution of Na^+ channel and paranodin in the tg/ASA(-/-) mice when compared to the controls. Analysis of paranodin stainings indicated a diffuse staining pattern in some regions of the sections, which was, however also observed in the controls.

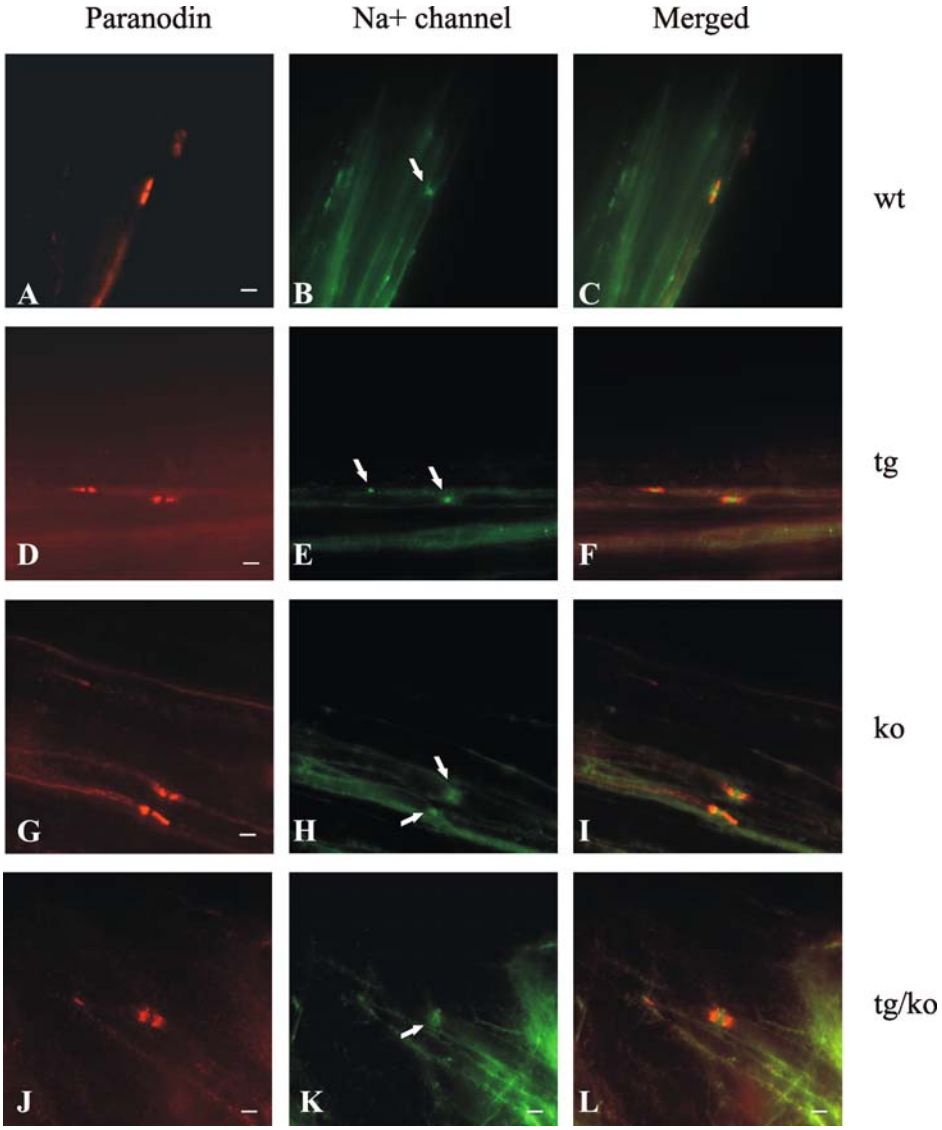

Figure 29: Sodium channel and paranodin stainings of sciatic nerve from PLP-CST mice. The nodal and paranodal regions of the axonal membrane of PLP-CST mice were stained for paranodin (A, D, G & J) and sodium channel (B, E, H & K), respectively. Stainings were done on wt (A, B & C), tg (D, E & F), ko (G, H & I) and tg/ko (J, K & L) mice. (C, F, I & L) represent the merged pictures. wt-ASA(+/-), tg-tg/ASA(+/-), ko-ASA(-/-), tg/ko-tg/ASA(-/-). Scale bar: 5µm (A-L).

5. Discussion

5.1 Role of PSA-NCAM in oligodendrocyte differentiation and myelination

Myelin membrane is an electrically insulating layer that ensheath the axons. Myelin is synthesized by oligodendrocytes in the CNS and Schwann cells in the PNS, respectively. The formation and maintenance of myelin membrane involves biosynthesis and degradation of various lipids, proteins and carbohydrates. De-regulation in the expression of genes involved in these regulatory mechanisms results in changes in myelin formation, structure, maintenance and stability leading to different pathological conditions like demyelination. Proliferation, migration and differentiation of oligodendrocytes are an integral part of myelin biogenesis. Oligodendrocyte maturation and onset of myelination in the central nervous system is regulated by several positive regulators like electrical activity in axons (Barres and Raff, 1993) and cell adhesion molecules and negative regulators like sulfatide (Bansal et al., 1999) and PSA (Charles et al., 2000). Some of these signals are expressed during proliferation and migration and downregulated during maturation of oligodendrocytes. PSA-NCAM is one such negative regulator which is expressed in migratory oligodendrocyte progenitor cells (Wang et al., 1994), whose expression facilitates the cells to respond to external signals spatially and temporally (Rutishauser and Landmesser, 1996).

PSA-NCAM expression is downregulated when oligodendrocytes undergo differentiation to become myelin forming mature oligodendrocytes (Trotter et al., 1989; Bartsch et al., 1990). Downregulation of PSA in oligodendrocytes is proposed to be due to downregulation of PST in oligodendrocytes (Stoykova et al., 2001). Although PSA downregulation plays a role during myelination, the answer to the question whether PSA downregulation is important for oligodendrocyte differentiation and myelination was not clear. Hence, in order to address this question, in this study, transgenic mice overexpressing PST under the control of PLP promoter was generated and analyzed.

Expression of PLP gene is upregulated in differentiated oligodendrocytes. Hence, by expressing PST under the control of PLP promoter, the downregulation of PST is prevented in adult animals and the NCAM-120 in differentiated oligodendrocytes of transgenic mice remain polysialylated. Analysis of transgenic mice indicated an upregulation in transgene expression in postnatal day 1 and 7-week-old animals, with a reduction in the endogenous mRNA (Fig. 4B) in accordance with published results of PST expression in adult mouse brain (Ong et al., 1998). Overexpression of PST led to PSA expression in the white matter regions

of the brain (Fig. 5A). Immunofluorescence stainings of PSA and MBP showed a partial co-localisation of PSA and MBP in oligodendrocytes clearly indicating localization of PSA in myelin (Fig. 6A & B).

Analysis of myelin showed loss of myelin in transgenic mice, which was evident from the reduction in myelin weight in 12-week-old transgenic animals. Despite myelin loss, there were, however, no behavioural deficits observed in the transgenic mice. Structural abnormalities in the transgenic mice, as revealed by electron microscopy, like axonal degeneration, redundant myelination and hypomyelination indicate that myelin formation is affected in these mice (Fewou et al., 2007). Although there was myelin loss and structural abnormalities in myelin, myelin formation did occur in the transgenic mice. This in a way shows that PSA downregulation is not necessarily required for myelin formation. Unstable myelin in the transgenic mice suggests a possible role of PSA in maintenance and stabilization of myelin.

Apart from NCAM several gangliosides are also oligosialylated and gangliosides like GM1 are one of the important components of the myelin membrane. Data from Sheikh et al., (1999) suggest that mice lacking sialylated gangliosides also display axonal degeneration and myelin related abnormalities. Hence, the likelihood of alterations in brain gangliosides in transgenic mice was analyzed, which however indicated no major difference in ganglioside composition between the transgenic and wild-type mice (Fig. 10). Thus, the observations above indicate that most of the effects on myelin due to PST overexpression are a result of polysialylation of NCAM in oligodendrocytes.

In vitro oligodendrocyte cultures from transgenic mice showed no significant difference in differentiation except that there was lower number of branches in oligodendrocyte cultures from transgenic mice when compared to that from wild-type mice (Fig 13A & B). PSA staining in oligodendrocytes from transgenic mice was not only found in the branches and membrane extensions of oligodendrocytes, but was also concentrated around the cell body (Fig. 11 & 12). Such perinuclear localization of PSA was also reported by Franceschini et al., (2004) and Lavdas et al., (2006) who overexpressed PSA by transducing neural precursors or Schwann cells with retroviral vectors encoding PST or STX, respectively.

Extension of cellular processes during oligodendrocyte differentiation is essential for myelination. During the process of oligodendrocyte differentiation, cytoskeletal rearrangement occurs in these cells, characterized by an extended branched morphology in differentiated oligodendrocytes. Data from Klein et al., (2002) showed that interaction of Fyn kinase with cytoskeletal protein Tau promotes process outgrowth of oligodendrocytes. Tau is

a microtubule associated protein that has been shown to induce microtubule assembly and bundle formation leading to process formation in oligodendrocytes (Brandt, 1996). Published reports show compartmentalization of NCAM-120 and Fyn kinase in the lipid rafts of oligodendrocytes (Kramer et al., 1999). Hence, it is quite likely that in oligodendrocyte cultures from transgenic mice due to overexpression of PST, the interaction between PSA-NCAM and Fyn kinase is affected causing interference in the Fyn-Tau-microtubule interactions, resulting in a lower number of branches in these oligodendrocytes. Further experiments need to be performed to verify this hypothesis.

PSA-NCAM is synthesized in the trans-Golgi network and transported via vesicles to the membrane. In the cultures from transgenic oligodendrocytes, NCAM co-localized with PSA in the membrane extensions but not in the perinuclear region (Fig. 16). Moreover, the overall distribution of NCAM or other glycosylated proteins like MAG were not altered in these cultures (Fig. 14, 16 & 17). Since, the distribution and expression of NCAM was not altered, it is quite likely that other proteins apart from NCAM could carry PSA. Published reports show that PST is autopolysialylated both *in vivo* and *in vitro*. *In vitro* studies with COS-1 cells show that autopolysialylated PST localises to the Golgi apparatus and cell surface of these cells (Mühlenhoff et al., 1996; Close et al., 1998). Although autopolysialylation of PST is not required for NCAM polysialylation, it does enhance NCAM polysialylation (Close et al., 2001). Since PST is overexpressed in the transgenic mice, the possibility of autopolysialylation of PST in these transgenic oligodendrocytes is quite likely. This autopolysialylated PST might localize around the Golgi apparatus and the perinuclear region as observed in the transgenic oligodendrocytes.

Increase in PSA expression on NCAM-120 led to a decrease in the number of differentiated oligodendrocytes in the corpus callosum of PLP-PST mice. This was evident from the *in situ* hybridisation analysis of 1-week-old mouse brains for mature oligodendrocyte markers like PLP (Fewou, 2005), MBP and MAG (Fig. 8). Although PLP is a marker for mature oligodendrocytes a subset of OPCs also express an isoform of PLP, namely DM-20 (Spassky et al., 1998). Hence, the decrease in differentiated PLP positive cells could actually be a decrease in this subset of OPCs. But, analysis of other markers of mature oligodendrocytes, other than PLP, like MBP and MAG, also showed a reduction in the number of oligodendrocytes expressing these markers in the corpus callosum of 1-week-old PST transgenic mice. This in a way indicates a decrease in the number of differentiated oligodendrocytes in the 1-week-old PLP-PST transgenic mice. However, analysis of 4-week-old mice did not show a significant decrease in PLP expressing cells (Fewou, 2005).

Altogether, these results indicate the possibility of a delay in differentiation of oligodendrocytes in 1-week-old mice, which at later time points is compensated by an increase in the differentiation process to reach normal values.

Presence of PSA on NCAM is known to decrease NCAM mediated membrane-membrane interactions (Rutishauser, 1998). Moreover, removal of PSA can enhance the interactions between NCAM and NCAM or NCAM and other cell adhesion molecules like L1, NgCAM, cadherins and receptors like FGF receptors. PSA in general is believed to cause steric inhibition of membrane-membrane apposition causing a decrease in cell adhesion (Rutishauser and Landmesser, 1996) by either preventing interaction of NCAM on two adjacent cells or the same cell or by NCAM-independent interactions (Fujimoto et al., 2001). This in a way could influence the membrane-membrane adhesion and change the intercellular space upon removal of PSA-NCAM or influence clustering of NCAM.

The exact role of PSA-NCAM in myelination is still not clear. The persistence of PSA expression in oligodendrocytes could interfere with NCAM interactions within the oligodendrocytes as well as between oligodendrocytes and neurons. Moreover, as mentioned above, the interaction of NCAM and other adhesion molecules and receptors could also be altered. NCAM along with cadherins and other members of the immunoglobulin superfamily like L1 and MAG play a role in axon-glia interactions (Doyle and Colman, 1993; Payne et al., 1996). PSA-NCAM on axons acts as a negative regulator of myelination (Charles et al., 2000). Since axon-oligodendrocyte interaction is critical for myelination, PSA overexpression in oligodendrocytes could lead to disruption of homophilic NCAM-NCAM or heterophilic NCAM-cell adhesion molecules interactions between oligodendrocytes and axons. This could have an impact in the adhesion and ensheathment of myelin sheath around axons, despite the formation of myelin sheath, leading to improper myelin compaction and myelin instability as observed in the transgenic mice.

The involvement of PSA in signal transduction cascades, besides modulating homophilic/heterophilic interactions has been recently reported. Role of PSA in brain derived neurotrophic factor (BDNF) signalling cascade in cortical neuron differentiation (Vutskis et al., 2001) and in long term potentiation (Muller et al., 2000) has been reported. Seidenfaden et al., (2003) reported that EndoN removal of PSA from NCAM activates the MAP kinase pathway in neuroblastoma and rhabdomyosarcoma cell lines. The exact mechanism as to how PSA is involved in oligodendrocyte differentiation and myelination is far from clear. Although an anti-adhesive property of PSA on NCAM is one explanation, the other possibility could be due to alterations in signaling cascades. Kramer et al., (1999) showed that

NCAM-120 is compartmentalized in the same subdomain of lipid rafts as Fyn kinase in oligodendrocytes and the possibility of NCAM interacting with Fyn could lead to activation of the src, non receptor tyrosine kinase, pathway. Published data show that activation of Fyn kinase is required for oligodendrocyte differentiation (Osterhout et al., 1999; Klein et al., 2002). Hence, the possibility of interaction of NCAM with Fyn kinase needs to be studied further to substantiate this hypothesis. A detailed analysis of the interaction partners and signaling cascades involved in myelination would definitely shed more light on the mechanisms of how PSA-NCAM mediates oligodendrocyte differentiation and myelination.

Altogether, it is clear from the above results that PSA downregulation is important but not a prerequisite for oligodendrocyte differentiation and myelin formation and its presence in myelin interferes with myelin maintenance and stability.

Published results suggest that PSA-NCAM facilitates oligodendrocyte migration (Decker et al., 2000; Franceschini et al., 2004). Since, oligodendrocyte migration is a key step in the process of myelination, it will be interesting to observe whether overexpression of PST increases the migratory potential of oligodendrocytes.

PST expression is not limited to oligodendrocytes of CNS but is also prominently expressed in Schwann cells of PNS. Analysis of changes in peripheral nervous system myelin and Schwann cell migration, differentiation and myelination will enable to better understand the function and regulation of PSA-NCAM in CNS and PNS respectively.

5.2 Effect of increased sulfatide accumulation in ASA(-/-) mice and its significance to MLD

The differentiation of oligodendrocytes to mature myelin forming cells involves synthesis of variety of lipids and proteins. The myelin membrane is composed of 70% lipids and 30% proteins (Baumann and Pham-Dinh, 2001). Of the different lipids, glycosphingolipids like sulfatide and GalC play a crucial role in myelin formation, maintenance and stability (Bosio et al., 1996; Coetzee et al., 1996; Honke et al., 2002). De-regulation in the degradation pathways of these lipids can lead to severe myelin associated disorders like MLD (von Figura et al., 2001).

Sulfatide storage is a critical step for the disease manifestation in humans. ASA(-/-) mice show only 1.4-fold increase in sulfatide at 2 years of age (Saravanan et al., 2004) when compared to late infantile MLD patients where sulfatide levels are increased 3 to 4-fold (Kolodny, 1995). In adult MLD patients, there is only less than 2-fold increase in sulfatide (von Figura et al., 2001), possibly due to residual ASA activity in these patients. Hence,

ASA(-/-) mice exhibit sulfatide storage that is less than that in infantile MLD, which could probably be contributing to the lack of demyelination in the older mice. Therefore, an animal model that exhibits increased sulfatide storage and the characteristic symptoms of the patients including demyelination can enable us to better understand and elucidate the molecular mechanisms and treatment options of the disease. Therefore, to increase sulfatide storage, an improved mouse model was generated by overexpressing cerebroside sulfotransferase (CST) gene under the control of the PLP promoter in ASA(-/-) mice, so that these mice [tg/ASA(-/-)] accumulate an increased amount of sulfatide in oligodendrocytes.

Analysis of transgenic mice revealed an increase in transgene expression in the brain of tg/ASA(-/-) mice (Fig. 18B). CST assay showed a substantial increase in CST activity in the transgenic mice when compared to wild-type controls (Fig. 20). Comparison of CST activity between tg mice at 3-weeks and 3-6 months of age showed that at 3-weeks, CST activity is higher when compared to 3-6 months of age. The activity of PLP promoter in mice reaches its peak at around 3-weeks postnatal; consequently, PLP mRNA expression also reaches a maximum at around 3-weeks. On the other hand the expression of CST mRNA is maximum at postnatal day-14, followed by a decrease in its expression at later time points (Yaghootfam et al., 2005). Hence, the higher CST activity of tg mice at 3-weeks is due to the maximum PLP promoter activity at this time point when compared to tg animals at 3-6 months of age, at which time point the PLP promoter activity is decreased.

Lipid analysis of tg/ASA(-/-) mice showed a 1.7 to 2-fold increase in sulfatide level in 7-months and 1.4-fold increase in 18-months-old mice brain when compared to ASA(-/-) mice (Fig. 22). Lipid analysis of sciatic nerve from 18-month-old tg/ASA(-/-) animals showed a 1.5-fold increase in sulfatide level when compared to ASA(-/-) mice (Fig. 23). Although the concentration of sulfatide in the tg/ASA(-/-) mice increased with age (7-months - ~10µg/mg wet weight when compared to 18-months - ~25µg/mg wet weight), there was a reduction in the relative net sulfatide accumulation between the tg/ASA(-/-) and ASA(-/-) mice of 7-months and 18-months (from 2-fold to 1.4-fold). The reason for this reduction could be due to the demyelination in older animals resulting in a loss of myelin membrane. However, it was interesting to observe that the tg/ASA(+/-) mice did not show a significant increase in sulfatide level when compared to wt/ASA(+/-) mice, despite the nearly 60 to 200-fold increase in CST activity. This shows that CST activity may not be the limiting factor for sulfatide synthesis. Moreover, this also in a way highlights the complex biochemical mechanisms regulating lipid synthesis. One reason for a no increase in sulfatide level in tg/ASA(+/-) mice can be that there is an increase in the turnover of sulfatide in tg/ASA(+/-)

mice. Reports from Burkart et al., (1981) show that during the active period of myelination in mice, a pool from the synthesized sulfatide is transported via vesicles to the lysosomes and rapidly degraded in the lysosomes before getting incorporated into the myelin membrane. Normally sulfatide is transported from the Golgi apparatus to the myelin membrane via vesicles and from the myelin membrane sulfatide is endocytosed and then transported to lysosomes for the degradation of sulfatide. Hence, it is possible that in the tg/ASA(+/-) mice, sulfatide from the synthesized pool is transported directly to the lysosomes for degradation thereby increasing the turnover of sulfatide. The alternate explanation can be that there is a decrease in ceramide synthesis leading to the decreased GalC synthesis, so that, GalC becomes the limiting factor. One cannot also rule out the possibility of a reduction in sulfate donor PAPS, so that there is inefficient transfer of sulfonate group to GalC, leading to decreased sulfatide accumulation than expected. This scenario is also true for CGT transgenic mice which showed only a marginal increase in GalC and a reduction in sulfatide level despite signficant increase in CGT activity (Fewou et al., 2005).

In MLD patients, along with the increase in sulfatide accumulation, a decrease in GalC level has been observed, indicating the metabolic alterations as a result of sulfatide accumulation. Since both GalC and sulfatide levels are altered in patients, the most sensitive indicator for alterations in lipid metabolism is not the absolute amount of sulfatide stored, but the ratio of GalC:sulfatide (von Figura, 2001). GalC:sulfatide ratio in humans decreases from 4 in normal white matter to 0.5 in MLD patients (Norton and Poduslo, 1982). In accordance to that reported for patients, the GalC:sulfatide ratio in tg/ASA(-/-) mice was also significantly reduced in both younger and older animals to nearly 1 and 0.5 respectively (Fig. 22). The exact reason for this decrease in GalC level is still not clear. The possible explanation can be that, as a result of sulfatide accumulation, the GalC synthesis is somehow inhibited. Thus, it is clear that the tg/ASA(-/-) mice accumulate sulfatide to significantly higher levels in both central and peripheral nervous system compared to ASA(-/-) mice and show a reduction in GalC:sulfatide ratio, a key indicator of the disease.

The main clinical manifestations of MLD patients include ataxia, tremors, dementia, postural abnormalities and progressive spastic quadriparesis (weakening of all four limbs). Increased sulfatide storage in older tg/ASA(-/-) mice resulted in behavioural abnormalities like motor co-ordination deficits, progressive hind-limb weakness, decreased nerve conduction velocity and paralysis akin to MLD patients which is in contrast to the mild behavioural phenotypes observed in 2-year-old ASA(-/-) mice (Fig. 24). Electrophysiological studies also showed a decreased muscle action potential and spontaneous muscle activity, which could indicate

axonal degeneration and muscle denervation in the peripheral nervous system (Table 11). It still remains to be verified whether tg/ASA(-/-) mice also display any forms of memory deficits like MLD patients. Though the tg/ASA(-/-) mice undergo progressive demyelination, the average life span of these mice when compared to ASA(-/-) mice was not significantly different.

Electron microscopic analysis of tg/ASA(-/-) mice indicated demyelination, axonal degeneration and uncompacted myelin in both central and peripheral nerves (Fig. 26 & 27). Many storage granules containing sulfatide were also observed, resembling the metachromatic granules seen in MLD patients. These storage materials could be phagocytic macrophages engulfing the degenerated myelin. Regions of uncompacted and thin myelin sheaths are indications for demyelination and remyelination in these mice. From the analysis of the neuropathological symptoms, the behavioural deficits in tg/ASA(-/-) mice could be attributed to demyelination in central and peripheral nervous system, as a result of sulfatide storage.

Comparison of MBP protein levels in 7-months-old tg/ASA(-/-) and ASA(-/-) mice showed no difference in the protein expression. However, MBP protein expression was reduced in 17-18 month old tg/ASA(-/-) animals when compared to ASA(-/-) mice. The reduction in MBP levels in 17-18 months old mice suggests demyelination in these mice. As there was no change in the GFAP expression level, astrogliosis could not be detected at least at the biochemical level in the tg/ASA(-/-) mice (Fig. 25).

The ultimate goal of an animal model for MLD is to understand the molecular mechanisms of the disease and explore the therapeutic options for MLD. Therapeutic interventions have been tried successfully for lysosomal storage diseases like e.g. Fabry disease, Tay-Sachs disease and Krabbe's disease (Gieselmann et al., 2003). Till date, though therapies like bone marrow stem cell based gene therapy (Matzner et al., 2000; Matzner et al., 2002) and enzyme replacement therapy (Matzner et al., 2005) have been proposed and tested on ASA(-/-) mice as a possible cure for MLD, due to lack of demyelination in the nervous system of these mice, the significance of ASA(-/-) mouse model for therapy related research is still debatable. The main setback in the treatment of MLD is the inability of ASA to effectively cross the blood brain barrier of the CNS. Enzyme replacement therapy in ASA(-/-) mice led to a major reduction in sulfatide only in peripheral nerves and to a small extent in CNS. The reduction in CNS is mainly due to sulfatide clearance from phagocytes representing activated microglial cells rather than from neurons or oligodendroglia (Matzner et al., 2005). Hence, demyelination in MLD per se may not be effectively treated with enzyme replacement therapy. In contrast to ASA(-/-) mice, tg/ASA(-/-) mice display progressive demyelination in

both CNS and PNS. Electron microscopy revealed hypertrophic neuropathy, axons surrounded by Schwann cells without myelin, and axons surrounded by uncompacted myelin in the peripheral nervous system. These observations indicate that tg/ASA(-/-) mice have the capacity to remyelinate demyelinated axons. Though the problems associated with gene therapy or enzyme replacement therapy (ERT) are still valid, hints of remyelination in tg/ASA(-/-) mice, opens some new possibilities for treatment.

The possible signs of demyelination and remyelination in tg/ASA(-/-) mice open the possibility of analyzing the expression of PSA-NCAM in these mice. Reports from multiple sclerosis patients suggest that PSA-NCAM expression is an inhibitor of remyelination in the patients (Charles et al., 2002). Hence, from an academic and therapeutic point of view, it is interesting to analyse whether PSA-NCAM is re-expressed in demyelinated axons of tg/ASA(-/-) mice and if so whether removal of PSA-NCAM facilitates remyelination in these mice.

Although tg/ASA(-/-) mice show increased accumulation of sulfatide and demyelination, one cannot neglect the fact that CST transgene is overexpressed leading to 60 to 200-fold higher CST activity in these mice. It cannot be ruled out completely that such an increase in transgene expression could induce stress in the cells of these animals, thereby inducing the expression of stress induced proteins like heat shock proteins or cytokines like TNF-α.

In many of the lysosomal storage disorders, the connection between lipid metabolism and demyelination is far from clear, especially in MLD, where sulfatide accumulation leads to progressive demyelination. Sulfatide storage is not just limited to the lysosomes but also to the lipid rafts in the plasma membrane, particularly myelin (Eto et al., 1976; Malone et al., 1966; Poduslo et al., 1982). Sulfatide plays an important role in signal transduction cascades, myelin formation, maintenance and function. Hence, sulfatide increase, as in MLD, can alter the raft stoichiometry and distribution of raft associated lipids and proteins. Recent reports suggest that sulfatide storage leads to a negative regulation of myelin and lymphocyte (MAL) protein synthesis (Saravanan et al., 2004), demonstrating a link between the regulatory mechanisms of lipid and protein synthesis. MAL is a myelin proteolipid protein that binds to glycosphingolipids, particularly sulfatide. Both sulfatide and MAL are part of lipid rafts in myelin. Analysis of tg/ASA(-/-) show a decrease in MBP level. This decrease could be due to demyelination observed in these mice. Hence, it will be more interesting to analyse the expression of MAL protein in the tg/ASA(-/-) mice, because MAL has been shown to be required for proper maintenance of myelin and stability of axon-glia interactions (Schaeren-Wiemers et al., 2004). Altogether, it is possible that transport of MAL to lipid rafts of myelin

membrane is interfered due to increase in sulfatide accumulation and disrupts the myelin stability.

Reports from Brown et al., (1993) show that sulfatide and proteolipid protein (PLP) are co-transported in vesicles to the myelin membrane. The fact that both sulfatide and PLP are transported in very close association highlights the significance of this lipid-protein interactions. PLP is a myelin protein that plays an important role in stabilizing membrane junctions after compaction. Hence, it is quite possible that any changes in the metabolism of sulfatide could affect the metabolism of PLP, thereby affecting myelin stability and compaction.

In conclusion, tg/ASA(-/-) mice is the first improved mouse model of MLD with increased sulfatide storage, leading to progressive demyelination both in CNS and PNS and exhibiting the neuropathological symptoms like hindlimb weakness, paralysis, slow nerve conduction velocity and hypertrophic peripheral neuropathy similar to human MLD patients. Further analysis of these mice would enable to better understand and resolve the molecular mechanisms of the disease, besides, exploring the therapeutic options for MLD patients with this mouse as a model system.

6. References

Alcaraz G. and Goridis C. (1991) Biosynthesis and processing of polysialylated NCAM by AtT-20 cells. Eur J Cell Biol. 55(1):165-73.

Baader S.L, Sanlioglu S., Berrebi A.S., Parker-Thornburg J., Oberdick J. (1998) Ectopic overexpression of engrailed-2 in cerebellar Purkinje cells causes restricted cell loss and retarded external germinal layer development at lobule junctions. J Neurosci. 18(5):1763-73.

Bansal R., Winkler S., Bheddah S. (1999) Negative regulation of oligodendrocyte differentiation by galactosphingolipids. J. Neurosci. 19(18):7913-24.

Barres B.A. and Raff M.C. (1993) Proliferation of oligodendrocyte precursor cells depends on electrical activity in axons. Nature. 361(6409):258-60.

Barthels D., Santoni M.J., Wille W., Ruppert C., Chaix J.C., Hirsch M.R., Fontecilla-Camps J.C., Goridis C. (1987) Isolation and nucleotide sequence of mouse NCAM cDNA that codes for a Mr 79,000 polypeptide without a membrane-spanning region. EMBO J. 6(10):3202.

Bartsch U., Kirchhoff F., Schachner M. (1990) Highly sialylated N-CAM is expressed in adult mouse optic nerve and retina. J. Neurocytol. 19(4):550-65.

Bartsch U., Faissner A., Trotter J., Dorries U., Bartsch S., Mohajeri H., Schachner M. (1994) Tenascin demarcates the boundary between the myelinated and nonmyelinated part of retinal ganglion cell axons in the developing and adult mouse. J. Neurosci. 14(8):4756-68.

Baumann N and Pham-Dinh D. (2001) Biology of oligodendrocyte and myelin in the mammalian central nervous system. Physiol Rev. 81(2):871-927.

Becker C.G., Artola A., Gerardy-Schahn R., Becker T., Welzl H., Schachner M. (1996) The polysialic acid modification of the neural cell adhesion molecule is involved in spatial learning and hippocampal long-term potentiation. J. Neurosci Res. 45(2):143-52.

Beggs H.E., Baragona S.C., Hemperly J.J., Maness, P.F. (1997) NCAM140 interacts with the focal adhesion kinase p125(fak) and the SRC-related tyrosine kinase p59(fyn). J. Biol. Chem. 272, 8310–8319.

Bhat S. and Silberberg D.H. (1986) Oligodendrocyte cell adhesion molecules are related to neural cell adhesion molecule (N-CAM). J. Neurosci. 6(11):3348-54.

Boison D., Stoffel W. (1994) Disruption of the compacted myelin sheath of axons of the central nervous system in proteolipid protein-deficient mice. Proc Natl Acad Sci U S A. 91(24):11709-13.

Boison D., Bussow H., D'Urso D., Muller H.W., Stoffel W. (1995) Adhesive properties of proteolipid protein are responsible for the compaction of CNS myelin sheaths. J. Neurosci. 15(8):5502-13.

Bosio A., Binczek E., Stoffel W. (1996) Functional breakdown of the lipid bilayer of the myelin membrane in central and peripheral nervous system by disrupted galactocerebroside synthesis. Proc Natl Acad Sci U S A. 93(23):13280-5.

Brandt R. (1996) The tau proteins in neuronal growth and development. Front Biosci. 1:d118-30.

Brown M.C., Besio Moreno M., Bongarzone E.R., Cohen P.D., Soto E.F., Pasquini J.M. (1993) Vesicular transport of myelin proteolipid and cerebroside sulfates to the myelin membrane. J Neurosci Res. 35(4):402-8.

Bunge M.B., Bunge R.P., Pappas G.D. (1962) Electron microscopic demonstration of connections between glia and myelin sheaths in the developing mammalian central nervous system. J. Cell Biol. 12:448-53.

Bunge R.P. (1968) Glial cells and the central myelin sheath. Physiol Rev. 48(1):197-251.

Bunge R.P. and Fernandez-Valle. (1995) Neuroglia, edited by Kettenmann H. and Ransom B.R., New York: Oxford Univ. Press. p. 44-57.

Burkart T., Hofmann K., Siegrist H.P., Herschkowitz N.N., Wiesmann U.N. (1981) Quantitative measurement of in vivo sulfatide metabolism during development of the mouse brain: evidence for a large rapidly degradable sulfatide pool. Dev Biol. 83(1):42-8.

Burkart T., Caimi L., Siegrist H.P., Herschkowitz N.N., Wiesmann U.N. (1982) Vesicular transport of sulfatide in the myelinating mouse brain. Functional association with lysosomes? J. Biol. Chem. 257(6):3151-6.

Burne J.F., Staple J.K., Raff M.C. (1996) Glial cells are increased proportionally in transgenic optic nerves with increased numbers of axons. J. Neurosci. 16(6):2064-73.

Butt A.M., Ibrahim M., Ruge F.M., Berry M. (1995) Biochemical subtypes of oligodendrocyte in the anterior medullary velum of the rat as revealed by the monoclonal antibody Rip. Glia. 14(3):185-97.

Charles P., Hernandez M.P., Stankoff B., Aigrot M.S., Colin C., Rougon G., Zalc B., Lubetzki C. (2000) Negative regulation of central nervous system myelination by polysialylated-neural cell adhesion molecule. Proc Natl Acad Sci U S A. 97(13):7585-90.

Charles P., Reynolds R., Seilhean D., Rougon G., Aigrot M.S., Niezgoda A., Zalc B., Lubetzki C. (2002) Re-expression of PSA-NCAM by demyelinated axons: an inhibitor of remyelination in multiple sclerosis? Brain. 125(Pt 9):1972-9.

Close B. E. and Colley K. J. (1998) In vivo autopolysialylation and localization of the polysialyltransferases PST and STX. J. Biol. Chem. 273, 34586-34593

Close B.E., Wilkinson J.M., Bohrer T.J., Goodwin C.P., Broom L.J., Colley K.J. (2001) The polysialyltransferase ST8Sia II/STX: posttranslational processing and role of autopolysialylation in the polysialylation of neural cell adhesion molecule. Glycobiology. (11):997-1008.

Coetzee T., Fujita N., Dupree J., Shi R., Blight A., Suzuki K., Suzuki K., Popko B. (1996) Myelination in the absence of galactocerebroside and sulfatide: normal structure with abnormal function and regional instability. Cell. 86(2):209-19.

Cremer H., Lange R., Christoph A., Plomann M., Vopper G., Roes J., Brown R., Baldwin S., Kraemer P., Scheff S., Barthels D., Rajewsky K., Wille W. (1994) Inactivation of the N-CAM gene in mice results in size reduction of the olfactory bulb and deficits in spatial learning. Nature. 367(6462):455-9.

Crossin K.L. and Krushel L.A. (2000) Cellular signaling by neural cell adhesion molecules of the immunoglobulin superfamily. Dev. Dyn. 218, 260–279.

Cunningham B.A., Hemperly J.J., Murray B.A., Prediger E.A., Brackenbury R., Edelman G.M. (1987) Neural cell adhesion molecule: structure, immunoglobulin-like domains, cell surface modulation and alternative RNA splicing. Science. 236(4803):799-806.

Decker L., Avellana-Adalid V., Nait-Oumesmar B., Durbec P., Baron-Van Evercooren A. (2000) Oligodendrocyte precursor migration and differentiation: combined effects of PSA residues, growth factors, and substrates. Mol Cell Neurosci. 16(4):422-39.

de Ferra F., Engh H., Hudson L., Kamholz J., Puckett C., Molineaux S., Lazzarini R.A. (1985) Alternative splicing accounts for the four forms of myelin basic protein. Cell. 43:721-7.

D'Hooge R., Hartmann D., Manil J., Colin F., Gieselmann V., De Deyn P.P. (1999) Neuromotor alterations and cerebellar deficits in aged arylsulfatase A-deficient transgenic mice. Neurosci Lett. 273(2):93-6.

Dierks T., Schmidt B., von Figura K. (1997) Conversion of cysteine to formylglycine: A protein modification in the endoplasmic reticulum. Proc Natl Acad Sci. 94: 11963-68.

Doetsch F., Garcia-Verdugo J.M., Alvarez-Buylla A. (1997) Cellular composition and three-dimensional organization of the subventricular germinal zone in the adult mammalian brain. J. Neurosci. 17(13):5046-61

Doyle E., Nolan P.M., Bell R., Regan C.M. (1992) Hippocampal NCAM180 transiently increases sialylation during the acquisition and consolidation of a passive avoidance response in the adult rat. J. Neurosci Res. 31(3):513-23.

Doyle J.P. and Colman D.R. (1993) Glial-neuron interactions and the regulation of myelin formation. Curr Opin Cell Biol. 5(5):779-85.

Eckhardt M., Muhlenhoff M., Bethe A., Koopman J., Frosch M., Gerardy-Schahn R. (1995) Molecular characterization of eukaryotic polysialyltransferase-1. Nature. 373(6516):715-8.

Eckhardt M., Gerardy-Schahn R. (1998) Genomic organization of the murine polysialyltransferase gene ST8SiaIV (PST-1). Glycobiology. 8(12):1165-72.

Eckhardt M., Fewou S.N., Ackermann I., Gieselmann V. (2002) N-glycosylation is required for full enzymic activity of the murine galactosylceramide sulphotransferase. Biochem J. 368(Pt 1):317-24.

Eto Y., Meier C., Herschkowitz N.N. (1976) Chemical compositions of brain and myelin in two patients with multiple sulphatase deficiency (a variant form of metachromatic leukodystrophy). J. Neurochem. 27, 1071–1076.

Fedokova L., Rutishauser U., Prosser R., Shen H., Glass J.D. (2002) Removal of polysialic acid from the SCN potentiates nonphotic circadian phase resetting. Physiol Behav. 77(2-3):361-9.

Fewou S.N. (2005) Functional impacts of transgenic overexpression of UDP-galactose: ceramide galactosyl transferase and polysialyltransferase on the development of oligodendrocytes and myelin maintenance Dissertation. p. 92-110., p. 39-56.

Fewou S.N, Büssow H., Schaeren-Wiemers N., Vanier M.T., Macklin W.B., Gieselmann V., Eckhardt M. (2005) Reversal of non-hydroxy:alpha-hydroxy galactosylceramide ratio and

unstable myelin in transgenic mice overexpressing UDP-galactose:ceramide galactosyltransferase. J. Neurochem 94:469-481.

Fewou S.N., Ramakrishnan H., Bussow H., Gieselmann V., Eckhardt M. (2007) Down-regulation of polysialic acid is required for efficient myelin formation. J Biol Chem. 282(22):16700-11.

Filbin M.T. (1996). The muddle with MAG. Mol Cell Neurosci. 8(2-3):84-92.

Finne J., Finne U., Deagostini-Bazin H., Goridis C. (1983). Occurrence of alpha 2-8 linked polysialosyl units in a neural cell adhesion molecule Biochem Biophys Res Commun. 112(2):482-7.

Finne J., Bitter-Suermann D., Goridis C., Finne U. (1987) An IgG monoclonal antibody to group B meningococci cross-reacts with developmentally regulated polysialic acid units of glycoproteins in neural and extraneural tissues. J. Immunol. 138(12):4402-7.

Frail D.E., Webster H.D., Braun P.E. (1985) Developmental expression of the myelin-associated glycoprotein in the peripheral nervous system is different from that in the central nervous system. J. Neurochem. 45(4):1308-10.

Franceschini I., Vitry S., Padilla F., Casanova P., Tham T.N., Fukuda M., Rougon G., Durbec P., Dubois-Dalcq M. (2004) Migrating and myelinating potential of neural precursors engineered to overexpress PSA-NCAM. Mol Cell Neurosci. 27(2):151-62.

Friedman B., Hockfield S., Black J.A., Woodruff K.A., Waxman S.G. (1989) In situ demonstration of mature oligodendrocytes and their processes: an immunocytochemical study with a new monoclonal antibody, rip. Glia. 2(5):380-90.

Fuda H. Shimizu C. Lee Y.C., Akita H., Strott C.A. (2002) Characterization and expression of human bifunctional 3'-phosphoadenosine 5'-phosphosulphate synthetase isoforms. Biochem J. 365(Pt 2):497-504.

Fujimoto I., Bruses J. L., Rutishauser U. (2001) Regulation of cell adhesion by polysialic acid: Effects on cadherin, IgCAM and integrin function and independence from NCAM binding or signaling activity. J. Biol.Chem. 276:31745–31751.

Gard A.L. and Pfeiffer S.E. (1993) Glial cell mitogens bFGF and PDGF differentially regulate development of O4+GalC- oligodendrocyte progenitors. Dev Biol. 159(2):618-30.

Gennarini G., Hirsch M.R., He H.T., Hirn M., Finne J., Goridis C. (1986) Differential expression of mouse neural cell-adhesion molecule (N-CAM) mRNA species during brain development and in neural cell lines. J. Neurosci. 6(7):1983-90.

Gieselmann V., Matzner U., Hess B., Lullmann-Rauch R., Coenen R., Hartmann D., D'Hooge R., DeDeyn P., Nagels G. (1998) Metachromatic leukodystrophy: molecular genetics and an animal model. J. Inherit Metab Dis. 21(5):564-74.

Gieselmann V., Matzner U., Klein D., Mansson J.E., D'Hooge R., DeDeyn P.D., Lullmann Rauch R., Hartmann D., Harzer K. (2003) Gene therapy: prospects for glycolipid storage diseases. Philos Trans R Soc Lond B Biol Sci. 358(1433):921-5.

Goridis C., Deagostini-Bazin H., Hirn M., Hirsch M.R., Rougon G., Sadoul R., Langley O.K., Gombos G., Finne J. (1983) Neural surface antigens during nervous system development. Cold Spring Harb Symp Quant Biol. 48 Pt 2:527-37.

Gravel M., Peterson J., Yong V.W., Kottis V., Trapp B., Braun P.E. (1996) Overexpression of 2939-cyclic nucleotide 39phosphodiesterase in transgenic mice alters oligodendrocyte development and produces aberrant myelination. Mol Cell Neurosci. 6: 453–466, 1996.

Hardy R. and Reynolds R. (1993) Rat cerebral cortical neurons in primary culture release a mitogen specific for early (GD3+/04-) oligodendroglial progenitors. J. Neurosci Res. 34(5):589-600.

Harrison R.G. (1924) Neuroblast versus cell sheath in the development of peripheral nerves. J. Comp. Neurol. 37:123-205.

Harzer K. and Kustermann-Kuhn B. (1987) Brain galactolipid content in a patient with pseudoarylsulfatase A deficiency and coincidental diffuse disseminated scleroses and in patients with metachromatic, adreno and other leukodystrophies. J. Neurochem. 48:62-6.

He H.T., Barbet J., Chaix J.C., Goridis C. (1986) Phosphatidylinositol is involved in the membrane attachment of NCAM-120, the smallest component of the neural cell adhesion molecule. EMBO J. 5(10):2489-94.

Hemperly J.J., Edelman G.M., Cunningham B.A. (1986) cDNA clones of the neural cell adhesion molecule (N-CAM) lacking a membrane-spanning region consistent with evidence for membrane attachment via a phosphatidylinositol intermediate. Proc Natl Acad Sci U S A. 83(24):9822-6.

Hess B., Saftig P., Hartmann D., Coenen R., Lullmann-Rauch R., Goebel H.H., Evers M., von Figura K., D'Hooge R., Nagels G., De Deyn P., Peters C., Gieselmann V. (1996) Phenotype of arylsulfatase A-deficient mice: relationship to human metachromatic leukodystrophy. Proc Natl Acad Sci U S A. 93(25):14821-6.

Hildebrandt H., Becker C., Murau M., Gerardy-Schahn R., Rahmann H. (1998) Heterogeneous expression of the polysialyltransferases ST8Sia II and ST8Sia IV during postnatal rat brain development. J. Neurochem. 71(6):2339-48.

Hirahara Y., Tsuda M., Wada Y., Honke K. (2000) cDNA cloning, genomic cloning, and tissue-specific regulation of mouse cerebroside sulfotransferase. Eur J Biochem. 267(7):1909-17.

Hirahara Y., Bansal R., Honke K., Ikenaka K., Wada Y. (2004) Sulfatide is a negative regulator of oligodendrocyte differentiation: development in sulfatide-null mice. Glia. 45(3):269-77.

Honke K., Hirahara Y., Dupree J., Suzuki K., Popko B., Fukushima K., Fukushima J., Nagasawa T., Yoshida N., Wada Y., Taniguchi N. (2002) Paranodal junction formation and spermatogenesis require sulfoglycolipids. Proc Natl Acad Sci U S A. 99(7):4227-32.

Ikenaka K., Kagawa T., Mikoshiba K. (1992) Selective expression of DM-20, an alternatively spliced myelin proteolipid protein gene product, in developing nervous system and in nonglial cells. J. Neurochem. 58(6):2248-53.

Ishibashi T., Dupree J.L., Ikenaka K., Hirahara Y., Honke K., Peles E., Popko B., Suzuki K., Nishino H., Baba H. (2002) A myelin galactolipid, sulfatide, is essential for maintenance of ion channels on myelinated axon but not essential for initial cluster formation. J. Neurosci. 22(15):6507-14.

Ishizuka I. (1997) Chemistry and functional distribution of sulfoglycolipids. Prog Lipid Res. 36(4):245-319.

Johnson C.P., Fujimoto I., Rutishauser U., Leckband D.E. (2005) Direct evidence that neural cell adhesion molecule (NCAM) polysialylation increases intermembrane repulsion and abrogates adhesion. J. Biol Chem. 280(1):137-45.

Kaplan M.R., Meyer-Franke A., Lambert S., Bennett V., Duncan I.D., Levinson S.R., Barres B.A. (1997) Induction of sodium channel clustering by oligodendrocytes. Nature. 386(6626):724-8.

Kiss J.Z. and Rougon G. (1997) Cell biology of polysialic acid. Curr Opin Neurobiol. 7(5):640-6.

Klein C., Kramer E.M., Cardine A.M., Schraven B., Brandt R., Trotter J. (2002) Process outgrowth of oligodendrocytes is promoted by interaction of fyn kinase with the cytoskeletal protein tau. J Neurosci. 22(3):698-707.

Kolodny E.H. (1989) Metachromatic leukodystrophy and multiple sulfatase deficiency: Sulfatide lipidosis. In the metabolic bases of inherited disease. Vol. 2. C.R. Scriver, Beaudet, A.L., Sly, W.S., Valle D., editor. McGraw-Hill, New York. 1721-1750.

Kramer E.M., Klein C., Koch T., Boytinck M., Trotter J. (1999) Compartmentation of Fyn kinase with glycosylphosphatidylinositol-anchored molecules in oligodendrocytes facilitates kinase activation during myelination. J. Biol Chem. 274(41):29042-9.

Kuhn P.L., Petroulakis E., Zazanis G.A., McKinnon R.D. (1995) Motor function analysis of myelin mutant mice using a rotarod. Int J Dev Neurosci. 13(7):715-22.

Kurosawa N., Yoshida Y., Kojima N., Tsuji S. (1997) Polysialic acid synthetase (ST8Sia II/STX) mRNA expression in the developing mouse central nervous system. J. Neurochem. 69(2):494-503.

Lavdas A.A., Franceschini I., Dubois-Dalcq M., Matsas R. (2006) Schwann cells genetically engineered to express PSA show enhanced migratory potential without impairment of their myelinating ability in vitro. Glia. 53(8):868-78.

Li C., Tropak M.B., Gerlai R., Clapoff S., Abramow-Newerly W., Trapp B., Peterson A., Roder J. (1994) Myelination in the absence of myelin-associated glycoprotein. Nature. 369(6483):747-50.

Livingston B.D. and Paulson J.C. (1993) Polymerase chain reaction cloning of a developmentally regulated member of the sialyltransferase gene family. J. Biol Chem. 268(16):11504-7.

Lowry O.H., Rosenbrough N.J., Farr A.L., Randall R.J. (1951) Protein measurement with the Folin phenol reagent. J Biol Chem. 193(1):265-75.

Lubetzki C., Demerens C., Anglade P. Villarroya H., Frankfurter A., Lee V.M., Zalc B. (1993) Even in culture, oligodendrocytes myelinate solely axons. Proc Natl Acad Sci U S A. 90(14):6820-4.

Ludwin S.K. (1997) The pathobiology of the oligodendrocyte. J. Neuropathol Exp Neurol. 56(2):111-24.

Malone M.J., Stoffyn P. (1966) A comparative study of brain and kidney glycolipids in metachromatic leukodystrophy. J. Neurochem. 13:1037-45.

Marcus J., Honigbaum S., Shroff S., Honke K., Rosenbluth J., Dupree J.L. (2006) Sulfatide is essential for the maintenance of CNS myelin and axon structure. Glia. 53(4):372-81.

Marty M.C., Alliot F., Rutin J., Fritz R., Trisler D., Pessac B. (2002) The myelin basic protein gene is expressed in differentiated blood cell lineages and in hemopoietic progenitors. Proc Natl Acad Sci U S A. 99(13):8856-61.

Matzner U., Harzer K., Learish R.D., Barranger J.A., Gieselmann V. (2000) Long-term expression and transfer of arylsulfatase A into brain of arylsulfatase A-deficient mice transplanted with bone marrow expressing the arylsulfatase A cDNA from a retroviral vector. Gene Ther. 7(14):1250-7.

Matzner U., Hartmann D., Lullmann-Rauch R., Coenen R., Rothert F., Mansson J.E., Fredman P., D'Hooge R., De Deyn P.P., Gieselmann V. (2002) Bone marrow stem cell-based gene transfer in a mouse model for metachromatic leukodystrophy: effects on visceral and nervous system disease manifestations. Gene Ther. 9(1):53-63.

Matzner U., Herbst E., Hedayati K.K., Lullmann-Rauch R., Wessig C., Schroder S., Eistrup C., Moller C., Fogh J., Gieselmann V. (2005) Enzyme replacement improves nervous system pathology and function in a mouse model for metachromatic leukodystrophy. Hum Mol Genet. 14(9):1139-52.

Meyer-Franke A., Shen S., Barres B.A. (1999) Astrocytes induce oligodendrocyte processes to align with and adhere to axons. Mol Cell Neurosci. 14(4-5):385-97.

Milner R., Edwards G., Streuli C., Ffrench-Constant C. (1996) A role in migration for the alpha V beta 1 integrin expressed on oligodendrocyte precursors. J. Neurosci. 16(22):7240-52.

Molineaux S.M., Engh H., de Ferra F., Hudson L., Lazzarini R.A. (1986) Recombination within the myelin basic protein gene created the dysmyelinating shiverer mouse mutation. Proc Natl Acad Sci U S A. 83(19):7542-6.

Montag D, Giese KP, Bartsch U, Martini R, Lang Y, Bluthmann H, Karthigasan J, Kirschner DA, Wintergerst ES, Nave KA, Zielasak J., Toyka K.V., Lipp H.P. and Schachner M. (1994)

Mice deficient for the myelin-associated glycoprotein show subtle abnormalities in myelin. Neuron. 13: 229–tg246.

Morello D., Dautigny A., Pham-Dinh D., Jolles P. (1986) Myelin proteolipid protein (PLP and DM-20) transcripts are deleted in jimpy mutant mice. EMBO J. 5(13):3489-93.

Mühlenhoff M., Eckhardt M., Bethe A., Frosch M., and Gerardy-Schahn R. (1996) Autocatalytic polysialylation of polysialyltransferase-1. EMBO J. 15, 6943-6950

Muhlenhoff M., Eckhardt M., Gerardy-Schahn R. (1998) Polysialic acid: three-dimensional structure, biosynthesis and function. Curr Opin Struct Biol. 8(5):558-64.

Muller D., Wang C., Skibo G., Toni N., Cremer H., Calaora V., Rougon G., Kiss J.Z. (1996) PSA-NCAM is required for activity-induced synaptic plasticity. Neuron. 17(3):413-22.

Muller D., Djebbara-Hannas Z., Jourdain P., Vutskits L., Durbec P., Rougon G., Kiss J.Z. (2000) Brain-derived neurotrophic factor restores long-term potentiation in polysialic acid-neural cell adhesion molecule-deficient hippocampus. Proc Natl Acad Sci U S A. 97(8):4315-20.

Nakayama J., Fukuda M.N., Fredette B., Ranscht B., Fukuda M. (1995) Expression cloning of a human polysialyltransferase that forms the polysialylated neural cell adhesion molecule present in embryonic brain. Proc Natl Acad Sci U S A. 92(15):7031-5.

Nave K.A., Lai C., Bloom F.E., Milner R.J. (1987) Splice site selection in the proteolipid protein (PLP) gene transcript and primary structure of the DM-20 protein of central nervous system myelin. Proc Natl Acad Sci U S A. 84(16):5665-9.

Nave K. A. and Salzer J. (2006) Axonal regulation of myelination by neuregulin 1. Curr Opin Neurobiol. (5):492-500.

Newman S., Kitamura K., Campagnoni A.T. (1987) Identification of a cDNA coding for a fifth form of myelin basic protein in mouse. Proc Natl Acad Sci U S A. 84(3):886-90.

Norton W.T. and Poduslo S.E. (1973) Myelination in rat brain: changes in myelin composition during brain maturation. J Neurochem. 21(4):759-73.

Norton W.T. and Poduslo S.E. (1982) Biochemical studies in three siblings. Acta Neuropathol (Berl). 57:188-96.

Ong E., Nakayama J., Angata K., Reyes L., Katsuyama T., Arai Y., Fukuda M. (1998) Developmental regulation of polysialic acid synthesis in mouse directed by two polysialyltransferases, PST and STX. Glycobiology. 8(4):415-24.

Osterhout D.J., Wolven A., Wolf R.M., Resh M.D., Chao M.V. (1999) Morphological differentiation of oligodendrocytes requires activation of Fyn tyrosine kinase. J. Cell Biol. 145(6):1209-18.

Paratcha G., Ledda F., Ibanez C. (2003) The Neural Cell Adhesion Molecule NCAM Is an Alternative Signaling Receptor for GDNF Family Ligands. Cell. 113 (7), 867-879.

Payne H.R., Hemperly J.J., Lemmon V. (1996) N-cadherin expression and function in cultured oligodendrocytes. Brain Res Dev Brain Res. 97(1):9-15.

Pesheva P., Gloor S., Schachner M, Probstmeier R. (1997) Tenascin-R is an intrinsic autocrine factor for oligodendrocyte differentiation and promotes cell adhesion by a sulfatide-mediated mechanism. J. Neurosci. 17(15):6021.

Peyron F., Timsit S., Thomas J.L., Kagawa T., Ikenaka K., Zalc B. (1997) In situ expression of PLP/DM-20, MBP, and CNP during embryonic and postnatal development of the jimpy mutant and of transgenic mice overexpressing PLP. J. Neurosci Res. 50(2):190-201.

Pilz H. and Heipertz R. (1974) The fatty acid composition of cerebrosides and sulfatides in a case of adult metachromatic leukodystrophy. Z Neurol. 206(3):203-8.

Poduslo S.E., Miller K., Jang, Y. (1982) Biochemical studies of the late infantile form of metachromatic leukodystrophy. Acta Neuropathol. (Berl.) 57, 13– 22.

Poltorak M., Sadoul R., Keilhauer G., Landa C., Fahrig T., Schachner M. (1987) Myelin-associated glycoprotein, a member of the L2/HNK-1 family of neural cell adhesion molecules, is involved in neuron-oligodendrocyte and oligodendrocyte-oligodendrocyte interaction. J. Cell Biol. 105(4):1893-9.

Povlsen G.K., Ditlevsen D.K., Berezin V., Bock E. (2003) Intracellular signaling by the neural cell adhesion molecule. Neurochem Res. 28(1):127-41.

Pringle N.P. and Richardson W.D. (1993) A singularity of PDGF alpha-receptor expression in the dorsoventral axis of the neural tube may define the origin of the oligodendrocyte lineage. Development. 117(2):525-33.

Qiu J., Cai D., Filbin M.T. (2000) Glial inhibition of nerve regeneration in the mature mammalian CNS. Glia. 29(2):166-74.

Richardson W.D., Smith H.K., Sun T., Pringle N.P., Hall A., Woodruff R. (2000) Oligodendrocyte lineage and the motor neuron connection. Glia. 29(2):136-42.

Rintoul D.A. and Welti R. (1989) Thermotropic behaviour of mixtures of glycosphingolipids and phosphatidylcholine: effect of monovalent cations on sulfatide and galactosylceramide. Biochemistry. 10;28(1):26-31.

Roach A., Takahashi N., Pravtcheva D., Ruddle F., Hood L. (1985) Chromosomal mapping of mouse myelin basic protein gene and structure and transcription of the partially deleted gene in shiverer mutant mice. Cell. 42(1):149-55.

Ronn L.C., Berezin V., Bock E. (2000) The neural cell adhesion molecule in synaptic plasticity and ageing. Int. J. Dev. Neurosci. 18, 193–199.

Roth J., Taatjes D.J., Bitter-Suermann D., Finne J. (1987) Polysialic acid units are spatially and temporally expressed in developing postnatal rat kidney. Proc Natl Acad Sci U S A. 84(7):1969-73.

Rutishauser U. and Landmesser L. (1996) Polysialic acid in the vertebrate nervous system: a promoter of plasticity in cell-cell interactions. Trends Neurosci. 19(10):422-7.

Salzer J.L., Holmes W.P., Colman D.R. (1987) The amino acid sequences of the myelin-associated glycoproteins: homology to the immunoglobulin gene superfamily. J. Cell Biol. 104(4):957-65.

Sanes J.R., Schachner M., Covault J. (1986) Expression of several adhesive macromolecules (N-CAM, L1, J1, NILE, uvomorulin, laminin, fibronectin, and, a heparan sulfate proteoglycan) in embryonic, adult, and denervated adult skeletal muscle. J. Cell Biol. 102(2):420-31.

Santoni M.J., Barthels D., Barbas J.A., Hirsch M.R., Steinmetz M., Goridis C., Wille W. (1987) Analysis of cDNA clones that code for the transmembrane forms of the mouse neural cell adhesion molecule (NCAM) and are generated by alternative RNA splicing. Nucleic Acids Res. 15(21):8621-41.

Saravanan K., Schaeren-Wiemers N., Klein D., Sandhoff R., Schwarz A., Yaghootfam A., Gieselmann V., Franken S. (2004) Specific downregulation and mistargeting of the lipid raft-associated protein MAL in a glycolipid storage disorder. Neurobiol Dis. 16(2):396-406.

Sarlieve L.L., Neskovic N.M., Mandel P. (1971) PAPS-cerebroside sulphotransferase activity in brain and kidney of neurological mutants. FEBS Lett. 19(2):91-95.

Schachner M. (1997) Neural recognition molecules and synaptic plasticity. Curr. Opin. Cell Biol. 9, 627–634.

Schaeren-Wiemers N., Bonnet A., Erb M., Erne B., Bartsch U., Kern F., Mantei N., Sherman D., Suter U. (2004) The raft-associated protein MAL is required for maintenance of proper axon--glia interactions in the central nervous system. J. Cell Biol. 166(5):731-42.

Scheidegger P., Papay J., Zuber C., Lackie P.M., Roth J. (1994) Cellular site of synthesis and dynamics of cell surface re-expression of polysialic acid of the neural cell adhesion molecule. Eur J Biochem. 225(3):1097-103.

Schwab M.E., Schnell L. (1989) Region-specific appearance of myelin constituents in the developing rat spinal cord. J. Neurocytol. 18(2):161-9.

Seidenfaden R., Krauter A., Schertzinger F., Gerardy-Schahn R., Hildebrandt H. (2003) Polysialic acid directs tumor cell growth by controlling heterophilic neural cell adhesion molecule interactions. Mol Cell Biol. 23(16):5908-18.

Sheikh K.A., Sun J., Liu Y., Kawai H., Crawford T.O., Proia R.L., Griffin J.W., Schnaar R.L. (1999) Mice lacking complex gangliosides develop Wallerian degeneration and myelination defects. Proc Natl Acad Sci U S A. 96(13):7532-7.

Spassky N., Goujet-Zalc C., Parmantier E., Olivier C., Martinez S., Ivanova A., Ikenaka K., Macklin W., Cerruti I., Zalc B., Thomas J.L. (1998) Multiple restricted origin of oligodendrocytes. J. Neurosci. 18(20):8331-43.

Sprinkle T.J. (1989) 2',3'-cyclic nucleotide 3'-phosphodiesterase, an oligodendrocyte-Schwann cell and myelin-associated enzyme of the nervous system. Crit Rev Neurobiol. 4(3):235-301.

Stevens B., Porta S., Haak L.L., Gallo V., Fields R.D. (2002) Adenosine: a neuron-glial transmitter promoting myelination in the CNS in response to action potentials. Neuron. 36(5):855-68.

Stoykova L. I., Beesley J. S., Grinspan J. B., Glick M. C. (2001) ST8Sia IV mRNA corresponds with the biosynthesis of alpha2,8sialyl polymers but not oligomers in rat oligodendrocytes. J. Neurosci. Res. 66, 497-505.

Tang S., Shen Y.J., Debellard M.E., Mukhopadhyay G., Salzer J.L., Crocker P.R., Filbin M.T. (1997) Myelin-associated glycoprotein interacts with neurons via a sialic acid binding site at ARG118 and a distinct neurite inhibition site. J. Cell Biol. 138: 1355–1366.

Timsit S., Martinez S., Allinquant B., Peyron F., Puelles L., Zalc B. (1995) Oligodendrocytes originate in a restricted zone of the embryonic ventral neural tube defined by DM-20 mRNA expression. J. Neurosci. 15(2):1012-24.

Timsit S.G., Bally-Cuif L., Colman D.R., Zalc B. (1992) DM-20 mRNA is expressed during the embryonic development of the nervous system of the mouse. J. Neurochem. 58(3):1172-5.

Trotter J., Bitter-Suermann D., Schachner M. (1989) Differentiation-regulated loss of the polysialylated embryonic form and expression of the different polypeptides of the neural cell adhesion molecule by cultured oligodendrocytes and myelin. J. Neurosci Res. 22(4):369-83.

Umemori H., Sato S., Yagi T., Aizawa S., Yamamoto T. (1994) Initial events of myelination involve Fyn tyrosine kinase signaling. Nature. 367: 572–576.

van der Knaap M.S., Leegwater P.A., Konst A.A., Visser A., Naidu S., Oudejans C.B., Schutgens R.B., Pronk J.C. (2002) Mutations in each of the five subunits of translation initiation factor eIF2B can cause leukoencephalopathy with vanishing white matter. Ann Neurol. 51(2):264-70.1

van Echten-Deckert G. (2000) Sphingolipid extraction and analysis by thin-layer chromatography. Methods Enzymol. 312:64-79.

Varki A. (1999) Essentials of Glycobiology edited by Ajit Varki, Richard Cummings, Jeffrey Esko, Hudson Freeze, Gerald Hart, Jamey Marth; Plainview (NY): Cold Spring Harbor Laboratory Press. Chapter 15, Sialic acids.

von Figura K., Gieselmann V., Jaeken J. (2001) Metachromatic leukodystrophy. In: The metabolic and molecular basis of inherited disease. Eds.: Scriver, Beaudet, Valle, Sly Mc Graw Hill, New York, eighth edition, chapter 148, 3695-3724

Vutskits L., Djebbara-Hannas Z., Zhang H., Paccaud J.P., Durbec P., Rougon G., Muller D., Kiss J.Z. (2001) PSA-NCAM modulates BDNF-dependent survival and differentiation of cortical neurons. Eur J Neurosci. 13(7):1391-402.

Wang C., Rougon G., Kiss J.Z. (1994) Requirement of polysialic acid for the migration of the O-2A glial progenitor cell from neurohypophyseal explants. J. Neurosci. 14(7):4446-57.

Wang S, Sdrulla AD, diSibio G, Bush G, Nofziger D, Hicks C, Weinmaster G, Barres BA. (1998) Notch receptor activation inhibits oligodendrocyte differentiation. Neuron. 21(1):63-75.

Watanabe M., Sakurai Y., Ichinose T., Aikawa Y., Kotani M., Itoh K. (2006) Monoclonal antibody Rip specifically recognizes 2',3'-cyclic nucleotide 3'-phosphodiesterase in oligodendrocytes. J Neurosci Res. 84(3):525-33.

Waxman S.G. and Sims T.J. (1984) Specificity in central myelination: evidence for local regulation of myelin thickness. Brain Res. 292(1):179-85

Weinhold B., Seidenfaden R., Rockle I., Muhlenhoff M., Schertzinger F., Conzelmann S., Marth J.D., Gerardy-Schahn R., Hildebrandt H. (2005) Genetic ablation of polysialic acid causes severe neurodevelopmental defects rescued by deletion of the neural cell adhesion molecule. J. Biol Chem. 280(52):42971-7.

Wessel D. and Flugge U.I. (1984) A method for the quantitative recovery of protein in dilute solution in the presence of detergents and lipids. Anal Biochem 138(1):141-3.

Wittke D., Hartmann D., Gieselmann V., Lüllmann-Rauch R. (2004) Lysosomal sulfatide storage in the brain of arylsulfatase A-deficient mice: cellular alterations and topographic distribution. Acta Neuropathol. 108: 261-271.

Wood P.M. and Bunge R.P. (1986) Myelination of cultured dorsal root ganglion neurons by oligodendrocytes obtained from adult rats. J. Neurol Sci. 74(2-3):153-69.

Yaghootfam A., Gieselmann V., Eckhardt M. (2005) Delay of myelin formation in arylsulphatase A-deficient mice. Eur J Neurosci. 21(3):711-20.

Yang L.J., Zeller C.B., Shaper N.L., Kiso M., Hasegawa A. , Shapiro R.E., Schnaar R.L. (1996) Gangliosides are neuronal ligands for myelinassociated glycoprotein. Proc Natl Acad Sci USA 93: 814–818.

Yang P., Yin X., Rutishauser U. (1992) Intercellular space is affected by the polysialic acid content of NCAM. J. Cell Biol. 116(6):1487-96.

Yang P., Major D., Rutishauser U. (1994) Role of charge and hydration in effects of polysialic acid on molecular interactions on and between cell membranes. J. Biol Chem. 269(37):23039-44.

Yu W.P., Collarini E.J., Pringle N.P., Richardson W.D. (1994) Embryonic expression of myelin genes: evidence for a focal source of oligodendrocyte precursors in the ventricular zone of the neural tube. Neuron. 12(6):1353-62.

Zielasek J., Martini M., Toyka K.V. (1996) Functional abnormalities in P0-deficient mice resemble human hereditary neuropathies linked to P0 gene mutations. Muscle Nerve 19:946-952.